PREPARATION AND CHARACTERIZATION OF DCPD-FORMING CALCIUM PHOSPHATE CEMENTS AND OF CEMENT-PROTEIN DRUG MICROPARTICLE COMPOSITES FOR BONE TISSUE ENGINEERING

Dissertation zur Erlangung des akademischen Grades des
Doktors der Naturwissenschaften (Dr. rer. nat.)

eingereicht im Fachbereich Biologie, Chemie, Pharmazie
der Freien Universität Berlin

vorgelegt von

BURKHARD DICKENHORST
aus Kassel

Juni, 2010

1. Gutachter: Prof. Dr. Roland Bodmeier
2. Gutachter: Prof. Dr. Jürgen Siepmann
Tag der mündlichen Prüfung: 2010-07-05

To my parents

Acknowledgements

During the work on my thesis at the Freie Universität Berlin, many people helped me with their advice, patience and support. To all those, I want to express my thankfulness.

Special thanks go to Professor Dr. Roland Bodmeier for his advice, guidance and support throughout my graduate studies and for his slight pushing at the end. I am very thankful to him for the opportunity to let me work in his international research group as Ph. D. student and for allowing me to contribute in some collaborations.

I would also like to deeply thank Professor Dr. Jürgen Siepmann for co-evaluating my thesis. Thanks to Professor Dr. Johannes Surmann, Professor Dr. Heinz Pertz and Dr. Martin Körber for serving as members of my thesis committee.

Additional thanks go to all my colleagues in the Kelchstraße. I will not name all of you, as I may forget someone without intention. It was a real pleasure to work with you. However, some of you should be mentioned in irregular order: Dr. Martin Schulz for being my lab-mate for several years; Dr. Martin Körber for his advice and many fruitful discussions; Dr. Ingo Siebenbrodt for the nice state examinations in clinical pharmacy; Dr. Lothar Schwabe for his patience in our conflicts with the ZEDAT; Mr. Stefan Walter for prompt and diligent technical support; Mr. Alfred Protz for his help on all kinds of nitrogen; Mrs. Eva Ewest for prompt handling of orders and buffer preparation; Mrs. Angelika Schwarz and Mrs. Gabriela Karsubke for their assistance with administrative issues.

I would also like to thank Dr. Erich Schiffl for his advice and help during my internship in the industry and later on but especially for showing me, how a superior should be like.

Finally, I would like to express my deepest gratitude to my parents Wilfried and Ursula Dickenhorst and my girlfriend Katja Oelmann for their love, patience and ongoing support during my whole life and the last years, respectively.

Table of contents

1 Introduction

1.1 Bone

1.1.1 General

Bone is a highly complex tissue, consisting of living cells and a characteristically high amount of extracellular matrix. The latter one forms the rigid structures that are known as the skeleton.

Within all tissues of the body, bone has the unique ability to heal even very large defects without the formation of scars[1, 2]. However, this ability requires the prevention of "foreign tissue" ingrowth into the defect to be repaired, as the repair process is quite slow.

In most fractures, the defect is bridged by the forming hematoma. However, more than 800000 of the around 6.5 million fractures in the U.S. per year show poor healing and require the use of a void filler or implant[3].

For extensive information about bone tissue, it has to be referred to the literature. However, information on the most important aspects of bone with respect to the topic of this work will be given in the following.

1.1.2 Functions of bone

Bone provides different important functions in the body. The most obvious are the mechanical functions that include the provision of the shape of the body, the protection of internal organs against mechanical stresses, the participation in movement processes and, to a lower level, a role in sound transduction.

Bone has a central role in the homeostasis of ions in the body in general and blood in particular. Especially its storage capability for calcium and phosphate ions has to be mentioned here. About 99 % of the calcium and 85 % of the phosphorus content of the body are located in bone and the related materials dentin and enamel[4]. The phosphate ions in bone also play an important role in the pH homeostasis of the body.

Bone also acts as storage for growth factors like IGF or TGF, and – within the yellow bone marrow – for fatty acids. Within the red bone marrow, blood cells are produced. Besides, growth factors are synthesized in bone tissue.
Bone can act as a deep compartment for drugs (e.g. bisphosphonates) but also for toxins, especially bivalent heavy metal ions like cadmium or lead[5-7].

1.1.3 Anatomical structures in bone

The anatomy of bone is highly complex. Within this work, only some of the most important aspects can be touched.
The fundamental functional unit of (cortical) bone is called osteon. An osteon consists of concentric layers, so called *lamellae*, formed by bone matrix that surround a central canal (Haversian canal). Osteons are usually several millimeters in length and around 0.2 mm in diameter. The Haversian canal is filled with small blood vessels and may additionally include nerve fibers. Small channels diverting from the central Haversian canal lead to osteocytes (1.1.4.2), which are enclosed by the bone matrix.

1.1.3.1 Bone matrix

The bone matrix is the extracellular matrix (ECM) of bone tissue. Although every tissue has an ECM, the amount of ECM in human tissues is usually quite low. The only exceptions are cartilage and bone.
The bone matrix includes all acellular parts of bone, which is around 90 – 95 % of the total mass of living bone[8]. The bone matrix guarantees the mechanical properties of bone. Its mass in a standard human (70 kg) is just around 9 kg, still containing significant amounts of water. Calcium and phosphate, the abovementioned main constituents of the inorganic bone matrix, just account for approximately 2 kg of the matrix mass.
Compared to its low weight, the bone matrix provides exceptional compressive, high tensile and very good bending strengths (1.1.9, 1.5).
Bone matrix can be separated in an inorganic and an organic part. However, from a functional point of view, inorganic and organic parts cannot be separated as the mechanical properties of bone depend on both. Inorganic parts provide compressive strength, while organic parts provide tensile strength. In consequence, bending strength is a result of both properties.

The bone matrix (organic and inorganic parts) is initially deposited by osteoblasts (1.1.4.1) as unmineralized precursor substance called osteoid. The osteoid is then mineralized and transformed into the final bone matrix within a successive process involving enzymes like alkaline phosphatase and other substances, secreted into small vesicles from the osteoblasts and the forming osteocytes (1.1.4.2). The osteoblast-secreted vesicles then rupture and act as centers for crystal growth.

1.1.3.2 Inorganic matrix

Approximately 70 % of the mass of living bone can be attributed to the inorganic matrix. Its characterizing chemical constituent is hydroxylapatite (1.2.9). However, in natural bone pure hydroxylapatite is rare[4]. "Biological" hydroxylapatite often contains foreign ions, as magnesium or carbonate. Besides, its stoichiometry is often slightly different from pure hydroxylapatite, even without foreign ions. The last is usually called calcium deficient hydroxylapatite (CDHA). Fluoroapatite has a lower solubility and higher resistance to acids than hydroxylapatite. It is therefore a wanted "impurity" especially for dentin and enamel.
With the exception of fluorine, all impurities in "biological" hydroxylapatite increase the lattice strain and therefore the solubility. The impurities also have an effect on the size of the formed crystals. "Biological" hydroxylapatite has a much smaller crystal size than synthetically prepared hydroxylapatite, e.g. from hydroxylapatite-forming calcium phosphate cements (1.11).
Besides the mentioned apatites, other calcium salts, e.g. calcium carbonate, have been identified in bone tissue. Biltz et al.[9] reported a calcium-to-phosphate ratio of 1.77 for bone which is higher than that of hydroxylapatite and could therefore only be explained by the presence of non-phosphate-containing calcium salts within the inorganic matrix.
The inorganic matrix provides nearly the complete compressive strength of bone. However, the inorganic matrix is very brittle and a bone matrix just consisting of these inorganic parts would easily break on tensile loads or bending moments. In bone tissue, this brittleness is reduced by the organic matrix (1.1.3.3), which is in close contact to the inorganic.
Due to the macroscopic appearance of the structures of the inorganic matrix, two main types of bone are distinguished: Cortical bone (1.1.3.6) and trabecular bone (1.1.3.7). Each of them will be discussed later. Both types should not be seen isolated, as bone remodeling can

transform cortical bone into trabecular bone and vice versa in the attempt to optimize the ratio between bone strength and weight.

1.1.3.3 Organic matrix

Up to around 25 % of the mass of living bone are formed by the organic matrix. More than 95 % of the organic matrix are formed by collagen type I (type II is characteristic for cartilage). The collagen fibers are usually aligned along the osteons, forming an overall structure similar to (fiber) reinforced concrete. This alignment accounts for high tensile strength of lamellar bone.

1.1.3.4 Lamellar bone

Lamellar bone is characterized by the parallel orientation of the collagen fibers of the organic matrix and the osteons. Lamellar bone can be especially found in intact cortical bone. It has very good mechanical properties along its axis of orientation with respect to its compressive and its tensile strengths. The mechanical strengths orthogonal to this axis are significantly lower.
The formation of lamellar bone is a quite slow process that is predominant during permanent bone remodeling (1.1.5). After a fracture or the formation of any other larger bone defect, first woven bone is deposited.

1.1.3.5 Woven bone

Woven bone is characterized by a random orientation of the collagen fibers of the organic matrix. It is formed rapidly after fractures and other defects to close the gap and provide an initial amount of mechanical strength. The mechanical strength of woven bone is isometric, i.e. it exhibits the same compressive and tensile strengths in all directions. As the forces applied to bone usually have some preferred directions, woven bone is usually transferred into lamellar bone by the remodeling processes (1.1.5), optimizing the ratio between strength and weight.

1.1.3.6 Cortical bone

Cortical bone is characterized by its compact structure with only very few and very small gaps inside the bone matrix. This typical structure accounts for its English synonyms "compact bone" or "dense bone". Its Latin name is *substantia compacta*, derived from the same anatomical fact.
Cortical bone is usually seen at the outer layers of bone, the cortices. Pronounced cortices can be found especially with long bones like the femurs or tibias.
Cortical bone accounts for approximately 80 % of the total bone mass in adult humans and most of the mechanical strength (1.1.9)[10]. Compressive strengths of up to 180 MPa, tensile strengths of up to 151 MPa and elastic modulus values of up to 18 MPa are reported[11-14].

1.1.3.7 Trabecular bone

Trabecular bone is characterized by large pores between the structures of its bone matrix (1.1.3.1). Within these pores, the majority of the blood vessels supplying the bone itself and the bone marrow are embedded.
Trabecular bone is also named "cancellous bone" or "spongy bone", the latter derived from the medical Latin term *substantia spongiosa*. The name trabecular bone itself is derived from the Latin term *trabecula.* The *trabeculae* are beam or rod like elements of bone matrix that form the walls of the open pore network of "spongy bone".
Just around 20 % of the total bone mass in adult humans have to be attributed to trabecular bone. However, it accounts for more than 90 % of the total bone surface[10]. The mechanical strength (1.1.9) of trabecular bone is relatively low, with values of rarely more than 10 MPa for compressive strength reported[11, 12, 15-17].

1.1.4 Cells in bone

About 5 % of the mass of living bone is formed by cellular structures[8]. Besides some non-specific cells, e.g. from blood vessels, nerves or the immune system, two main groups of characteristic cells can be found in bone tissue.
The first group consists of cells forming new bone and providing its integrity, while the second one consists of cells resorbing existing bone matrix. Both groups are essential for the remodeling processes (1.1.5) and therefore correct bone function. Malfunctions in each group can cause severe diseases, like osteodystrophia dysformans, osteogenesis imperfecta, osteopetrosis or osteoporosis.
The group of (predominantly) bone forming cells consists of osteoblasts, osteocytes and bone lining cells while the bone resorbing second group is just represented by osteoclasts.

1.1.4.1 Osteoblasts

Osteoblasts are cuboidal single nucleated cells with an approximate diameter of 10 µm. They synthesize and deposit the precursor of the bone matrix, the osteoid. The osteoid is then calcified in a multi-step process to finally form the primarily hydroxylapatite containing bone matrix.
While an osteoblast is active, it encases itself in the produced bone matrix. An (inactive) osteoblast completely encased in the bone matrix is called osteocyte (1.1.4.2), while an inactive osteoblast at the surface of bone is called bone lining cell (1.1.4.3).
Osteoblasts are derived from a mesenchymal stem cell (MSC) lineage, making the use of MSCs in bone tissue engineering interesting (1.6.2).

1.1.4.2 Osteocytes

Osteocytes are living osteoblasts encased in the deposited bone matrix (1.1.3.1). The small hole in the bone matrix in which an osteocyte is located is called *lacuna*.
The main purpose of osteocytes is to serve as sensors for mechanical stimuli within bone tissue. Besides, they can deposit new bone matrix and destroy the bone matrix by osteocytic osteolysis, making them involved in remodeling processes (1.1.5).

To provide nutrition and communication, they are connected to other cells via cytoplasmatic extensions running through *canaliculi* within the inorganic matrix.

1.1.4.3 Bone lining cells

Bone lining cells are inactive osteoblasts located on the surface of bone[a]. Bone lining cells wait for external stimuli to start the secretion of osteoid to create new bone matrix or the secretion of degrading substances to dissolve the bone matrix. Bone lining cells are therefore involved in remodeling processes, too (1.1.5).
Bone lining cells allow the adaption of the bone diameter and therefore especially of bending strength (1.5). This parameter exponentially increases with the outer diameter of bone (Equation 1).

$$W = \frac{\pi}{32} \cdot \frac{\left(D^4 - d^4\right)}{D}$$

Equation 1: Calculation of the bending strength W of a tube with D as outer and d as inner diameter.

1.1.4.4 Osteoclasts

Osteoclasts are giant multi-nucleated cells with diameters of 20 to 100 µm. They secrete acids and enzymes (predominantly HCl and collagenase) that can break down inorganic and organic bone matrix very effectively.
Osteoclasts play an important role in bone remodeling (1.1.5) as they resorb old bone material. This is important, as the mass of a cylinder follows Equation 2, while its bending

[a] As bone is a quite porous structure, bone has different surfaces that can be distinguished: A periosteal surface which is the outer surface of bone, an endosteal surface as the general inner surface of bone, a Haversian surface inside the Haversian canals within the osteons and finally a trabecular surface as the outer surface of an individual *trabecula*. The most important surface for bone lining cells is the periosteal surface.

strength follows Equation 1. It is thus obvious that hollow, tubular structures have a better bending strength-to-mass ratio than compact ones. In combination with the bone lining cells, osteoclasts therefore account for the permanent optimization of the bone strength-to-mass ratio of the especially the *corticalis*.

$$m = \pi \cdot r^2 \cdot l \cdot \rho$$

Equation 2: Calculation of the mass m of a cylinder, where r is the cylinder's radius, l is its length and ρ is the density of the material.

Osteoclasts are also involved in the resorption of bone implants like calcium phosphate ceramics (1.9) and calcium phosphate cement (1.10).
Osteoclasts can be not only be activated for remodeling processes, but also to increase the calcium and phosphate concentrations in the blood, if these should fall below physiological limits. Therefore, they play an important role in the calcium and phosphate homeostasis of the body.
Different to osteoblasts, osteocytes and bone lining cells, osteoclasts are derived from the macrophage lineage.

1.1.5 Bone remodeling

Under physiological conditions, there is a balance between the formation of new bone and the resorption of existing bone. If certain parts of a bone are subjected to permanently increased stress, osteoblasts will create new bone in these regions to add mechanical stiffness. If another part is not used anymore, osteoclasts will degrade bone there, as unused bone would just create unnecessary weight and bind resources.
This mid-to-long term adaption process of bone to mechanical stresses is called bone remodeling[18, 19]. Bone remodeling includes anabolic and catabolic processes.
The formation of new bone by osteoblasts (1.1.4.1) is always accompanied by a resorption of some old parts of bone by osteoclasts (1.1.4.4). This combined action in the formation of new bone during remodeling has lead to speculation that the process could be induced by microcracks due to slight overloads[20-22]. These cracks had to be cleared by osteoclasts, before new bone matrix could be deposited.

Another theory on the induction of bone remodeling involves electricity[23, 24]. The calcium phosphate crystals in bone show piezoelectric properties. Every change in load will thus cause an electric stimulus, whose intensity is proportional to the applied load. Each load cycle produces two stimuli. With regard to the total amount of electric stimuli applied, the amount of load cycles and their frequency was also important. Effects of voltage and frequency of external electric stimuli on bone remodeling have been reported[25-29].

1.1.6 Fracture healing

The healing process of fractures and other (larger) bone defects is a multiple step process that can be divided into five phases:

1) Fracture and inflammatory phase
2) Granulation tissue formation
3) Callus formation
4) Lamellar bone deposition
5) Remodeling phase.

Within the first phase, a hematoma is formed at the site of the fracture. Most of the cells in the hematoma die, however fibroblasts in the hematoma area survive and start to replicate. In the second phase, the fibroblasts form a loose aggregate of cells, interspersed with small blood vessels, known as granulation tissue. The third phase comprises the replication and transformation of the cells of the *periosteum*. The periosteal cells proximal to the defect transform into chondroblasts and create hyaline cartilage, while the periosteal cells distal to the defect transform into osteoblasts and form woven bone (1.1.3.5). The fibroblasts within the granulation tissue also transform into chondroblasts producing hyaline cartilage. The process continues until the complete defect is filled with the formed callus, bridging the defect by hyaline cartilage and woven bone. The next phase involves the replacement of the formed hyaline cartilage and woven bone by lamellar bone (1.1.3.4). The structure of the new-formed lamellar bone is comparable to that of trabecular bone (1.1.3.7). At this point, the diameter of the healed bone is usually a little thicker than before the damage. The *status quo ante* including the presence of cortical bone (1.1.3.6) and original diameter is restored by remodeling processes.

Steps 4 and 5 are also known as endochondral ossification. This process is also seen in embryonic bone development and is controlled by several distinct growth factors (1.1.7) that show sophisticated expression profiles[30-33].

The size of defects that can be repaired with the described mechanism is virtually unlimited as long as the defect is not filled by other tissue and the concentration of growth factors within the defect is high enough.

For untreated bone defects, defect size thus can become limiting in practice. The maximum size of a defect that will completely heal without external help is called critical size. This size depends on factors like age and species, as well as on the location of the defect[34-41]. The critical size for adult humans is assumed to be 5 – 8 mm[42, 43].

Four challenges for an optimal treatment of large-scale bone defects can be postulated:

1) Immobilization of the adjacent periosteal sites
2) Prevention of scar tissue ingrowth
3) Sufficient provision of oxygen and nutrients at the site of the defect
4) Delivery of the right drug / growth factors at the right time and concentration.

These four postulates are identical within every species. However, especially the last mentioned point is also species dependent, as the sensitivity to growth factors is species dependent.

It has been mentioned that age of the patient and location of the defect have an influence on the healing process, too. As even the chemical composition of the bone matrix is not consistent within different species[9, 44], one-to-one transfers of results obtained from one species to another thus should be avoided.

1.1.7 Growth factors in bone

Several growth factors have been found in bone tissue and identified as important for bone formation. Some of them have already proved positive effects on the healing rate of bone defects in *in vivo* studies or are even already marketed[45, 46].

Besides non-specific growth factors, as IGF, PDGF or VEGF, a large group of growth factors specific to bone tissue has been identified. This group is known as bone morphogenetic proteins (BMPs).

The interactions between the several growth factors are highly complex; for extensive reviews it should be referred to the literature[47-49].

1.1.7.1 Bone morphogenetic proteins

Bone morphogenetic proteins (BMPs) are regulatory proteins, playing different important roles in bone formation, healing and remodeling[50-52]. Their name was derived from their ability to induce bone formation as well as bone remodeling. Some of the members also show an effect on cartilage formation, showing the narrow connections between bone and cartilage.
BMPs are classified as members of the TGF-β superfamily, a large group of proteins, consisting of the three isoforms of TGF-β itself (TGF-β_1, TGF- β_2 and TGF-β_3) and more than 30 other proteins. Among these other proteins are the activins, the anti-Müllerian hormone (AMH), some growth and differentiation factors (GDFs) and the already mentioned bone morphogenetic proteins themselves[53].
Some of the GDFs, as GDF-6 or GDF-7, have also BMP synonyms, while others like GDF-5 do not although they are also involved in bone formation[54].
Twenty different bone morphogenetic proteins have been identified yet, with 15 of them also found in humans. According to the definition given before, BMP-1 is no real bone morphogenetic protein, since it does not belong to the TGF-β superfamily.
The functions of the different bone morphogenetic proteins have been widely studied as well as their signaling pathways[31, 55-57].
The osteogenic activity of different growth factors was compared e.g. by Cheng et al[58].
In their study, the induction of early and late osteogenic markers in osteoblastic progenitor cells was highest with the BMPs 2, 6 and 9. The same growth factors were found to be most effective in inducing matrix mineralization. When focusing on the alkaline phosphatase activity of mature osteoblasts the BMPs 2, 4, 6, 7 and 9 were most effective.
The release patterns of BMPs during fracture healing have been examined e.g. for mice[59], rats[60, 61] and rabbits[62].
The physiological content of BMPs in bone is estimated to around 1 µg/g[63]. Doses applied with bone implants are usually much higher, which can cause adverse effects as ectopic bone formation, is a bumbling step against reduced growth factor effects when delivered at wrong points of the healing process, and is not cost effective. For an optimal bone implant, growth factor release should mimic the physiological profiles[64, 65].

1.1.7.2 BMP-2

BMP-2 is among the just mentioned family of bone morphogenetic proteins one that shows the highest level of osteoinductivity *in vivo*. It has proved effective in improving healing of bone defects[45, 66-69]. Besides its functions on bone, BMP-2 plays also an important role in cardiac morphogenesis. It is also expressed in a variety of tissues such as lung, spleen, brain, liver, prostate/ovary and small intestine.

BMP-2 is a polypeptide consisting of 114 amino acids[68]. The physiologically active growth factor is a homodimer with two antiparallel BMP-2 chains, connected via a covalent bond between cysteinyl residues at position 78. The molecular weight of this dimer is 26.018 kDa.

The isoelectric point has been calculated to 8.21[70], but differing values can be found[71-73].

Like many members of the TGF-β family, BMP-2 shows a structure called "cystine knot". In BMP-2, it is formed by disulfide bonds between Cys^{43}-Cys^{111} and Cys^{47}-Cys^{113} forming a ring structure and by the Cys^{14}-Cys^{79} bond going through this ring.

BMP-2 shows many hydrophobic areas on its surface but has no distinct hydrophobic core. In its physiological homodimer the hydrophilicity of the total structure is even more reduced as the binding of the two BMP-2 molecules shields many of the polar groups of the protein.

In solution, BMP-2 is stable for approximately one week when stored at 4 °C. The lyophilized powder is stable at room temperature for several weeks. BMP-2 is soluble at more than 1 mg/ml at pH-values below 6.0[74]. The solubility is significantly lower at pH-values closer to its isoelectric point.

1.1.8 Interstitial fluid flow

The fluid flow through bone has been traced in several studies[75-77]. It was found that the flow was from the Haversian canals to the surface of the single osteons on a micro and from the endost to the periost on a macro level.

Interstitial fluid flow has been addressed as factor in the damping properties of bone[78] as well as for the development of bone atrophy or hypertrophy[79, 80]. It is therefore another factor affecting stress induced bone remodeling.

Studies on the effects of modified flow of the interstitial fluid due to bone implants could not be found.

Interstitial fluid flow has to be considered especially with the application of locally acting drugs, e.g. growth factors. Their systemic spread may cause reduced local action or avoidable systemic adverse effects.
Dillaman et al.[81] suggested a fluid flow velocity of 0.04 to 0.2 m/s through the bone matrix. This implies that drug containing matrix systems may be considerably permeated when implanted into bone, increasing their actual release rate compared to *in vitro* test systems like the USP I or USP II apparatus. Therefore, due to their high permeability, gels and larger matrix systems may not be suitable long term controlled drug delivery devices in bone.

1.1.9 Mechanical properties

Bone tissue provides resistance primarily to compressive forces (1.5). However, it also provides high tensile and bending strengths while being very light. Some of the mechanisms behind these exceptional mechanical properties have been mentioned before, e.g. the tube like structure of long bones and the mathematical reasons behind (Equation 1, Equation 2).
As the inner structure of bone depends on usually applied loads, due to the remodeling processes (1.1.5), no universally valid values for the mechanical properties of bone can be given. For cortical areas in long bones (1.1.3.6), values ranging from 131 – 224 MPa for compressive strength and 17 – 20 GPa for the Young's modulus have been reported. Due to the orientation of the osteons and fibers in cortical bone, its mechanical strength is highly anisometric. Trabecular bone (1.1.3.7) shows isometric mechanical strength but is generally much weaker, reaching compressive forces of 5 – 10 MPa and a Young's modulus of only 50 to 100 MPa[14, 16, 17, 82, 83].

1.2 Calcium phosphates

1.2.1 General

Calcium phosphates are chemical compounds consisting of calcium (Ca), phosphorus (P) and oxygen (O). Most compounds additionally contain hydrogen (H). Phosphorus and oxygen can form different phosphate ions, named as orthophosphate (PO_4^{3-}), metaphosphate (PO_3^-), pyrophosphate ($P_2O_7^{4-}$), and polyphosphate ($(PO_3)_n^{n-}$).

Within the mentions phosphate ions, the orthophosphates have the highest biological and technical relevance. Thus, the term phosphate will be used as synonym for orthophosphate in this work.

Good reviews on calcium orthophosphates are given by Dorozhkin[4, 84]. The most important facts will also be presented here. However, for data on crystallographic properties etc. it has to be referred to the literature.

Orthophosphates are salts of orthophosphoric acid (H_3PO_4). Up to three of the hydrogen ions from the acid can be removed, resulting in dihydrogen phosphate ($H_2PO_4^-$), hydrogen phosphate (HPO_4^{2-}) and phosphate (PO_4^{3-}) ions.

The acidity of the ions decreases in the given order. pK_a values are 2.161, 7.207 and 12.325, respectively.

The solubility of the formed salts usually decreases in the same order as acidity.

In calcium phosphates, the removed hydrogen ions are replaced by calcium ions (Ca^{2+}). Based on the aforementioned general properties of phosphates, $Ca(H_2PO_4)_2$ was the most acidic and soluble, and $Ca_3(PO_4)_2$ the least acidic and soluble calcium salt. Due to some additional calcium orthophosphates with more complicated stoichiometry, the order is right but there are less soluble calcium phosphates than $Ca_3(PO_4)_2$. The most prominent is hydroxylapatite ($Ca_5(PO_4)_3(OH)$). An overview on some chemical and physical properties of the most important calcium orthophosphates is given in Table 1.

The solubility of all calcium phosphates except $Ca(H_2PO_4)_2$ is quite low. A solubility diagram for the lower soluble calcium phosphates, depending on the pH of the dissolution medium is given in Figure 1.

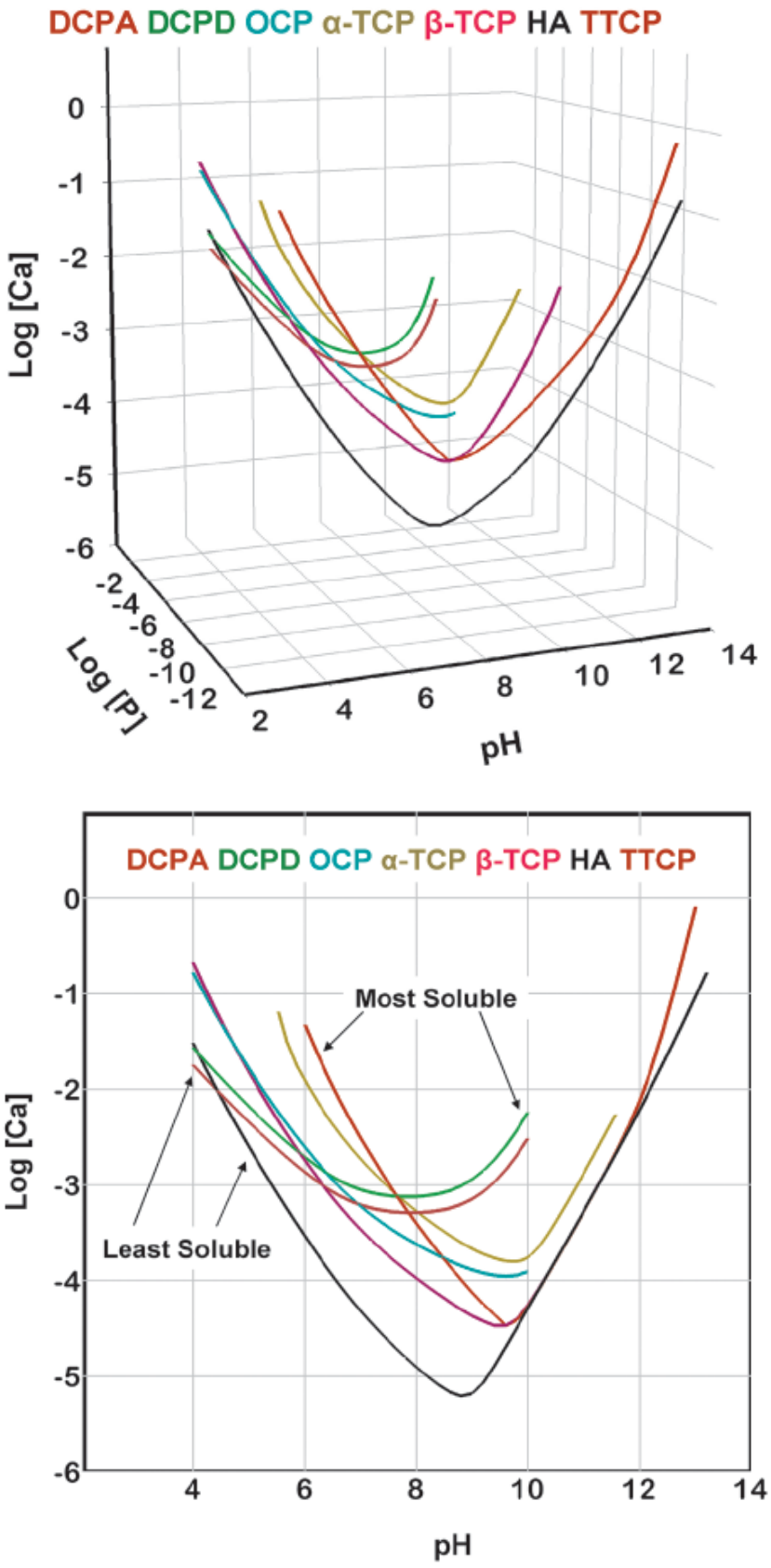

Figure 1: Solubility phase diagrams for the ternary system of $Ca(OH)_2$-H_3PO_4-H_20 at 37 °C taken from Chow[85].

Some of the different calcium phosphates can be precipitated from aqueous solutions. Others have to be prepared by solid state reactions[86].

It is obvious, that self-setting hydraulic calcium phosphate cements (1.10) can only form calcium phosphates that can be precipitated from aqueous solutions. These are calcium dihydrogen phosphate monohydrate (1.2.3), calcium hydrogen phosphate dihydrate (1.2.5), octacalcium phosphate (1.2.7), calcium deficient hydroxylapatite and hydroxylapatite (1.2.9).

The chemical nature of the precipitating calcium phosphate is predominantly determined by the pH of the calcium phosphate solution, from which precipitation occurs.

Table 1: Overview of the calcium orthophosphates. Based on Chow[87] and Dorozhkin[84], with data from other authors.

IUPAC name and common used names	Empirical formula	Ca/PO_4-ratio	pH stability range at 25 °C	Solubility in water, -log(K_{sp})		Density, g/cm^3
				at 25 °C	at 37 °C	
Calcium dihydrogen phosphate monohydrate (MCPM)	$Ca(H_2PO_4)_2 \cdot H_2O$	0.5	0.0 – 2.0	1.14[88]	Highly soluble	2.23
Calcium dihydrogen phosphate anhydrous (MCPA)	$Ca(H_2PO4)_2$	0.5	n/a	1.14[88]	Highly soluble	2.58
Calcium hydrogen phosphate dihydrate (DCPD)	$CaHPO_4 \cdot 2\ H_2O$	1.0	2.0 – 6.0	6.59[89]	6.63[90]	2.32
Calcium hydrogen phosphate anhydrous (DCPA)	$CaHPO_4$	1.0	n/a	6.90[89]	7.04[91]	2.89
Amorphous calcium phosphate	$Ca_x(PO_4)_y \cdot n\ H_2O$	1.2 – 2.2			25.7 (pH 7.4)[92]	n/a
Octacalcium phosphate (OCP)	$Ca_8H_2(PO_4)_6$	1.33	5.5 – 7.0	96.6[88]	95.9[93]	2.61
α-Tricalcium phosphate (α-TCP)	$Ca_3(PO_4)_2$	1.5	n/a	25.5[89]	25.5[94]	2.86
β-Tricalcium phosphate (β-TCP)	$Ca_3(PO_4)_2$	1.5	n/a	28.9[89]	29.5[95]	3.07
Hydroxylapatite (HA)	$Ca_5(PO_4)_3(OH)$	1.67	9.5 – 12.0	116.8[89]	58.6[96]	3.16
Tetracalcium phosphate (TTCP)	$Ca_4(PO_4)_2O$	2.0	n/a	38 – 44[89]	37.4[97]	3.05

1.2.2 Calcium dihydrogen phosphate anhydrous (MCPA)

Anhydrous calcium dihydrogen phosphate ($Ca(H_2PO_4)_2$) is a white, odorless, crystalline powder. In the English speaking literature it is also often referred to as monobasic calcium phosphate anhydrous (MCPA).
MCPA can be obtained by heating calcium dihydrogen phosphate monohydrate (1.2.3) to temperatures above 100 °C. The compound is then stable up to around 200 °C and decomposes at higher temperatures.
The density of MCPA is around 2.58 g/cm^3. Its calcium-to-phosphate ratio is 0.5, making it the calcium phosphate with the lowest calcium-to-phosphate ratio. Besides, it is quite acidic.
Anhydrous calcium dihydrogen phosphate is very hygroscopic and easily transforms into its monohydrate form (1.2.3). The reaction into the monohydrate is very fast when in contact with water; therefore, some given parameters like water solubility usually refer to the monohydrate.
Due to this hygroscopicity, its high solubility and the acidic pH formed upon dissolution, MCPA cannot be found in calcified tissue and is not biocompatible.

1.2.3 Calcium dihydrogen phosphate monohydrate (MCPM)

Calcium dihydrogen phosphate monohydrate ($Ca(H_2PO_4)_2 \cdot H_2O$), also referred to as monobasic calcium phosphate monohydrate (MCPM), is a white, odorless, crystalline powder. Just as MCPA, it is considered hygroscopic. However, hygroscopicity is much lower.
MCPM is the most stable calcium phosphate at pH-values below 2[86]. At temperatures above 100 °C, the substance loses its crystal water and transforms into MCPA (1.2.2).
Calcium dihydrogen phosphate is the most soluble calcium phosphate salt. Its water solubility is around 18 g/L at 20 °C. Solubility increases with increasing temperature.
The dissolution process of MCPM is very fast and results in the formation of a calcium phosphate solution of around pH 3 – 4.
Due to its high solubility and the acidity of the substance, MCPM cannot be found in calcified tissue. The low pH also results in poor biocompatibility. However, MCPM can be used in self-setting bone cements (1.10), since biocompatibility is not an issue during the short setting period of these cements[98-100].

1.2.4 Amorphous calcium phosphate (ACP)

Amorphous calcium phosphate has been of minor interest in the preparation of calcium phosphate bone cements, as it is not freely available and its exact stoichiometry cannot be given[84], making the preparation of cements with a predefined product stoichiometry impossible. However, it has been applied within calcium phosphate cements in some studies[101, 102].

ACP is reported to be the first product crystallizing out from supersaturated calcium phosphate solutions, being then transformed into more stable secondary products[103]. Anyway, ACP has been found in tissue calcifications *in vivo*[104], which is explained by a transformation inhibiting effect of several ions present under physiologic conditions[105].

The empirical formula for amorphous calcium phosphate is usually reported as $Ca_x(PO_4)_y \cdot n\ H_2O$. Therefore, an exact calcium-to-phosphate ratio in amorphous calcium phosphate cannot be given. The calcium-to-phosphate ratio is reported to be pH dependent[106], with higher pH-values leading to a more calcium rich ACP. Besides, an influence of the concentrations of the mixing solutions on the calcium-to-phosphate ratio is discussed[4].

Reported calcium-to-phosphate ratios vary between 1.18[84] and 2.3[107], with a mean of around 1.5 at physiological conditions[106, 108].

1.2.5 Calcium hydrogen phosphate dihydrate (DCPD)

Calcium hydrogen phosphate dihydrate ($CaHPO_4 \cdot 2\ H_2O$) is a white, odorless, crystalline substance. Other common names for the substance are dicalcium phosphate dihydrate (DCPD) or brushite. The last name honors the US mineralogist George Jarvis Brush (1831 – 1912) who first described the mineral in 1865. As the natural mineral is usually impurified with other ions, the name brushite should be avoided when talking about the pure substance, as it is chemically synthesized. Technical, cosmetical, food and pharma grades of DCPD are available. In the food industry, DCPD is commonly used as acidity regulator while it is applied as filler material in pharmaceutical oral dosage forms. In toothpastes, DCPD is used as intermediate for tooth remineralization and as gentle polishing agent.

DCPD crystallizes in a monoclinic lattice. The crystals are needlelike or prismatic to tabular and up to 2 cm long. They can also have a foliated appearance.

DCPD is sometimes considered as least soluble calcium phosphate compound at pH-values < 4.2. However, based on thermodynamical data, anhydrous calcium hydrogen phosphate (DCPA) is even more stable. There are also reports on hydroxylapatite being the least soluble calcium phosphate also at < 4.2[109]. The mentioned confusion about the least soluble calcium phosphate at low pH-values arises from the crystal formation rate of DCPD from supersaturated acidic calcium phosphate solutions, which is much faster than the one of DCPA or hydroxylapatite[110].

Partial conversion of DCPD into DCPA under certain storage conditions has been described[111]. At temperatures above 80 °C, this transformation is quite fast. The hardness of DCPD is 2.5; its density is around 2.328 g/cm^3.

Large natural deposits of DCPD/brushite can be found in guano-rich caves where it is formed by the interaction of guano with calcite and clay at a low pH. In humans, larger amounts of brushite can only be found in pathological calcifications like kidney stones, dental calculi, chondrocalcinosis or some carious lesions[104, 112-114].

DCPD is more acidic than the natural bone mineral hydroxylapatite and more soluble[90]. It is therefore less biocompatible and resorbed faster when applied as bone implant (1.12). However, biocompatibility is sufficient to be used as bone implant. Because of the higher pH in the body, DCPD implants are often reported to (partially) transform into hydroxylapatite at the implantation site[115, 116].

The mechanism (Figure 2) involves the pyrolysis of DCPD in a first step and the formation of octacalcium phosphate (1.2.7) in the presence of tricalcium phosphate (1.2.8) as a second. Octacalcium phosphate is then transferred into hydroxylapatite (1.2.9).

(A) $2\ CaHPO_4 \cdot 2\ H_2O \rightarrow Ca_2P_2O_7 + 5\ H_2O$

(B) $Ca_2P_2O_7 + 2\ Ca_3(PO_4)_2 + 6\ H_2O \rightarrow Ca_8H_2(PO_4)_6 \cdot 5\ H_2O$

(C) $2\ Ca_8H_2(PO_4)_6 \cdot 5\ H_2O \rightarrow 3\ Ca_2P_2O_7 + 2\ Ca_5(PO_4)_3OH + 11\ H_2O$

Figure 2: Mechanism of the conversion of calcium hydrogen phosphate monohydrate into hydroxylapatite. The three steps are subsequent processes taking place at pH > 4.2. (A) Conversion of calcium hydrogen phosphate into calcium pyrophosphate, (B) subsequent conversion of calcium pyrophosphate into octacalcium phosphate in the presence of calcium phosphate, (C) final conversion of octacalcium phosphate into calcium pyrophosphate and hydroxylapatite.

1.2.6 Calcium hydrogen phosphate anhydrous (DCPA)

Anhydrous calcium hydrogen phosphate ($CaHPO_4$) is often abbreviated as DCPA, standing for dibasic calcium phosphate anhydrous. The natural occurring mineral with the same chemical composition is called monetite.

DCPA is widely used, e.g. as abrasive in medical applications, as pharmaceutical excipient and in food industry to increase the calcium content or to buffer the pH.

Several preparation methods have been described[117, 118]. The most common used technical preparation method is the reaction of calcium hydroxide and orthophosphoric acid at high temperatures. If this reaction was carried out at temperatures below 100 °C, DCPD (1.2.5) would be formed.

Different to the aforementioned system MCPA / MCPM, a transformation of DCPA into DCPD under physiological conditions is very unlikely[110]. As mentioned before, DCPA is thermodynamically more stable than DCPD, therefore usually DCPD transforms into DCPA. For cements initially forming DCPD (1.12), this conversion is unwanted as it usually results a loss of mechanical strength[119, 120].

DCPA has not been found in any physiological or pathological calcifications. However, it can be used like its dihydrate form in many of its applications, including as reactant for hydroxylapatite-forming calcium phosphate cements (1.11).

1.2.7 Octacalcium phosphate (OCP)

Octacalcium phosphate (OCP) is a white, odorless, crystalline powder. It is widely regarded as intermediate in the formation of hydroxylapatite from aqueous solutions[115]. Octacalcium phosphate pentahydrate ($Ca_8H_2(PO_4)_6 \cdot 5\ H_2O$) precipitates as a precursor, which is then hydrolyzed into hydroxylapatite (Figure 2 C). This hydrolysis, which also takes place in biological systems, is believed to be a multi step process, involving crystalline structures of mixtures of a "hydrolyzed OCP" and hydroxylapatite (1.2.9). Within these structures, other ions may be entrapped, explaining for the quite high amount of foreign ions, e.g. carbonate, in biologic hydroxylapatite.

Suggesting OCP as a precursor for the formation of hydroxylapatite from aqueous solutions also solves the problem that hydroxylapatite would not form in the presence of biological fluids like serum at the observed rate, as its crystallization rate was too slow.

As OCP is less soluble than DCPD at physiological pH conditions, OCP can also form during the reported partial transformation of DCPD into hydroxylapatite *in vivo*[116].

1.2.8 Calcium phosphate / Tricalcium phosphate (TCP)

Calcium phosphate ($Ca_3(PO_4)_2$), usually called tricalcium phosphate (TCP) in the literature, is a white, odorless, crystalline substance. It cannot be precipitated from aqueous solutions. Two phases, α- and β-TCP, can be distinguished. Both are just poorly soluble in water and do not affect the pH of the formed solution.

1.2.8.1 α-Tricalcium phosphate

α-Tricalcium phosphate (α-TCP) is the high-temperature modification of calcium phosphate. It can be prepared by heating β-TCP (1.2.8.2) to temperatures above 1125 °C.

As metastable modification, α-TCP can transform into β-TCP at temperatures lower than 1125 °C. The solubility of α-TCP is slightly higher than that of the β-modification.

α-TCP has been used in some calcium phosphate bone ceramics and cements instead of β-TCP, but generally β-TCP has gained more interest[98].

1.2.8.2 β-Tricalcium phosphate (β-TCP)

The β-modification is the thermodynamically stable modification of tricalcium phosphate ($Ca_3(PO_4)_2$). It is usually abbreviated as β-TCP.
The substance cannot be precipitated from aqueous solutions but has to be prepared by solid state reactions[4, 86]. One common preparation method is the reaction of calcium hydrogen phosphate with calcium carbonate at high temperatures[121].

$$\mathbf{2\ CaHPO_4 + CaCO_3 \rightarrow Ca_3(PO_4)_2 + CO_2 + H_2O}$$

Another way applies the thermal decomposition of calcium deficient hydroxylapatite at temperatures above 800 °C[84].

$$\mathbf{Ca_2(HPO_4)(PO_4)_5(OH) \rightarrow 3\ Ca_3(PO_4)_2 + H_2O} \qquad \textbf{Equation 3}$$

Pure β-TCP cannot be found in biologic systems. However, there are reports on whitlockite being found in calcifications like dental calculus and bladder calculus[4, 113].
Whitlockite is a natural occurring calcium phosphate mineral, which is sometimes seen as third modification of $Ca_3(PO_4)_2$. However, as this mineral usually also contains other ions, it is discussed to define whitlockite as $(CaMg)_2(PO_4)_2$ or even $Ca_9(MgFe)(PO_4)$.
β-TCP has been used in calcium phosphate bone cements (1.10), but also as bone filler itself[122-124]. In some toothpastes, β-TCP is used as gentle polishing agent. In the food industry, several uses including bakery improver and anti-clumping agent have been described[4].

1.2.9 Hydroxylapatite (HA)

Hydroxylapatite (HA), also called hydroxyapatite, is a naturally occurring mineral from the family of calcium apatites. Its empirical formula is $Ca_5(PO_4)_3(OH)$, but often it is referred to as $Ca_{10}(PO_4)_6(OH)_2$ to denote that the crystal unit cell comprises two molecules[4].
In an attempt to make mineral names more logic, it was suggested in 2008 to rename the substance to apatite-(CaOH), to indicate the important elements and groups more easily[125].

The calcium-to-phosphate ratio of hydroxylapatite is only outnumbered by tetracalcium phosphate (1.2.10; Table 1). Hydroxylapatite has the lowest solubility of all calcium phosphates containing just calcium, phosphorus, oxygen and hydrogen at all pH-values > 4.2. Newer reports about HA suggest that it is also the least soluble compound at lower pH-values[109].

Hydroxylapatite has a hardness of 5 and a density of around 3.08 g/cm^3. While chemically pure HA is white, the natural minerals can also have a slight brownish to greenish appearance caused by foreign ions in the crystal lattice.

Pure hydroxylapatite can be prepared by precipitating it out of an alkaline (pH > 9) solution containing calcium and phosphate ions in the right stoichiometric ratio. The process has to be performed under exclusion of carbon dioxide at temperatures of around 100 °C as otherwise carbonated apatites may be formed[84]. Additional steps to purify the formed HA are often required as especially the first formed precipitates contain higher quantities of other calcium phosphates.

A faster way to produce high amounts of pure hydroxylapatite employs the solid-state reaction of a calcium phosphate like calcium hydrogen phosphate or OCP with calcium oxide at temperatures of around 1200 °C in a nitrogen water atmosphere.

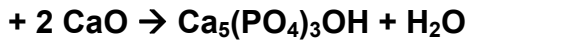

3 $CaHPO_4$ + 2 CaO → $Ca_5(PO_4)_3OH$ + H_2O

Other preparation methods have been described[84]. Besides the mentioned technically applied reactions, hydroxylapatite can be formed by some chemical reactions occurring during the setting of hydroxylapatite-forming calcium phosphate cements. These reactions will be discussed along with the cements (1.11).

Under *in vivo* conditions, hydroxylapatite is formed from its precursor OCP (Figure 2 C).

Chemically pure hydroxylapatite is not found in biological calcifications. However, the impurities are usually small enough to call the formed substances hydroxylapatite.

"Biologic" hydroxylapatite is the main constituent of the inorganic bone matrix (1.1.3.2). Around 90 % of the mass of the inorganic matrix can be attributed to this mineral or its calcium deficient form (CDHA, Equation 3). Most of the remaining 10 % are formed by carbonated apatites. In enamel and dentin, hydroxylapatite contents are even higher.

Its common appearance in bone and teeth has made hydroxylapatite a candidate of interest for all kinds bone implants (1.8) including calcium phosphate cements (1.11).

Hydroxylapatite implants usually show very good biocompatibility and good osteointegration. Therefore, hydroxylapatite has been used as coating material for metal implants to improve their integration into the physical bone structure[126-129].
Hydroxylapatite implants are resorbed by osteoclasts (1.1.4.4) in the permanent remodeling processes (1.1.5)[130]. Although this indicates a high level of biosimilarity instead of just biocompatibility, it also raised concerns about a too slow *in vivo* degradation.

1.2.10 Tetracalcium phosphate

Tetracalcium phosphate (TTCP), also called tetracalcium phosphate monoxide, has the empirical formula $Ca_4(PO_4)_2O$. The natural occurring mineral with the same chemical composition is called hilgenstockite. Like other calcium phosphates, TTCP is a white, odorless, crystalline substance.
TTCP is the most basic calcium phosphate and the one with the highest calcium-to-phosphate ratio (2:1). TTCP cannot be produced by precipitating it from aqueous calcium phosphate solutions[86]. It has to be produced via solid state reactions, e.g. between DCPA (1.2.6) and calcium carbonate at temperatures above 1300 °C in dry air or under nitrogen atmosphere[84]. The reaction can be summarized as follows:

$$\mathbf{2\ CaHPO_4 + 2\ CaCO_3 \rightarrow Ca_4(PO_4)_2O + 2\ CO_2 + H_2O}$$

The thereby prepared TTCP has to be cooled very fast to avoid its degradation into α-TCP (1.2.8.1) and HA (1.2.9) during cooling. Additionally, TTCP has to be stored at dry conditions as it is susceptible to hydrolysis. In the presence of moisture, TTCP slowly transforms it into hydroxylapatite and calcium oxide.

$$\mathbf{Ca_4(PO_4)_2O + H_2O \rightarrow 2\ Ca_5(PO_4)_3OH + 2\ CaO}$$

The mentioned required preparation and storage procedures explain the absence of TTCP in any biological calcifications. Its high pH reduces its biocompatibility, therefore it is not used as bone filler itself. However, it is the only calcium phosphate with a higher calcium-to-phosphate ratio than hydroxylapatite (1.2.9), making it very useful for the preparation of self-

setting hydroxylapatite-forming bone cements (1.11). As the compound will vanish during the setting reaction, long term biocompatibility issues are only of minor interest.

1.3 Lysozyme

Hen egg white lysozyme was used as model protein to replace BMP-2 (1.1.7.2) within this work, as it was much cheaper, highly stable and had some comparable basic physico-chemical parameters.

Lysozyme (EC 3.2.1.17) is a family of enzymes, discovered in 1909, produced by many animal organisms[131-134]. Lysozyme has hydrolytic activity, especially in catalyzing the hydrolysis of 1,4-β-linkages between *N*-acetylmuramic acid and *N*-acetyl-D-glucosamine residues in peptidoglycans as well as between *N*-acetyl-D-glucosamine residues in chitodextrins.

This catalytic activity is non-specifically targeted to bacterial cell membranes and related with the general non-specific defense of the body. Since lysozyme cannot penetrate cell walls, its antibiotic capacity is limited to Gram-positive bacteria.

The compositions of lysozyme are not consistent within all lysozyme-producing organisms, giving rise to some differences in the data found for lysozyme in the literature.

The number of amino acid residues (128 to 129) or the total molecular weight (14.3 to 14.7 kDa) vary as well as reported values on the isoelectric point, which range from 9.32[135] to 11.35[136].

In humans, lysozyme can be found in mucosal secretions like saliva and tears. However, concentrations are quite low. High concentrations of the enzyme can be found in chicken egg white in which it accounts for about 3 % of the total protein content.

Lysozyme has been widely applied as model-protein for general studies on proteins, e.g. their crystallization behavior, as well as for studies on protein encapsulation and release[137-143]. The main reasons for its popularity are its high stability and its low price. When working with lysozyme, it should always be considered that most other proteins will not show the same high stability but aggregate, oxidize or degrade in another way much faster.

1.4 Microparticles

Microparticles have been proposed as drug delivery systems, including protein drugs, for decades[144-146].

Various preparation techniques have been described[147]. The most common are several emulsion/dispersion techniques (o/w, w/o/w, s/o/w, etc.), induced phase separation/coacervation, melting techniques and spraying techniques.

The first two techniques can be performed without sophisticated equipment, making them ideal for lab-scale processes. However, the different methods produce very different stresses on the encapsulated entity, have different preferred particle size ranges and result in different microparticle morphologies.

Protein drugs are often encapsulated as solids via melting technologies or s/o/w techniques.

Van de Weert et al.[148] list the most important process parameters during microparticle preparation and their influence on protein stability in PLGA microparticles, but the results can be transferred to other polymers.

Especially the use of aqueous protein solutions and organic solvents (w/o techniques) is considered critical, as this implies the existence of an interface at which the protein can be destabilized and is therefore prone to degradation.

In addition, the organic solvent might cause a different folding of the protein due to hydrophobic interactions, not present in the physiological milieu of the protein. More hydrophilic organic solvents like ethyl acetate often induce less protein denaturation, than more hydrophobic ones like methylene chloride. However, Protein C has been shown to be more sensitive to degradation in contact with ethyl acetate[149].

Finally, the mechanical stress introduced by extensive mixing and stirring can facilitate protein denaturation and degradation[150].

Microparticles used as drug delivery systems can be made either of degradable or of non-degradable materials. Release mechanisms affecting both are diffusion through the polymer matrix and/or diffusion through pores. Additionally, degradable microparticles can release the incorporated drug by surface of bulk erosion (1.7.3.1, 1.7.3.2).

Surface eroding systems could release the incorporated drug continuously along with their degradation. The encapsulated drug was protected within the polymer until the degradation layer reached its position. Such system may thus be useful for drugs prone to undergo hydrolytic degradation.

Bulk eroding systems with a pure degradation based release mechanism would initially show no release, followed a short pronounced release phase.

The usually applied biodegradable materials, e.g. PLGA (1.7.5) or PCL (1.7.6), show bulk erosion, but usually the release of the encapsulated active is not only depending on polymer degradation processes. Diffusion of the drug through the intact polymer matrix or through created pores within the matrix are more often used as release mechanisms.

However, the polymer degrades in parallel to drug release. Therefore, depending on the release and the degradation rates, two- or three-phase release profiles are usually observed, both sharing an initial burst.

PLGA microparticles, observed for about one month often show triphasic release[151-153]. The third phase is a result of the changed diffusion properties of the degraded polymer and polymer erosion[154]. The very slow degrading PCL tends to show just biphasic release profiles.

For semicrystalline polymers like PLLA or PCL, diffusion is usually faster through amorphous parts of the polymer due to their lower density. As these parts degrade faster, the release rate from semicrystalline polymers may change already before significant bulk erosion becomes visible. The release can be reduced due to the higher crystallinity of the remaining bulk or increased due to an increased porosity of the remaining structures[155].

1.5 Testing mechanical strength

Mechanical strength is a crucial factor for bone (1.1) and bone implants (1.8). Four different types of mechanical strength, i.e. the ability to withstand a mechanical stress, should be clarified: Compressive, tensile, bending and shear strength. The main force vectors applied to the sample during the determination of each strength are depicted in Figure 3.

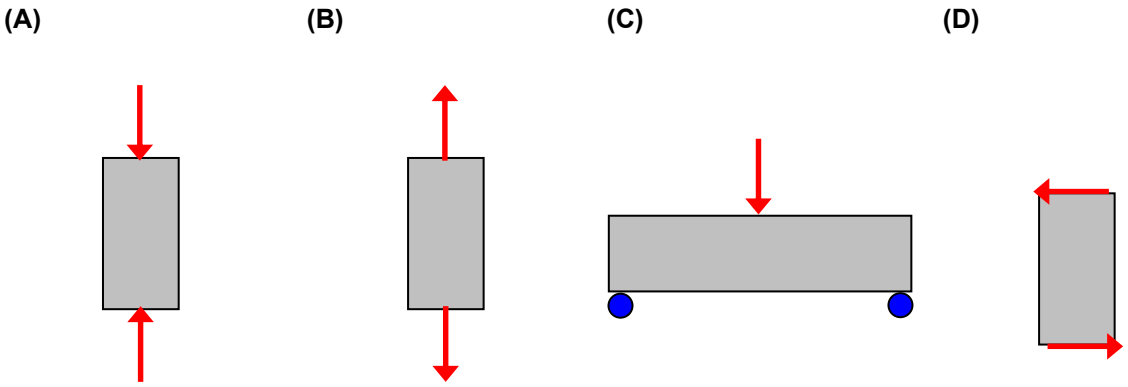

Figure 3: Vectors of the introduced forces for (A) compressive, (B) tensile, (C) bending and (D) shear stress

The most important strength for bone and any bone implant is the compressive strength, as providing compressive strength is the main objective of bone.

Other stresses are of less importance, but should be considered, too. Especially bending and shear moments are often applied to bones, predominantly to the long bones of the extremities. However, bending and shear stress are closely related to compressive and tensile stresses as the forces introduced while bending and shearing can be separated in compressive and tensile parts. For example, the upper surface of Figure 3 C just has to face compressive loads, while the lower surface has to face only tensile loads. In consequence, only compressive and tensile strengths need to be determined for an adequate characterization of the mechanical strength of a sample.

Measuring compressive and tensile strengths of a sample is not trivial. For extensive information about the effects of sample geometry etc. it should be referred to the literature[156]. Besides, for calcium phosphate cements (1.10), measurements in dry state have to be clearly separated from measurements in wet state, as the first results in much higher values.

The most common tests for determining the compressive strength of a sample are the uniaxial direct compression test and the indirect compression test ("Brazilian test")[157]. Direct compression tests have been widely performed on bone and bone implants[158-164].

Although both tests are called compression tests, especially the second does not really give values on compressive strength but on a mixture of compressive and tensile strength. As the main forces finally leading to mechanical failure of the sample are tensile loads, the values obtained by the indirect compression tests are usually named "ultimate tensile stress". However, they cannot be directly compared to values obtained from real tensile strength tests where only tensile loads are applied. Correction factors between the values obtained from the uniaxial direct compression method and the indirect method have been proposed[165].

1.6 Tissue engineering

1.6.1 General

"Tissue Engineering is the application of principles and methods of engineering and life sciences toward fundamental understanding of structure-function relationships in normal and pathological mammalian tissues and the development of biological substitutes to restore, maintain, or improve tissue function"[166].

This first definition of tissue engineering was given in 1988 in the proceedings of a NSF workshop[167]. However, the first appearance of "tissue engineering" on PUBMED is in an article by Wolter and Meyer in 1984[168]. Interestingly, the next entry "Development of hybrid compliant graft: Rapid preparative method for reconstruction of a vascular wall"[169], is dated not earlier than 1989 and includes already many of the concepts of tissue engineering still used today.

In 1993 Langer and Vacanti published an article called "Tissue engineering" in Science[170]. In their definition tissue engineering "is an interdisciplinary field that applies the principles of engineering and the life sciences toward the development of biological substitutes that restore, maintain or improve tissue function".

The most important goal of tissue engineering, which can be deducted from the definitions, is the curing of chronic diseases caused by the depletion of normal tissue functions. In an ageing society, this is of course a very promising idea as it could prolong healthy life while also cutting costs due to the now dispensable chronic treatment.

Important diseases addressed by many research groups should therefore be e.g. arthrosis, atherosclerosis, cirrhosis or diabetes. According to a study of the NSF[167] 22 % of the articles published with the keywords "tissue engineering" during the period of 1984 to 2001 covered cartilage and bone, whereas just 2 % covered hepatic and 1 % pancreatic tissue. Thus, there is an obvious discrepancy between medical need and actual research.

Bone and cartilage may have found so much attention due to several facts: Bone has unique healing abilities (1.1.1), giving rise to the idea of understanding the healing process here and then transfer it to other tissues. Cartilage on the other hand has very bad healing capacities, but there is a great need for cartilage repair. Implants for bone and cartilage predominantly require good mechanical properties, making it ideal for researchers from material sciences to get into tissue engineering, while functional tissues are much more complicated to handle for

"outsiders". Other reasons for the high number of articles dealing with bone and cartilage may be added.

Large numbers of articles about the superior mechanical properties of a new implant or the exceptional biocompatibility of a new polymer "for tissue engineering" can be found, although not every proposed system seems reasonable. This might lead to the sneaking suspicion of a misuse of the term tissue engineering to get better funding, as many of the concepts today related with "tissue engineering" have been proposed years to decades before.

The large number of research fields covered by the definition of tissue engineering can explain the sometimes quite different approaches to the solution of the same problem. While biologists naturally often tend to prefer cell-based tissue replacements, engineers tend to prefer artificial tissue substitutes. Physicians and biochemists often prefer the application of growth factors, chemists prefer polymers and material scientists prefer ceramics and cements. Cell based approaches are focusing on soft tissues, e.g. muscles or nerves or the special tissue of organs like the liver, the heart or the kidneys, while the focus for hard tissues like cartilage and bone (both with a physiologically higher amount of ECM) is on artificial implants.

With more than 18500 articles on PUBMED found by using "tissue engineering" as keyword and more than 5500 articles additionally related to bone as of June 6th, 2010, it has clearly to be pointed to the literature for more extensive information.

1.6.2 Cell based tissue engineering

Cell based tissue engineering employs living cells as material for the engineering of new tissues. Depending on the target tissue, different cell types are used, e.g. fibroblasts for skin replacement, chondrocytes for the repair of cartilage or osteoblasts for bone regeneration[(171)].

One of the main problems of experimental cell based tissue engineering was solved in 1998: The extension of telomeres[(172)]. This allowed the production of immortalized cell lines, without the use of cancerous cells[b]. However, for an implant of practical use, many problems remain. For immunologic reasons cells from the same patient (autologous cells) are desirable, but as they had to be removed from the same individual which is going to get the final implant, their number is often very limited. For some genetically caused diseases, they might

[b] Before this discovery, laboratory cultures of healthy, noncancerous mammalian cells could only divide a fixed number of times, up to the so-called Hayflick limit.

not even be available. This problem might be overcome by the use of stem cells. Within the different types of stem cells, multipotent mesenchymal stem cells (MSC) have gained great interest, as they are easily to harvest and ethically more accepted than the pluripotent embryonic stem cells (ESC)[173-176]. However, they are also very limited.

Due to the mentioned limitations in directly available cells, their number has to be multiplied *in vitro* during implant preparation. Within this step, the provision of the necessary stimuli to guarantee correct proliferation and differentiation is paramount. As the exact stimuli to guide these processes, e.g. time and concentration profiles of growth factors or influences from the extracellular matrix, are not completely understood yet, the often proposed use of stem cells is still far from clinical practice[177, 178]. In addition, differentiated cells tend to loose their function, when exposed to the wrong external conditions.

The preparation time for cell based tissue engineering constructs negatively correlates to the number of seed cells in the implant. Therefore, the use of autologous cells was more time restricted than the use of allogenic (from the same species) or even xenogenic (from another species) cells. The use of syngenic (from a genetically identical organism) cells could solve issues with immunogenicity and pathogen transduction but opens big ethical issues as it is related to cloning.

The mechanical strength of cell based tissue engineering constructs is quite low. In addition, they cannot mimic the high amount of ECM present in bone, therefore pure cell based approaches seem not very promising for bone tissue engineering.

1.6.3 Tissue engineering using artificial implants / scaffolds

Artificial tissue implants can be used to avoid the mentioned problems with cell based tissue engineering. The implants are either called implants or scaffolds, mostly depending on the author, not on their properties. However, the term scaffold is more prominent with polymer implants, while inorganic implants prefer also the term implant.

General requirements especially for polymer scaffolds, but not limited to them, have been postulated[179]. These requirements are often just put next to each other without structuring or weighing them. In the following, the most important parameters will be briefly discussed based on their importance and inherent dependency on other parameters.

While biocompatibility and degradability (often incorrectly called “biodegradability”, see 1.7.2) are usually seen as basic requirements for any tissue engineering implant, the

importance of all others seems to vary greatly depending on the intended application or the used material. However, each of them can still decide whether an implant will work or finally fail in practice.

1.6.3.1 Biocompatibility

Every scaffold implanted into the body has to be biocompatible. This is usually no issue for polymers, as long as they either do not degrade or degrade into non-toxic products. The term "non-toxic" has to be defined very broad, as degradation products like lactic acid (1.7.5) are usually considered non-toxic but may lead to unwanted side effects anyway. In fact, necrosis inside larger PLGA scaffolds used in bone tissue engineering has been reported and was attributed to the accumulation of acidic degradation products, which could not be removed from the implant site and therefore led to a pronounced pH drop[180, 181].
Besides the chemical nature of the used implant material, the physical surface structure of a polymer and the size of eventually formed or administered particles can affect biocompatibility[182]. Very small particles might be taken up by macrophages or other cells and cause adverse reactions, that could not be seen with the large bulk[183-185].

1.6.3.2 Degradability

For any implant or scaffold aiming for regenerative tissue engineering, degradation within the conditions of the body is mandatory. Only the degradation, removal and successive replacement by new formed tissue allow a real healing to a status in which the treated tissue does not show any signs of the defect anymore.
Challenges from the degradation of the implant can arise especially with mechanical properties (1.6.3.4) and, as mentioned before, with some degradation products of polymers. The two main types of (polymer) erosion will be addressed in 1.7.3.
As the degradation process has to take place in a biological system, it is very often termed "biodegradation". However, as can be seen from the definition of biodegradation (1.7.2), real biodegradation is not necessary.

1.6.3.3 Porosity

Porosity is an important parameter in the design of most tissue engineering implants. It is often seen as a key factor for allowing tissue ingrowth and therefore defect regeneration. However, the high level of interest it has acquired, especially with polymer scaffolds, is a side effect of the bulk eroding properties of the usually used polymers (1.7.3.2). Considering a purely surface eroding implant (1.7.3.1), there was no need to put major focus on porosity, as the scaffold would keep the mechanical function in the center of the defect, while new grown tissue provided the mechanical function in the periphery.

However, in bulk eroding polymers the erosion process takes place throughout the whole structure. Thus, mechanical strength lost due to the degradation, has to be compensated by new formed tissue throughout the implant. This requires cell growth and tissue formation already within the still intact implant and therefore a certain degree of porosity into the initial scaffold.

Several preparation methods for polymer scaffolds and their abilities to create pores have been described[(186)]. Interestingly, many authors just focus on total porosity of their constructs while leaving pore size, shape and interconnectivity more or less unmentioned. While the optimal pore size and shape are related to the respective tissues – and will therefore be addressed later (1.8.2) – any pore interconnectivity below 100 % has to be seen critical. Lower pore interconnectivities result in areas without cell ingrowth and thus in areas that do not provide tissue functions immediately after the degradation of the scaffold. Supposing a scaffold with a pore size of 25 µm and a pore interconnectivity of 90 %, the chance to reach the 10^{th} pore in a row (e.g. one in a depth of just 2.5 mm) is already down to 35 %.

Like degradability, porosity is closely related to the mechanical properties of the implant.

1.6.3.4 Mechanical stability

The importance of the mechanical properties of an implant varies with the mechanical stresses it has to face at its site of implantation. This includes static loads as well as dynamical stresses.

For soft tissue implants, mechanical properties are usually of much lower importance than for implants intended as temporal cartilage or bone replacement.

Mechanical properties for bulk eroding implants are much harder to control than for surface eroding ones, as the mechanical properties are affected by degradation process. With regard to static loads, the implant usually gets just weaker. With regard to dynamic stresses, bulk degradation can make the implant more flexible and less rigid due to shorter mean chain lengths. However, with semicrystalline polymers or polymer blends, the stiffness of the construct might as well increase, as the ratio between usually more rigid crystalline and usually more flexible amorphous regions within the polymer bulk can increase due to different degradation rates.

1.6.3.5 Physiological surface properties

For surface eroding (1.7.3.1) solid void fillers, surface properties may be widely disregarded, as direct cell attachment was not intended. Pure biocompatibility was enough, as no temporary integration of the implant into the tissue was desired. However, surface properties are of crucial importance for porous bulk eroding scaffolds (1.7.3.2). This becomes obvious when the term "surface properties" becomes translated into its consequences: Cell attachment, cell proliferation and cell differentiation.

Most cells in the body are directly connected to other cells and attached to an extracellular matrix (ECM). The latter one had long been seen just as void filler between the living cells, but it has become evident that it plays a great role in cell attachment, proliferation and differentiation. An ideal tissue engineering scaffold thus should mimic the physiological ECM of the target tissue.

Although pure cell attachment usually is not dependent on the ECM, it has been shown that appending small fragments of the ECM, called RGD sequences, onto the surface of a scaffold promotes cell attachment[187-189]. However, more ambitious goals, e.g. improved cell proliferation and cell differentiation, which was paramount with stem cells, will require more sophisticated ECM constructs.

While the introduction of RGD sequences is part of the surface chemistry of the scaffold, a proper reconstruction of the ECM will also have to emulate other aspects of the ECM like roughness, pore size and pore shape.

The surface pH of the scaffold in the beginning and during its degradation process is of great importance, too. Unphysiological pH-values may prevent cell attachment or even result in necrosis of already attached cells[180, 181].

External chemical stimuli, as growth factors or hormones, should be considered for a perfect ECM mimicking, too. However, they are not directly related to the properties of scaffold itself.

1.7 Polymers in tissue engineering

1.7.1 General

Much work has been done on the preparation and design of polymeric scaffolds in tissue engineering. Many well-known polymers have been applied for that, but also a large number of new polymers have been synthesized[190-197]. However, the number of approved polymers is quite short. Within the synthetic polymers, four groups/substances will be shortly discussed. More extensive information can be found in the literature.

A short overview will be given on:

- Polyacrylates and polymethacrylates (1.7.4), as they have been extensively used as "bone cements" during the last decades
- Polylactides and polyglycolides (1.7.5), as they are widely used for microparticles, implants and polymer scaffolds
- Polycaprolactone (1.7.6), as it is often used for polymer scaffolds and as it was the polymer selected for further work, due to its exceptional biocompatibility
- Polyurethanes (1.7.7), as they have gained increasing interest during the last years, due to their biocompatibility and ability to easily form sponge-like structures.

However, some terms that will be used or have already been used will have to be clarified first.

1.7.2 Biodegradation / Bioerosion

"Biodegradation" is defined as a process in which biologic systems, e.g. enzymes, are directly involved in the degradation process, i.e. in the cleaving of bonds within the polymer backbone[198, 199]. Polymers susceptible for biodegradation are very often polyesters and polyamides, as the ester or peptide bonds within their polymer chains are common substrate structures for (unspecific) esterases or proteases prevalent in nearly every living organism.

On the other hand, "bioerosion" is related to the cleavage of the polymer backbone by unspecific mechanisms, e.g., acid catalyzed hydrolysis. It does not mean that biological systems are involved in the erosion process but that the erosion takes place in biological systems. As the mentioned hydrolysis requires the presence of bonds susceptible to hydrolytic cleavage, bioerosion can be found like biodegradation with polyesters and polyamides.

The synonymic use of biodegradation and bioerosion finally arises from the fact, that any degradable polymer brought into a biologic system will usually face biodegradation as well as bioerosion. However, the proportions in which the two mechanisms are involved in the degradation of a specific polymer depend on several factors like the monomers or the chain length of the polymer. The proportion thus can change during polymer degradation, starting with virtually pure bioerosion and an then increasing amount of biodegradation as the polymer chains are getting shorter and can be better bound by cleaving enzymes.
An even more sophisticated system on the differentiation of polymer degradation behavior was suggested by Hutmacher[179]. He defined biodegradable, bioresorbable, bioerodable and bioabsorbable polymers.

1.7.3 Erosion (polymer bulk)

The term erosion is used for the loss of material from the polymer bulk[198]. This process requires the degradation of the polymer into soluble oligomers or monomers, but the focus is not on the single chain's properties but on those of the bulk, e.g. mass, outer dimension or mechanical stability. Two basic mechanisms are distinguished: Surface erosion (1.7.3.1) and bulk erosion (1.7.3.2). However, pure forms of the described erosion processes are rare.

1.7.3.1 Surface erosion

Surface erosion is characterized by a degradation and mass loss process localized merely at the polymer's surface[198].
Surface erosion is linked to the precondition that the agent needed for degradation, e.g. water, cannot penetrate the polymer bulk. Hence, only polymer chains at the surface of the bulk can be cleaved and transferred into soluble oligomers or monomers. Not until their removal, the polymer chains of the next layer can be degraded.
This mechanism explains for the usually observed very constant rate of weight loss (based on the surface area) and the continuous changes in the outer dimensions of the polymer bulk throughout the entire erosion process. The mechanical properties of the remaining polymer bulk do not change within the complete erosion process.

Surface erosion can be found with many polyorthoesters, but the regulatory state of most of these compounds is still far from being approved for medical use, leaving bulk eroding polymers the predominant option for polymers in tissue engineering.

1.7.3.2 Bulk erosion

Bulk erosion is characterized by uniformly distributed degradation throughout the polymer bulk[198]. Ideally, the probability of chain cleaving is evenly distributed within the complete bulk. As long as the polymer chains are still insoluble, they cannot leave the bulk. Every polymer showing bulk erosion therefore usually retains most of its mass over quite a long time before finally showing a fast mass loss. This loss is correlated with the loss of the now soluble shortened polymer chains that leave the bulk's structure.

Different to the mass, the mechanical properties continuously change during the erosion process. Bulk erosion requires the agent forcing chain degradation to penetrate faster into the bulk than a thought "front of degradation". In most biodegradable polymers, water is this agent as it allows hydrolytic cleavage of the polymer chains. Thus, water permeability of the bulk determines whether a polymer undergoes bulk erosion.

The degradation rate of a bulk-eroding polymer is relatively independent of its shape, as long as no additional factors are involved. As many polyesters show autocatalyzation effects during their degradation, accelerating the further degradation, different diffusion pathways for the leaving of formed acidic degradation products can change the degradation behavior. This can explain e.g. the different reported degradation times of PLGA scaffolds *in vitro* and *in vivo* as well as of samples of different sizes[200-202].

It has also been shown, that the ratio between amorphous and crystalline parts of semicrystalline polymers can change during erosion. As crystalline regions within a polymer bulk usually have lower water permeability, their degradation rate tends to be slower than that of amorphous parts. Therefore, the relative amount of crystalline regions within the bulk will increase during degradation process, affecting e.g. the rate of the further degradation and the bulk's mechanical properties[203]. The same principle has to be applied to co-polymers with larger blocks[204].

1.7.3.3 Effects of erosion type on implant design

Depending on the designed application of the implant, bulk erosion as well as surface erosion may be favorable. However, for load-bearing bone implants, surface erosion seems more suitable as it allowed the design of a more compact and therefore strong implant that would keep its strength throughout its erosion phase. With a surface-eroding bone implant, new tissue would grow into the cleared areas from the outsides and subsequently fill the whole defect. The mechanical strength of the initial implantation site would gradually be transferred from the shrinking implant to the growing bone. Ideally, erosion was not faster than tissue ingrowth as otherwise the mechanical stability of the implant site could not be guaranteed due to a forming gap between implant and tissue.
For bulk-eroding polymers, internal scaffold design is a much larger challenge as two basic requirements porosity (1.6.3.3) and mechanical strength (1.6.3.4) contradict each other.

1.7.4 Polyacrylates and polymethacrylates

Polyacrylates and -methacrylates are widely used in pharmaceutical applications e.g. as release modifying coatings for tablets or pellets (e.g. Eudragit®). Besides, they have been applied in clinical use for more than 40 years, e.g. as "bone cements" to fixate metal bone implants (e.g. Endurance®, Osteobond®, Palacos®, Simplex® P). The polymer itself is highly biocompatible[205, 206]. However, the use as "acrylic bone cement" requires the application of the monomers to the patient, as the fixation is caused by the polymerization of the "cement". The acute toxicities of the monomers (acrylic acid and methacrylic acid) are quite high[207, 208], thus short contact times and complete polymerization to eliminate any monomer remnants have to be guaranteed. Besides toxicity, the exothermic polymerization reaction is another problem. For the use, e.g. as adhesive for hip implants, temperatures of more than 70 °C at the site of polymerization and the immediately surrounding tissue have been reported[209-211]. These high temperatures can cause necrosis in surrounding tissue[208, 209, 212-214]. While this is seen negative for the fixation of implants, as it increases the size of the defect and weakens the interface, it is sometime seen positive for the filling of bone defects as it reduces the risk of a relapse after bone tumor resection.
Polyacrylates/-methacrylates are non-biodegradable. This can cause the weakening of the fixation and the successive failure of the attached implant, as remodeling of the surrounding

bone can lead to a loosening of the contact between the "cement" and bone. As biodegradability was one of the basic demands for an implant (1.6.3.2), these polymers are not suitable for regenerative tissue engineering.

1.7.5 Polylactides (PLA), polyglycolides (PGA), polylactide-co-glycolides (PLGA)

Polylactic acid (PLA) and poly-glycolic acid (PGA) as well as mixtures thereof, called poly-lactic-co-glycolic acid (PLGA) have been in clinical use since the beginning of the 1970s[215-217]. They are also used for pharmaceutical products like microparticles or small implants, acting as biodegradable drug reservoirs. PLA/PGA/PLGA offer the advantages of being clinically approved, well known and biodegradable. They showed a high biocompatibility in lots of studies. As the polymers degrade, acidic degradation products are formed. The end products of the degradation are lactic acid (pK_a 3.85) and glycolic acid (pK_a 3.83) (Figure 4), which are both non-toxic and excreted via the lungs (after incorporation in the tricarboxylic acid cycle) or the urine[218].

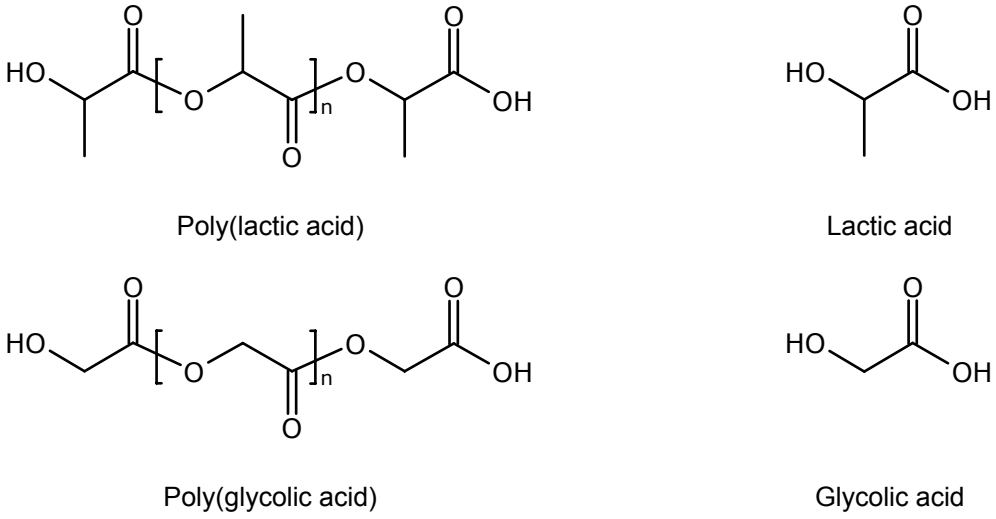

Figure 4: Poly(lactic acid), poly(glycolic acid) and their respective monomers.

The acidity of the degradation products does not play a role, as long as they are quickly removed from the implantation site. Thus, for drug releasing implants in soft tissue, acidity usually is no issue. However, there are reports on local necrosis inside larger degrading PLGA scaffolds used as bone implants caused by a local pH drop to values below 4[180, 181]. For these

large scaffolds the reported *in vivo* degradation times of PLGA were also significantly longer than expected from values derived e.g. from microparticle formulations.

The degradation rate of PLGA largely depends on its composition. While both pure polymers, i.e. pure PGA and pure PLA, show relatively slow degradation, mixtures degrade significantly faster. The highest degradation rates have been reported for 50:50 mixtures[219]. In the cited study, the degradation half-life was 5 months for PGA, 6.1 months for PLA and just around one week for PLGA 50:50. Besides, the molecular weight of the polymer chains affects the degradation rate, as smaller molecular weight chains are likely to become soluble earlier than large ones.

As the pure substances degrade slower than the blends, their biocompatibility is usually higher[220].

An autocatalyzation of polymer degradation has been reported for PLA, PGA and PLGA[200, 201]. Due to the different degradation rates, autocatalytic effects for PLA can only be seen with longer running studies. Effects of the enantiomeric composition on the degradation rate have been shown[221].

An overview on the expected degradation times for larger implants is given in Table 2.

PLA, PGA and PLGA have been successfully used for the delivery of a wide variety of drugs, including peptides and proteins[65, 139, 140]. Due to its adjustable degradation time, PLGA is usually preferred for drug delivery systems, e.g. microparticles (1.4).

Table 2: Degradation times of some biodegradable polymers.

Polymer	Degradation time
PLGA	Adjustable
PLA	12 – 16 months
PLLA	> 24 months
PGA	6 – 12 months
PCL	> 24 months

1.7.6 Polycaprolactone (PCL)

Poly(ε-caprolactone) (polycaprolactone, PCL) is a synthetic, biodegradable linear polymer often made by ring-opening polymerization from ε-caprolactone (Figure 5)[222].

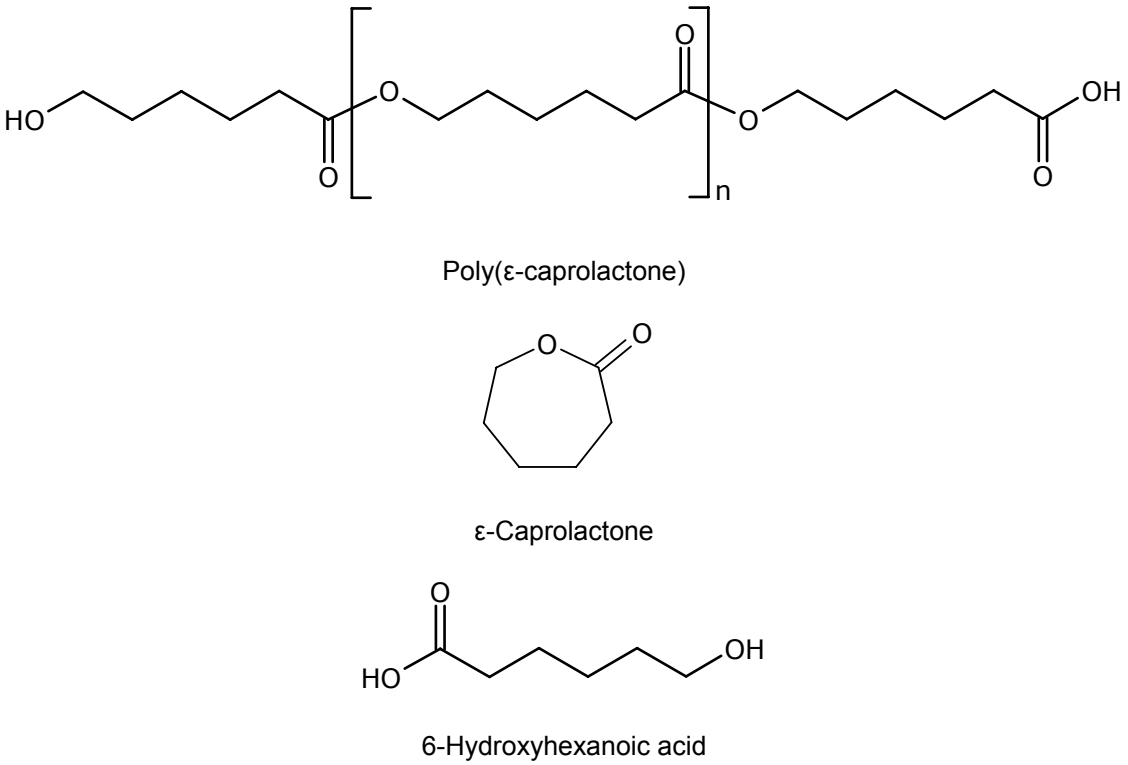

Figure 5: Poly(ε-caprolactone), its monomer ε-caprolactone and the degradation product 6-hydroxyhexanoic acid.

PCL has proved high biocompatibility in many studies[223, 224]. Even the monomer has only low toxicity. PCL undergoes a very slow bulk-degradation into 6-hydroxyhexanoic acid as end product. Compared to lactic or glycolic acid, 6-hydroxyhexanoic acid is much weaker (pK_a 4.75). This significantly reduces the risk of pH dependent side effects as the aforementioned pH-induced tissue necrosis. The weak acidity of the degradation products also explains the missing of autocatalyzation effects during degradation[204, 225].

Studies on the *in vivo* degradation of PCL have been performed by Pitt et al.[203] or Woodward et al.[226] in the 1980s. They claimed a two-stage process, consisting of a non-enzymatic hydrolytic cleavage, followed by an intracellular degradation primarily in macrophages. The second step was considered not to start before the molecular weight of the PCL chains dropped below approximately 3000 Da. The mass of the tested implants did not show any

significant mass loss, until the molecular weight of the chains had reduced to around 5000 Da. This indicated that longer chain degradation products could not leave the polymer bulk either due to limited diffusivity or to insolubility.

Chen et al.[227] found an increased degradation rate with the addition of lipase (approx. factor two). Without these degradation enhancements *in vitro* degradation times of around 12 to 24 months have been reported[228]. Often no weight loss could be found during the first 6 months. The *in vitro* degradation rate was thus comparable to PLLA[229].

The glass transition temperature (T_g) of PCL is approximately -63 °C, while the melting point (T_m) is around +60 °C, both depending on the crystallinity of the sample. Thus, the mechanical properties of polycaprolactone at body temperature are very good and combine a certain degree of flexibility, a medium compressive and a relatively high tensile strength.

Flexibility and tensile strength correlate with the mean molecular weight of the polymer chains. Higher molecular weight PCLs show better mechanical properties, especially lower brittleness and higher flexibility. Elongations before rupturing of more than 500 % could be found.

PCL has a high tendency to form crystallized structures, thus PCL is usually a semi-crystalline material. The amount of crystallinity is negatively correlated to the mean molecular weight. Higher molecular weight polycaprolactones show lower amounts of crystallinity, since the longer polymer chains cannot form highly ordered structures while hardening as easy as shorter chains.

As typical for semicrystalline polymers showing bulk erosion (1.7.3.2), amorphous areas of the polymer bulk degrade faster than crystalline ones, as water permeability is higher in these areas. In conclusion, the ratio between the amorphous and the crystalline fraction of the bulk changes during degradation, increasing the fraction of the crystalline parts[227, 230].

Despite its better biocompatibility and lower costs, PCL has been used remarkably less for drug delivery systems than e.g. PLA/PGA/PLGA (1.7.5). This may be explained by the slow degradation of PCL, which resulted in much longer residence times than required for most implantable drug delivery systems. On the other hand, before degradability was introduced as important factor with tissue engineering, other polymers, e.g. PMMA (1.7.4), had gained more attention as by then implanted structures were thought to stay in the body for the rest of the life. However, polycaprolactone has been used as FDA-approved biodegradable suture material since the 1970s[231].

Polycaprolactone is soluble in several organic solvents, including dichloromethane, trichloromethane and ethyl acetate. However, the solubility in ethyl acetate is significantly lower than in the other mentioned solvents.

Polycaprolactone has been applied in various drug delivery systems, including microparticles (1.4)[224, 232, 233]. The incorporated drugs ranged from small molecules like levobunolol[234] or papaverine[235] to large protein drugs like human growth hormone[236].

Diffusion through the polymer matrix was identified as release mechanism for smaller drug molecules[235, 237], while diffusion through pores was discussed for large molecules. Pores were usually created by blending polycaprolactone with a water soluble polymer as PEG[238].

1.7.7 Polyurethanes

Polyurethanes have been proposed as biocompatible and – depending on the used monomers – also biodegradable polymers for tissue engineering[239-241]. Polyurethanes seem very promising void fillers, as they can be injected via small needles and form a highly porous, elastic network upon polymerization. The temperature increase during polymerization is much smaller than for polyacrylates (1.7.4) and monomer toxicity can be minimized by choosing appropriate substances. However, there is a certain risk in the use of the necessary isocyanate monomers, which are thought to be able to cause allergies and even cancer.

Due to the high porosity of the formed foam structures, the release of incorporated drugs is quite fast. Hafeman et al.[239] found 75 % of their model drug PDGF released within 24 h and around 85 % within 48 h, followed by a very slow release of around 5 % during the next 25 days. If used as drug delivery systems, these polyurethane foams will therefore need additional drug delivery systems.

1.8 Bone implants

1.8.1 General

Bone implants are artificial structures implanted into bone. Metal implants like nails have been used for decades, just as e.g. artificial hip implants. These "first generation" bone implants have to face several drawbacks. One is a lack of integration into the physiological structures of the body leading to loosening of the implant and consecutive failure of the whole system. Another is often the lifetime of the artificial implants themselves. Modern hip implants should be able to stay in the patient for approximately 15 years before they need replacement. However, as the number of possible replacements is limited, the current implants still have to be seen as *ultima ratio,* i.e. their use has to start as late in the patients life as medically defensible.

Coatings of the implant surface for improved bone integration have been effectively tested since the 1970s[127-129, 242]. However, metal implants cannot be seen as acceptable implants with respect to a regenerative tissue engineering approach.

Various bone implants that are compatible with the ideas of tissue engineering have been proposed, including grafted natural bone from different sources, coral skeletons, polymer scaffolds, ceramic calcium phosphate scaffolds (1.9) and calcium phosphate cements (1.10). Overviews on these and other filler families used in bone tissue engineering can be found in the literature[243].

Today, pure polymer scaffolds showing an adequate level of porosity for tissue ingrowth are still much too weak for any load-bearing applications, limiting their use mainly to void fillers. However, they have been tested as bone implants, too[244-248]. It is not surprising that the published results in this field usually focus on cell attachment and cell compatibility rather than reporting mechanical properties.

All bone implants, independent of their material have to take care of the standard requirements for an artificial implant in tissue engineering (1.6.3.1 - 1.6.3.5).

Porosity will have to be now extended by the left out factor pore size (1.8.2), specific to bone tissue. A closer look to surface properties will also be performed (1.8.3).

Polymer scaffolds will be excluded from further observation, due to their low mechanical strength. Therefore, the rest of this work will focus on preformed bone implants, represented

by calcium phosphate ceramics (1.9) and non-preformed bone implants, represented by the self-setting calcium phosphate cements (1.10).

1.8.2 Pore size

As explained before (1.6.3.3), providing tissue ingrowth is essential especially for bulk eroding bone implants. As calcium phosphate cements (1.10) are usually more surface eroding, pore size may be of less interest with this kind of implants. However, a high level of porosity in combination with an optimal size of the pores may facilitate tissue ingrowth and therefore remodeling and healing processes (1.1.5, 1.1.6). Besides, porosity and pore size are important factors for calcium phosphate ceramics (1.9).

The determination of the optimal pore size for bone ingrowth seems complicated. Some authors, using rats as tested species, report a size of 300 – 400 µm[249, 250] as optimal. This is in good agreement with another source, where a pore size of 300 µm was found to be better than 200 µm or 500 µm[251]. Other authors, using rabbits as tested species, report optimal bone ingrowth for pore sizes of around 200 µm[252] or they report that bone ingrowth is nearly independent of the pore size[253]. However, the latter ones just tested pore sizes of 50 – 125 µm where they could not determine any significant differences. This would not mean that there could be no better bone ingrowth in larger pores.

Larger pores (260 µm) showed better bone ingrowth than pores of 150 µm diameter in a study on Göttingen minipigs[254]. A better bone ingrowth could also be observed for hydroxylapatite scaffolds with pore sizes of 300 – 600 µm, compared to those with just 50 – 250 µm pore diameter[255].

While these studies are consistent with most other reports, that indicate a better bone ingrowth for larger pores, there is also at least one report of a better ingrowth for smaller pores[256]. However, it seems more likely that the observed slower ingrowth into the implant with larger pores had to be attributed to a worse pore interconnectivity, as the authors themselves reported a higher level of interconnections between those samples with smaller pore sizes.

For human osteoblast-like MG63 cells, a better scaffold colonization was found for a pore size of 600 µm, than for a size of 200 µm[257]. Another study showed a better ingrowth of human osteosarcoma cells in channels of 421 µm than in ones of 170 µm[258].

In conclusion: If there is any optimum pore size for bone ingrowth, it is likely to be in the range of 300 – 400 µm. Depending on the used species and the exact structure of the used

scaffold, values slightly differing from this range may be obtained. This large optimum pore size was the reason for choosing microparticles of that large size for the cement-microparticle composite within this work (3.1).

1.8.3 Surface properties

It has already been mentioned that the surface properties of an implant have a distinct effect on parameters like cell adhesion and cell ingrowth (1.6.3.5).

HA-coatings improved bone adhesion and integration of metal implants significantly. For calcium phosphate based bone implants, differences in the cell attachment and osteogenicity have been reported, based on their preparation procedures. A very good biocompatibility was found for all hydroxylapatite-based implants. However, cell attachment and ingrowth was faster for cements than for sintered scaffolds. Within sintered HA-scaffolds, differences in osteointegration were observed. Scaffolds sintered at 900 °C showed a higher osteogenicity than those sintered at 1100 °C[255]. This has most likely to be explained by the different roughness of the surfaces. Calcium phosphate cements are just precipitated and therefore rough crystals, while in sintered HA-scaffolds the crystals are fused together and therefore less rough. Fusion and reduction of surface roughness are proportional to the sintering temperature[259].

1.9 Calcium phosphate ceramics

Calcium phosphate ceramics have been proposed as bone implants in the 1970s and gained much interest since[260]. Calcium phosphate ceramics are usually preformed implants, i.e. their shape has to be fixed before the last steps of their preparation. This may require either two surgical procedures (one two find the size of the defect, and one to implant the accordingly shaped scaffold) or the shaping of an off-the-shelf implant to the defect shape at the patient-site or the defect to the implant shape. All options are inconvenient and can increase cost, patient risk and healing time (if the defect was expanded).

Most calcium phosphate scaffolds are prepared by sintering chemically synthesized hydroxylapatite (1.2.9). Besides, coral skeletons can be transformed into highly porous hydroxylapatite scaffolds by relatively low temperatures – compared to the temperatures used for sintering. The thermal treatment of the coral skeletons is used to eliminate organic impurities that might cause adverse reactions upon implantation. The low preparation temperatures of these implants often result in slightly better cell attachment than for sintered implants, but porosity issues may also account here.

While the coral skeleton structures are already highly porous, porosity has to be introduced in synthetic calcium phosphate ceramics by using pore formation techniques. Besides gas foaming[260], several pore formers which burn ("pyrolyze") during the sintering process have been used to create the desired level of porosity in the final scaffold[261, 262].

The pore formation techniques allow the creation of highly porous implants with still sufficient mechanical strength. The biocompatibility is usually good and resorbability is given, too. Some authors even claim osteoinductive properties[263, 264].

Besides these advantages, preformed calcium phosphate ceramics require long preparation times, usually offer just insufficient mechanical fit to complex shaped defects and have a very high brittleness. This brittleness may become a problem in load-bearing implants as it increases the risk of fatigue cracks and consecutive failure of the implant itself and the implantation site.

Some authors have reported less osteoblast ingrowth in the preformed scaffolds than in calcium phosphate cements, despite their higher porosity.

This difference is commonly attributed to the different surface structures in cements and sintered scaffolds. While the surface in cements shares the same properties as in natural bone,

as both are derived from the precipitation of hydroxylapatite from supersaturated solutions, the surface of the sintered scaffolds is quite different.

The different surface structure is also considered to be one reason for the sometimes reported retarded resorption of sintered hydroxylapatite scaffolds[89].

Cell attachment and ingrowth could be improved by coating the ceramics with RGD-sequences. However, this was not more effective than a coating with blood serum[265].

To avoid the need for a complicated implant shaping, the use of porous ceramic calcium phosphate granules has been proposed. However, the off-the-shelf availability of this system is accompanied by a very low mechanical strength of the formed implant, making the ceramic granules pure void fillers. Marketed products are available, e.g. CONDUIT® TCP granules.

1.10 Calcium phosphate cements (CPC)

1.10.1 General

Self-setting calcium phosphate cements (CPC) are mixtures of calcium and phosphate containing powders or liquids that set in the presence of water by forming a solid microporous crystal network consisting of calcium phosphate[85, 87, 266].

The biggest advantage of calcium phosphate cements is probably their ability to fit into defects of any shape directly off-the-shelf. There is no need for time-consuming implant preparation, complicated shape adjustments of the implant or shape corrections of the defect prior to use.

This advantage can also be found with other non-preformed bone fillers. However, there are only a few and all of them have to face large drawbacks that are not present with calcium phosphate cements:

- PMMA-cements, reinforced with hydroxylapatite particles have been proposed as void fillers[267], but their in situ polymerization causes the same problems as described with PMMA before (1.7.4). Besides, the formed implants are not completely degradable.
- The formation of porous implants from injectable polymer formulations has yet been shown just for polyurethanes (1.7.7). However, the mechanical strength of these implants was just sufficient for pure bone void fillers that do not have to support any mechanical function.
- Calcium sulfate has been proposed as bone replacement material already in 1892[268]. However, it is quite soluble and therefore rapidly removed from the implantation site. Besides, a low mechanical strength compared to natural bone has limited its application in practice[269, 270]. Modifications of calcium sulfate implants by the addition of slow resorbing polymers have been suggested to reduce their drawbacks[271, 272], but could not completely solve them.

Calcium phosphate cements are named by their products. These products are, due to physico-chemical reasons, usually either hydroxylapatite (1.2.9) or calcium hydrogen phosphate dihydrate (1.2.5). Due to the very slow formation of HA under certain conditions, OCP (1.2.7) and ACP (1.2.4) have been reported as products, too[273]. However, in biological environments, OCP and ACP have to be seen as intermediate products, which will transform into HA.

Many reactants have been used to create self-hardening calcium phosphate cements[98, 101, 274]. Usually mixtures of different calcium phosphate salts, one with higher and one with lower calcium-to-phosphate ratio than the product are applied, e.g. MCPM + β-TCP or DCPD + TTCP, but many other formulations will result in the formation of a precipitated calcium phosphate crystal network, too. Compositions like $CaCO_3$ + H_3PO_4 have been suggested as well as formulations with up to four different compounds.

The selection of the reactants does not only affect the formed product, but can also control the reaction rate. As the reaction rate is partially pH-dependent, the use of H_3PO_4 as setting liquid usually results in quite fast setting[274, 275].

The setting process itself is driven by the different solubilities of different calcium and phosphate containing salts at a given condition. In principle, the setting can be described as follows:

The first step involves the dissolution of the reactants in an aqueous medium. Simultaneously, a calcium phosphate solution with a given pH is formed. The solubility of the reactants at the given pH is higher than that of another calcium phosphate – the formed product. Therefore, the formed solution will start to supersaturate with respect to the product. In the next step, the product will precipitate out of the supersaturated solution, while new calcium and phosphate ions from the reactants dissolve and reestablish the old amount of supersaturation. This process continues until all reactants have dissolved and the formed solution is not supersaturated with respect to the product anymore.

Based on these explanations, the setting of the cement can be modified by a variation in the dissolution rate of the reactants, a variation in the pH of the formed solution and a modification of the crystal formation rate of the product.

The dissolution speed can be controlled e.g. by the particle size of the reactants and by lowering the pH. The pH itself can be controlled either by external pH-adjustment or by the used reactants. Finally, the crystallization rate can be modified by the addition of so-called setting modifiers. These substances can be intended to either increase or decrease the crystal formation rate.

Attempts to change the reaction rate by adjusting the pH have to consider that at pH-values above 4.2 hydroxylapatite or its precursors will be formed, while at lower pH DCPD will be the reaction product. This pH-dependent reaction product leads to the HA-forming calcium phosphate cements (1.11) and the DCPD-forming calcium phosphate cements (1.12).

Calcium phosphate cements are crystalline and therefore very brittle structures. A reduction of the brittleness, often correlated with an increased tensile strength, was attempted by several modifications, including the addition of fibers[276], polymers like chitosan-lactate[277] or xanthan gum[278].

Some authors have claimed osteoinductive properties for their cements[279]. However, it is more likely that they just observed osteoconductive properties in combination with the normal remodeling (1.1.5) and fracture healing mechanisms (1.1.6).

All calcium phosphate cements are degraded by resorption within remodeling processes (1.1.5) or, especially DCPD-forming calcium phosphate cements, dissolved and removed by body fluids.

During degradation or due to fractures of the brittle cement, cement particles may be formed at the implantation site. Pioletti et al.[183] tested the effect of those particles of different sizes and materials on osteoblast function. They found that particles smaller than 10 µm showed negative effects on osteoblast function but could not see significant differences between the particle material.

1.10.2 Injectability

Calcium phosphate cements are intended to be applied as aqueous self-setting slurries or pastes by most authors. The application is often thought to be performed via a syringe-needle-system, allowing a "keyhole" application with decreased wound size, faster wound healing and a lower risk of complications due to infections.

This desired mode of application is not trivial for calcium phosphate cements. Although most authors claim injectability for their CPC slurries, the injectability of the cements is typically quite poor[280-282].

Many authors have investigated mechanisms of improving the injectability of calcium phosphate cements. However, neither their findings on the poor injectability nor their results on improving this parameter are surprising when considering the applied CPC slurries as highly concentrated dispersions.

For example, Ishikawa et al.[283] showed that spherical cement particles resulted in a better injectability than irregularly shaped particles. While this is easy to understand as the ability to interact with each other is much smaller with spherical particles, it is interesting that they also found a lower mechanical strength of the cements prepared with the spherical particles.

This suggests a relationship between the initial shape of the reactants and the shape of the formed particles. Based on the general mechanism of the setting reaction for calcium phosphate cements, this had to be either due to an incomplete setting reaction, leaving particles of the reactants in the final product, and/or due to reactant particles working as "seed crystals" for the new formed particles.

Khairoun et al.[284] investigated the effects of the powder-to-liquid ratio on the injectability as well as some other factors and found an increased injectability with lower powder-to-liquid ratios. This effect could be explained by the increased mean distances between the dispersed particles, a thus reduced probability of direct particle interactions and a reduced total viscosity.

Bohner et al.[282] did an extensive mathematical approach on the injectability of cement pastes. However, their model cement was non-setting, making it lack the additional problems arising from this factor and more related to conventional dispersions. Besides, their basic results could easily be predicted by common knowledge about suspensions and hydrodynamics, e.g. they found that smaller needle diameters impede injectability as well as longer needles.

1.10.3 Time

Time is a critical factor for self-setting calcium phosphate cements as the powder mixtures immediately start to react and thereby set when brought into contact with water. Several terms are used for different periods during cement preparation and setting. Unfortunately, different authors sometimes tend to use different definitions of the same term. This can make direct comparisons of given numbers hard or even impossible. In an attempt to clarify the meaning of the different "time definitions", the most important terms will be defined and explained briefly.

1.10.3.1 Dough time

The dough time is the period between the addition of the setting liquid to the CPC powder and that point of time where any further mixing of the cement had an irreversible negative impact on the formation of the crystal network forming during cement setting. As a consequence,

mixing after the dough time will result in a reduction of the mechanical strength of the set cement[285].

Dough time may be very short with fast setting calcium phosphate cements, eventually leaving an interval of just some seconds.

1.10.3.2 Cohesion time

The cohesion time is defined as the amount if time necessary to develop a sufficient cohesion within the cement after the addition of the setting liquid. Before reaching the cohesion time the cement slurry behaves like a concentrated dispersion, i.e. it would be immediately disintegrated and simply washed away from the implantation side by surrounding body fluids[284] instead of staying together as a compact implant.

Several authors have addressed on reducing the cohesion time by the addition of gelling agents like HPMC, alginate or chitosan[286-288]. However, the addition of these agents usually did not just shorten the cohesion time, as the cement particles were already entrapped in a high viscosity network, but also reduced the final mechanical strength of the modified cement, as the network formation of the cement crystals itself was hindered.

1.10.3.3 Working time

For a useful application of any CPC slurry, the cement should be already cohesive enough not to be washed away, but not already as far in its setting process that any further manipulation would cause damage to its mechanical strength providing structure. Unfortunately, cohesion time is usually longer than dough time, so practically working time can only be defined as “the time the cement paste can still be worked with”. Longer working times can easily be obtained by either starting the working time earlier or by letting it end later. While the first is often seen by starting the working time with the addition of water, ignoring the cohesion time, the latter is even more subjective, as it clearly depends on the author which hardness of the cement is seen as still sufficient to allow its application.

1.10.3.4 Setting time

In principal, the setting time should be defined as the period of time in which any chemical reaction involved in the transformations responsible for the cement setting is completed. A precise determination of this period is therefore more or less impossible. From a practical point of view, it is often more useful to define the setting time by the acquired mechanical strength of the cement. Two setting time terms have to be distinguished: Initial and final setting time.

The initial setting time is usually defined as the time used to gain a certain, predefined mechanical strength. It should be noted that this is a convention method so the application of different thresholds for the mechanical strength will lead to different values for the initial setting time.

The final setting time is an absolute value, which is usually defined as the time to build up the maximum mechanical strength of the set cement. Values for the final setting time should be (slightly) shorter but still closely correlated to the completeness of the chemical setting processes within the cement sample.

1.10.4 Porosity

While injectability and the mentioned times are especially important during preparation and application of the cement slurry, porosity, pore size and pore interconnectivity are often considered as important parameters for the set implant. Porosity was already mentioned as important parameter for implants before (1.6.3.3, 1.8.2). Considering the conclusions made there, calcium phosphate cements seem quite bad implants. All three major parameters, total porosity, pore size and pore interconnectivity, are usually far from the mentioned optima and much harder to control than with preformed implants.

While microporosity can, at least to some extend, be altered e.g. by modifications in the powder-to-liquid ratio, reducing the density of the set cement, the introduction of macropores seems to depend on the use of pore formers. The method then strongly resembles the different solvent casting/particulate leaching approaches used to create porous polymer scaffolds. As the leaching step had to happen *in vivo*, toxicity of the porogen has to be considered as well as a not too high solubility, as this could mean a leaching of the porogen before the cement had

hardened. Several materials like sucrose, mannitol or $NaHCO_3$ granules have been tested[161, 276, 289].

1.10.5 Mechanical strength

Mechanical strength is an important factor for calcium phosphate cements applied to load-bearing areas of bone. For any bone implant, the most critical parameter is the compressive strength, as it will have to resist primarily compressive forces. However, tensile and bending strengths are also of importance.

The mechanical strengths reported for calcium phosphate cements used as bone implants largely vary. This refers not only to actual differences in the strength of the cements, but also to different measurement conditions – especially dry or wet – and sample geometries (1.5).

HA-forming cements (1.11) are inherently much harder than DCDP-forming ones (1.12). A ratio between them of 2.7 in tension, 3.4 in shear and 7.0 in compression was reported by Charrière et al.[290]. They related the different ratios to the fact that compressive strengths were more related to the bulk material properties, while tensile and shear strengths were more connected to microstructural defects.

Besides, the crystal shape of DCPD (1.2.5) an HA (1.2.9) differs. DCPD forms more platelet-like crystals, while HA often precipitates in a more needle-like shape[291, 292]. This will have an effect on the entanglement of the crystals within the formed cement network and thereby on the mechanical strength of the implant.

Some exemplary values for compressive and tensile strength are given in Table 3, in which the values for the compressive strengths are maximum values, i.e. most cements fail to reach these high strengths, while the tensile strengths are in the range of the usually reported values.

Table 3: Comparison of the mechanical strength of HA-forming and DCPD-forming calcium phosphate bone cements based on Hofmann[293] and Charrière[290]

Cement type	Compressive strength, MPa	Tensile strength, MPa
HA-forming	67 - 187[c]	3.5
DCPD-forming	24 - 32[c]	1.5

The mechanical strength of the set cement sample can be influenced mainly by adjusting the density of the cement, e.g. by compression[294, 295] or the powder-to-liquid ratio[99, 296].
Effects of different particle sizes were reported[297] but it remains unclear if the different mechanical strength was not caused by a changed, incomplete setting with larger particles.
As the density of the sample is correlated with its porosity (1.10.4), it is obvious that a higher porosity will result in a lower mechanical strength. This opens the question, if one of the two parameters might be less important. For calcium phosphate cements, the importance of porosity enabling bone ingrowth can be neglected as long as the cement implant was degrading in a fashion comparable to the surface erosion of polymers (1.7.3.1). When water penetrates into the cement, it will dissolve calcium and phosphate ions. This dissolution will start at the implant surface. If this dissolution process was fast enough, the water diffusing deeper into the cement was already saturated with calcium and phosphate ions. Therefore, it could not dissolve the inner parts of the implant any more. This would result in a perfect surface eroding system. However, bulk erosion (1.7.3.2) can take place if the dissolution of the cement was slower.

1.10.6 Premixed calcium phosphate cement pastes

Some authors have focused on preparing premixed cement pastes that can be used off-the-shelf. This would avoid powder mixing and slurry compounding prior to cement application. More accurate mixing and improved injectability are claimed as additional benefits.
As any amount of water would immediately start the setting reaction, the used liquids have to be absolutely free of water. Besides, they have to be biocompatible and at least partially soluble in water, as only this allowed hardening at the site of implantation.

[c] The higher values relate to samples compressed prior or during setting.

This limits the amount of usable liquids mainly to polyethylene glycols (PEG)[99] and the hygroscopic glycerol[99, 298, 299].

Injectability is often really improved, as the higher viscosity of the external phase reduces sedimentation problems. Premixed calcium phosphate cement pastes can also prolong the working time as the cement setting is slowed down due to the retarded penetration of water into the paste.

However, premixed cement pastes have to face also some drawbacks. The setting of the cement may be extremely prolonged, as the outer parts of the implant will set quite fast after the water has reached the cement particles here, forming a dense calcium phosphate network that hinders the diffusion of the external phase out of the implant and thus also the diffusion of water into the implant. As a result these implants tend to have hardened surfaces while still being paste like in their centers[99].

1.10.7 Drug delivery from calcium phosphate cements

Set calcium phosphate cements are in principle large calcium phosphate matrices, located directly at the site of the defect. This makes them interesting as drug delivery systems especially for local acting antibiotics[300-304], anti-inflammatory/analgesic drugs[305, 306], anti-cancer drugs[307] and proteins[308-310]. A review on their use as drug delivery system was given by Ginebra et al.[311]

The application of calcium phosphate cements as delivery systems for proteins is based on the results of e.g. Tiselius et al.[312] who applied calcium phosphates as column material for the separation of proteins and other large molecules. Urist et al.[313] reported the purification of bovine bone morphogenetic protein on a hydroxylapatite-loaded column, showing good separation and the retention of bioactivity. However, the adsorption of another protein to the charged cement surface may cause protein destabilization, facilitating its degradation[314].

Although the principle concept of using hydroxylapatite as a carrier matrix for protein adsorption and release was therefore easily proved, the practical use of this observation in drug delivery is quite limited as the required retention times for chromatography and long term drug release are quite different.

Drug loading of calcium phosphate cements is usually performed by mixing the drug with the cement powder before initiated setting. This results in a good homogeneity of drug dispersion in the formed matrix, but may influence the setting process.

It has been reported, that many drugs, e.g. tetracycline[304] that could form calcium complexes, prolonged setting times. Pronounced positive on the mechanical strength of the set cement are described as well as negative[302, 315]. Both effects were usually correlated to the amount of drug available in the setting cement system.

Direct loading of the cement matrix should result in a drug release pattern according to the Higuchi equation[316], at least for the first 60 % of the total dose. A different release behavior has to be expected with very poorly soluble drugs, as here the dissolution and not the diffusion through the matrix will become rate limiting.

The influence of the matrix porosity, leading to a release pattern best described by a modified Fick's law approach has been observed, too. As expected, higher porosities resulted in faster release profiles[293].

The release of incorporated drugs is quite fast. Also low porosity cements, usually release the active within several days. Thus, pure calcium phosphate cements seem unable to provide controlled long term drug release, as it was necessary to mimic the physiological profiles of growth factors as BMP-2 in bone healing (1.1.7).

1.10.8 CPC-polymer composites

Most CPC-polymer composites described in the literature have been prepared to reduce the brittleness of the CPC, to increase its porosity and degradation or to deliver actives from the cement[46, 163, 276, 317-320]. Brittleness is usually addressed by the addition of solid fibers, while microparticles are preferred for drug delivery.

Habraken et al.[318] included up to 20 % (w/w) of PLGA microspheres with a mean particle size of 33 µm in their cement to increase the macroporosity of their composite. The addition of the microparticles had a pronounced negative effect on the mechanical strength of their samples. Compressive strength was reduced by approximately 40 % (50 → 30 MPa). With polymer degradation, the compressive strength further reduced to around 12 MPa for 10 % microparticle loading and just 4.3 MPa for 20 % loading. Besides, the pH of the release medium (PBS) dropped to pH 4.0 after 12 weeks due to PLGA degradation.

A nearly zero order release over more than 90 days from a gentamicin loaded apatitic CPC-PLGA-microparticle composite was reported by Schnieders et al.[163], while the release from the pure microparticles showed the typical triphasic release profile of PLGA microparticles and complete release within around 30 days.

In contrast to the study presented before, the prepared implants, loaded also with up to 20 % (w/w) microparticles, showed no significantly lower compressive strength than the pure CPC samples. Moreover, a significantly increased mechanical strength of the composites with microparticles prepared from higher molecular weight polymers was reported. This is interesting as it implies a significant increase of the compressive strength of the total structure by a component which itself did not show significant mechanical strength. As the microparticles were in the size range of 7 to 14 µm, they might have increased the total density of the composite instead of reducing it as in the previous study.

Ruhe et al.[321] included PLGA microparticles loaded with rhBMP-2 in a hydroxylapatite-forming calcium phosphate cement. They used a ratio of 30:70 based on the weight of the components and found a significant decrease in the mechanical properties of the set cement upon addition of the microparticles. The composites had only approximately one sixth of the strength of the pure cement. The release of rhBMp-2 from the composites was a lot slower than from the PLGA microparticles alone, reaching only about 3.1 % compared to around 18.0 % after 28 days in pH 7.4 buffer. As approximately 1.1 % of the protein was released from the composites within the first day, the following release was extremely slow. They also reported a slight influence of the pH of the release medium on the release rate. Compared to the release rates at pH 7.4, the release rates at pH 4.0 from the composite was faster, while it was slower for the pure microparticles.

1.11 Hydroxylapatite-forming calcium phosphate cements

Self-setting hydraulic hydroxylapatite-forming calcium phosphate cements as potential materials for dental applications were first described by Brown and Chow in 1985[322].
Various compositions have been described[86, 323, 324]. However, if just calcium phosphate salts should be used, hydroxylapatite-forming calcium phosphate cements have to use TTCP (1.2.10) as one of their reactants because of its high calcium-to-phosphate ratio.
From a theoretical point of view any other aforementioned calcium phosphate (1.2) can be combined with TTCP to form HA (1.2.9) as product. The resulting setting reactions can be found in the literature[86].
The setting reaction of a HA-forming CPC using TTCP and DCPD (1.2.5) as reactants can be given as:

$$Ca_4(PO_4)_2O + CaHPO_4 \cdot H_2O \rightarrow Ca_5(PO_4)_3(OH) + H_2O$$

As with all calcium phosphate cements, the reaction is driven by the supersaturation of the formed solution with respect to the product, which is hydroxylapatite under neutral to alkaline conditions.
DCPD is the preferred combination partner for TTCP, as it dissolves quite fast and does not negatively affect the pH of the formed solution. TCP (1.2.8) and OCP (1.2.7) also do not lower the pH but dissolve too slow under the pH conditions required for hydroxylapatite formation. MCPM (1.2.3) tends to change the pH and thereby form DCPD instead of HA. However, formed DCPD may react with additional TTCP to HA in a second step.
In contrast to the DCPD-forming calcium phosphate cements (1.12), the setting reaction of TTCP + DCPD is a pure crystalline transformation reaction. Water is not irreversibly bound in the formed product, but only used as dissolution and transport medium for the ions of the cement.
Pure HA-forming calcium phosphate cements often show a quite slow setting which is a result of the low crystallization rate of HA. The reported setting times for non-modified HA cements are often in the range of 30 min or longer[161, 273, 325, 326]. Therefore, several attempts to decrease the setting time of these calcium phosphate cements have been made. The proposed methods include the addition of chemicals as setting accelerators as well as the use of hydroxylapatite seed crystals[308, 327-330].

The stability of hydroxylapatite cements *in vitro* has been addressed, e.g. by Breding et al.[331] who studied the "resorption" of the cements at pH 3, 5 and 7. They reported the cement to be the most stable at pH 7, while more "resorption" could be seen at the lower, not physiologic pH-values. This is in perfect agreement with the pH-dependent solubility of HA.

The degradation of hydroxylapatite cements *in vivo* has been addressed by several authors[332-334]. The degradation of the compact cement implant is sometimes seen as too slow; therefore, methods to increase the resorption have been suggested[317].

HA-forming calcium phosphate cements are marketed from different companies under names as Biobon®, Callos® or Norian® SRS.

1.12 DCPD-forming calcium phosphate cements

DCPD-forming calcium phosphate cements are the second most important subtype of calcium phosphate cements. One of the first articles dealing with DCPD-forming cements is dated from 1988[335].

The general principle of the setting of DCPD-forming calcium phosphate cements is the same as for all calcium phosphate cements. However, there are some important differences during their setting and in their properties after setting compared to the previously described HA-forming calcium phosphate cements (1.11).

The first difference compared to HA-forming cements is the pH of the surrounding medium. In contrast to HA-forming cements, which set at neutral to alkaline pH, the pH has to be acidic (< 4.2) with DCDP-forming cements since DCPD (1.2.5) had a higher solubility than HA at higher pH.

DCPD-forming cements are usually prepared from mixtures of MCPM (1.2.3) and β-TCP (1.2.8.2)[99, 100, 294, 336-338]. This has the advantage of having a sufficiently acidic component in the formulation, which will keep the pH of the formed calcium phosphate solution in the desired range during most of the setting period[339].

Even after setting, the pH inside DCPD-forming cements may stay lower than physiological. However, biocompatibility has been shown in several studies[336, 340].

The setting reaction of a DCPD-forming calcium phosphate cement using MCPM and β-TCP as reactants can be given as:

$$\beta\text{-}Ca_3(PO_4)_2 + Ca(H_2PO_4)_2 \cdot H_2O + 7\ H_2O \rightarrow 4\ CaHPO_4 \cdot 2\ H_2O$$

It should be noted that, different to the standard composition of HA-forming cements presented before (1.11), water is now irreversibly bound in the reaction.

Just as with the HA-forming cements, many other compositions of reactants can also be used, e.g. H_3PO_4 as acidic component. However, H_3PO_4 is much more acidic than MCPM. This accelerates the dissolution of the reactants and the total setting rate. Besides, it can cause local adverse reactions.

An acceleration of the cement setting is usually not wanted with DCPD-forming cements, as already DCPD-forming calcium phosphate prepared from MCPM and β-TCP exhibit very fast

setting rates. Working/setting times of down to 30 s have been reported[335], however the usual range is 1 – 3 min.

The main reason for the fast setting of DCPD-forming calcium phosphate cements is the high crystallization rate DCPD; besides, the solubility and dissolution rate of the reactants is higher than with HA-forming cements, due to the lower pH of the formed solution.

Based on solubility products, the formation of anhydrous calcium hydrogen phosphate (DCPA, 1.2.6) was expected instead of the dihydrate form. However, DCPD crystals form much faster than DCPA crystals. In consequence, the thermodynamically less stable DCPD is the only formed product upon setting. However, cements produced at higher temperatures (> 55 °C) also revealed fractions of DCPA[341], which were attributed to the direct formation of DCPA not a transformation of formed DCPD into DCPDA.

This conversion of DCPD into DCPA has been observed during storage[120, 335, 342]. The (partial) conversion was usually accompanied by a loss in mechanical strength.

Due to the general chemistry of calcium phosphates (1.2), the possible transformations of DCPD are not limited to DCPA. As DCPD is not the least soluble calcium phosphate at physiologic pH, a conversion into HA was expected and observed[116, 159].

The problem of too short setting times has been addressed by the addition of chemical setting modifiers and by changing the particle size of the reactants.

As MCPM is very soluble at the pH-values present during the setting, it is easier to modify the dissolution rate of the less soluble β-TCP. Increasing the particle size of β-TCP has shown to slow down the setting reaction[343]. However, an increase of the particle size of β-TCP can also result in reduced total reaction, leaving unreacted β-TCP particles within the cement. Reduced total reaction was also reported for strongly (100 MPa) compressed cements[294].

Various setting modifiers have been used to retard the setting of DCPD-forming calcium phosphate cements. The long list of successfully tested substances include pyrophosphates[338, 344], citrate ions[345], sulfate ions[100, 345], glycolic acid[346] and magnesium stearate[347]. Also relatively strange potential retardants like chondroitin 4-sulfate and silica gel polymers have been tested, however their effects were negligible[348].

Marketed DCPD-forming cements include products like Eurobone®, chronOs® or VitalOs®.

1.13 Objectives

The objectives of this work were the characterization of a DCPD-forming calcium phosphate and its use in a cement-microparticle composite system intended for controlled long term release of protein drugs.

Particular goals were the characterization of the mechanical properties of the pure cement and the composites, characterization and modification of the reaction rate, and the evaluation of the cement's ability to be stored as premixed powder. Besides, the release behavior of the proposed cement-protein drug microparticle composite system was evaluated under several mechanical stress conditions.

2 Materials and methods

2.1 Materials

Poly(ε-caprolactone) (PCL; M_n approx. 80 kDa), lysozyme, micrococcus lysodeikticus, calcium dihydrogen phosphate monohydrate (monobasic calcium phosphate monohydrate, MCPM), β-calcium phosphate (β-tricalcium phosphate, β-TCP) (Sigma-Aldrich Chemie GmbH, Steinheim, Germany); dichloromethane, sodium citrate (Carl Roth GmbH & Co. KG, Karlsruhe, Germany); polyvinyl alcohol (PVA; Mowiol 4-88, Kuraray Europe GmbH, Frankfurt, Germany); Coomassie Plus (Bradford) Protein Assay (Thermo Fisher Scientific, Waltham, MA, USA); calcium hydrogen phosphate dihydrate (DCPD), sodium azide (Merck KGaA, Darmstadt, Germany).

2.2 Methods

2.2.1 DCPD-forming calcium phosphate cements containing polycaprolactone microparticles for controlled protein drug delivery: Release behavior and mechanical properties

2.2.1.1 Microparticle preparation

Polycaprolactone microparticles were prepared by a w/o/w double emulsion solvent evaporation technique. Briefly, approximately 20 or 40 mg of lysozyme was dissolved in 1 ml deionized water. This aqueous solution was emulsified into a solution of 800 – 1600 mg PCL dissolved in 10 ml dichloromethane by intensive stirring for about 1 min on a magnetic stirrer (RCT basic, IKA Labortechnik GmbH & Co. KG, Staufen, Germany). This w/o-emulsion was emulsified into 1500 ml of an aqueous PVA solution (0.25 % w/w) with a propeller stirrer at 250 rpm and stirred for 65 min to allow the organic solvent to evaporate. The hardened microparticles were filtered off, washed with deionized water and dried in a desiccator.

2.2.1.2 Lysozyme activity (Micrococcus lysodeikticus assay)

The activity of the encapsulated lysozyme was checked by a *Micrococcus lysodeikticus* assay[349-351]. Briefly, a bacteria suspension was prepared and tempered to 25 °C. 3000 µl of the suspension were added to 100 µl of the lysozyme solution to be tested in a quartz cuvette standing in the light path of an UV-Vis spectrophotometer (HP 8453, Hewlett Packard Company, Palo Alto, CA, USA; thermostat 89090A, Agilent Technologies Inc., Santa Clara, CA, USA). The changes in light absorption during the following 120 s were recorded using the kinetics mode of the software (UV-Vis ChemStation, rev. A.06.03 [48], Hewlett Packard Company, Palo Alto, CA, USA). Acquired data were analyzed with Microsoft Excel (version 11, Microsoft Corporation, Redmond, WA, USA). Relative lysozyme activity was calculated by comparing the slope of the samples absorption curve to those of reference solutions.

2.2.1.3 Encapsulation efficiency

The encapsulation efficiency in percent was calculated as actual protein content / theoretical protein content · 100.

Approximately 20 mg microparticles (n = 3), accurately weighed (AT 261 Delta Range, Mettler Toledo GmbH, Greifensee, Switzerland), were placed into 1.5 ml microcentrifuge tubes (Standard Reaktionsgefäß 3810X, Eppendorf AG, Hamburg, Germany) and dissolved in 1 ml dichloromethane by vortexing for 1 min (Omnilab Reax 2000, Omnilab-Laborzentrum GmbH & Co. KG, Bremen, Germany). After centrifugation at 14500 g for 5 min at room temperature (Biofuge 13 Haemo, Heraeus Instruments GmbH, Osterode, Germany), the supernatant was carefully removed (Research 100 – 1000 µl micropipette, Eppendorf AG, Hamburg, Germany) without destroying the formed protein pellet sediment. This procedure was repeated twice. After the last removal of the supernatant, the remaining dichloromethane was evaporated under vacuum (VT5042EKP, Heraeus GmbH, Hanau, Germany) at room temperature. The protein pellet was dissolved in deionized water, transferred into a volumetric flask and filled up to 25.0 ml volume. Three samples (500 µl each) were drawn from each flask and analyzed for protein concentration using the Coomassie assay[352] in a modified version as described by the manufacturer. Briefly, the samples were mixed with 500 µl reagent solution, stored at room temperature for 10 min and measured spectrophotometrically at 595 nm (UV-2101 PC, Shimadzu Corporation, Kyoto, Japan running UV-2102/3102 PC

software, Version 3.0). The readings were transferred into protein concentrations by comparison with standard curves prepared from the same Coomassie batch as used for the sample measurements.

2.2.1.4 Preparation of cement-based delivery systems

Pure cement tablets, cement-microparticle tablets and cement-microparticle implants were prepared to study the protein release and possible effects of compression force on the drug release.

The DCPD-forming calcium phosphate cement (CPC) was prepared by mixing equimolar amounts of MCPM and β-TCP. MCPM was ground in a mortar to a mean particle size of around 80 µm, while β-TCP (mean particle size approx. 2 µm) was used as received. Particle size data were obtained by dry powder laser diffractometry (Helos BF, Sympatec GmbH, Clausthal, Germany).

For the pure cement samples, 12.0 g CPC were mixed with 20 mg lysozyme and compressed into tablets (300 mg, 9 mm in diameter, approx. 3 mm in height) with a single punch tablet press (EK0, Korsch AG, Berlin, Germany). Tablet hardness was adjusted to approx. 8 N to enable their save handling.

The cement-microparticle composites were prepared by first blending the microparticles with the CPC powder. Cement-microparticle tablets were then prepared as described above. CPC tablets were not set prior to release testing.

Cement-microparticle implants were prepared by filling the blend into cylindrical molds and compressing within the molds with a texture-analyzer (TA.XTplus, Stable Micro Systems, Godalming, United Kingdom; compression speed 0.16 mm/s) to predefined compression forces (10, 20, 40, 80, 160 N). Force limits were guaranteed by software (Texture Exponent 32, version 4.0.8, Stable Micro Systems Ltd., Godalming, United Kingdom). The implants were set inside the mold by immersing them in small amounts of deionized water (approx. 1 to 2 ml per sample). The hardened rod-like samples (length approx. 10 mm, diameter 5 mm) were removed, dried in a desiccator and used for the release tests.

2.2.1.5 Protein release

The samples were placed in closed glass vessels containing 30 ml water (0.1 % w/v NaN_3 added as preservative) as release medium and shaken at 37 °C, 100 rpm in a horizontal shaker (Innova 4230, New Brunswick Scientific, Edison, NJ, USA). 500 µl samples were drawn at predetermined time points and analyzed spectrophotometrically after staining with Coomassie blue as described above. The removed volumes were immediately replaced with fresh release medium. Each value was taken at least in triplicate (n = 3 – 10).

2.2.1.6 Scanning-electron microscopy (SEM) imaging

SEM images were taken on a Hitachi S-520 (Hitachi High-Technologies Europe GmbH, Krefeld, Germany) using 20 kV acceleration voltage and a secondary electron detector. Samples used for imaging were gold coated, while energy dispersive x-ray (EDX) analysis was performed on carbon sputtered samples, using an IDFix system (SAMx, Saint Laurent Du Var, France). Additional images were taken on a Hitachi TM-1000 SEM equipped with a BSE detector.

2.2.1.7 Mechanical testing

In an indirect compression test[157], the force is applied like in a compression test, but the normal failure occurs orthogonal to the introduced force and therefore in the direction of tensile stresses on the sample. The ultimate tensile strength of a sample calculates as:

$$\sigma_{uts} = \frac{2 \cdot F}{A}$$ **Equation 4**

Where σ_{uts} is the ultimate tensile strength in Pascal (Pa), F is the applied force in Newton (N) and A is the area in m^2. If the area is calculated in mm^2, the ultimate tensile strength is obtained directly in MPa.
The tensile strength of the cylindrical samples was calculated as:

$$\sigma_{uts} = \frac{2 \cdot F}{\pi \cdot d \cdot h}$$ **Equation 5**

The samples were placed on the base of the texture analyzer and compressed with a circular plunger of 4 mm diameter with a plunger speed of 0.07 mm/s. The forces needed to rupture the samples were recorded and exported to Microsoft Excel for further evaluation.
Each measurement was performed at least in triplicate (n = 3 – 5).

2.2.2 Effect of temperature and citrate-addition on the setting time of a DCPD-forming calcium phosphate cement and on the mechanical properties of DCPD

2.2.2.1 Cement preparation

Prior to use, MCPM was ground in a mortar to a mean particle size of around 80 µm, measured by dry powder laser diffractometry (Helos BF, Sympatec GmbH, Clausthal, Germany). The same method revealed a mean particle size of the purchased β-TCP powder of around 2 µm.
Both powders were thoroughly mixed in equimolar ratio to form a premixed calcium phosphate cement (CPC). The powder was kept in closed container until sample preparation and DSC measurements. No used cement powder was older than 36 h before initiating the setting reaction by adding either deionized water or aqueous sodium citrate solution (62.5, 125, 250, 500, 750 and 1000 mmol/l, respectively).

2.2.2.2 Isothermal DSC measurements

Kinetics of the setting reaction was observed via isothermal differential scanning calorimetry (iDSC) at temperatures within 4 °C to 40 °C for the unmodified cement and at 30 °C for the cements using sodium citrate solutions as setting liquid.
25 – 40 mg CPC, accurately weighed (Mettler M3, Mettler Toledo GmbH, Gießen, Germany) into 40 µl aluminum crucibles were placed in a DSC apparatus (DSC 821e, Mettler Toledo GmbH, Gießen, Germany) and calibrated to the desired temperature in the closed sample

chamber. The chamber was opened for approximately 5 – 10 s to initiate the setting reaction by adding 20 µl setting liquid. The sample chamber was closed again immediately and the energy required to keep the sample at the preset temperature was recorded over 20 min. Obtained data were used as measure for the heat flux from the sample due to the exothermic setting reaction.

Machine control and basic thermogram evaluation was performed using Star^{e} Software (version 8.10, Mettler Toledo GmbH, Gießen, Germany). Further thermogram evaluation was performed via Microsoft Excel 2003 (Microsoft Corporation, Redmond, WA, USA).

Raw thermograms (Figure 18) were normalized based on their weight and time of liquid addition (Figure 6). For some curves (250, 500, 750 and 1000 mmol/l citrate solutions), no clear exothermic peak maximum could be identified due to a continuously increasing baseline. The peak maxima of these curves had to be distinguished from the minimum change in the slope of the curve. No maximum could be identified for the 1000 mmol/l sodium citrate solution within the observed period of 20 min as the minimum slope was found at the last recorded value.

Values for each concentration and temperature were taken at least in duplicate (n = 2 – 3).

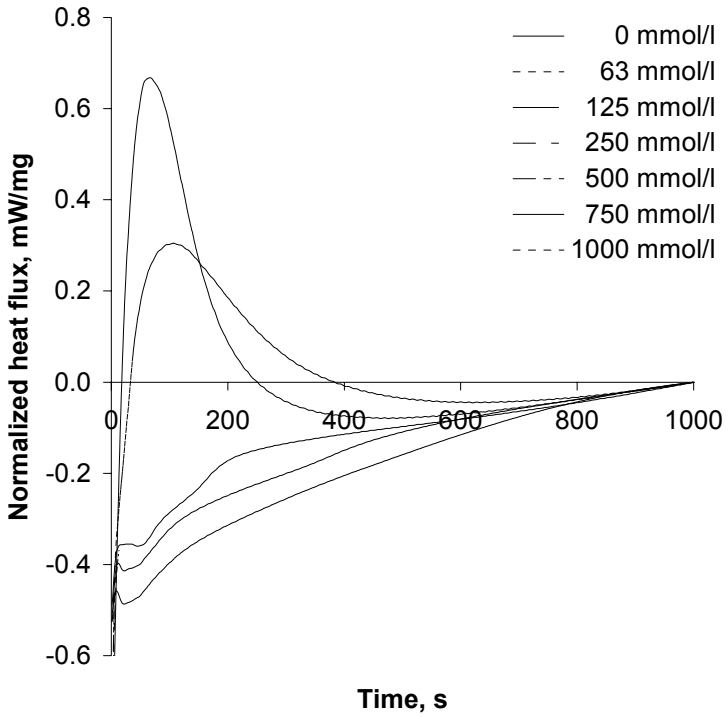

Figure 6: Normalized heat flux curves generated via isothermal DSC at 30 °C for the setting of a CPC with different citrate concentrations in the setting medium. Curves are starting at the maximum initial deflection of the heat flux curves.

2.2.2.3 Mechanical tests on isothermal DSC samples

Mechanical testing on hardened cement samples obtained from the iDSC measurements (iDSC samples) was performed using a modified needle test. A needle of approximately 0.8 mm diameter was attached to an aluminum block mounted to the arm of a texture analyzer (TA.XT plus, Stable Micro Systems Ltd., Godalming, United Kingdom). The machine was equipped with a 5 kg load cell. Samples were used as obtained by the described iDSC procedure after storing them for approximately 24 h at room conditions to achieve an equal amount of humidity in all samples.

The cement-filled DSC pans were placed on the base of the texture analyzer with the needle adjusted 2 mm above the base. During the measurement, the needle was moved down 1.5 mm, preventing any contact of the needle with the bottom of the DSC pan. Five measurements were performed at different points of each sample. Machine control and recording of the forces needed to penetrate the cement was done using the Exponent 32

software (Version 4.0.6, Stable Micro Systems Ltd., Godalming, United Kingdom). Further evaluation was performed with Microsoft Excel.
The quite small insertion depth of the needle due to the spatial limitations of the DSC pans reduced the effective diameter of the needle to just about 0.5 mm, as the broader parts of the needle did not get in contact with the cement.
Values were taken from five different locations in each sample. At least two samples were used per concentration and temperature.

2.2.2.4 Cement compression and tests on ultimate tensile strength

Cement rods of 10 mm height and 5 mm diameter were prepared for tests on the ultimate tensile strength of the cement. The premixed cement powder was filled into cylindrical molds and compressed with a texture-analyzer (compression speed 0.16 mm/s) to predefined compression forces (10, 25, 79, 250 and 500 N). The samples were then immersed in the setting liquid, which was either pure deionized water or a sodium citrate solution. The samples were allowed to set for 24 h before drying in a desiccator and mechanical testing after at least 48 h of drying.
Mechanical testing was performed as indirect compression test[157], measuring the ultimate tensile strength of the sample which is for cement samples usually much lower than their compressive strengths but allows easier sample preparation and more robust results. The samples were put on the base of the texture analyzer and compressed with a circular plunger moving onto the sample with a speed of 0.07 mm/s. The forces needed to break the samples were recorded and exported for further evaluation.

2.2.2.5 X-ray diffractometry (XRD)

X-ray diffractometry was performed using a powder x-ray diffractometer (PW2273/20 copper anode, PANalytical B.V., Almelo, The Netherlands; PW 1830 x-ray generator, PW 1710 diffraction control unit and PW 1820 vertical goniometer, Philips Industrial and Electro-acoustic Systems Division, Almelo, The Netherlands). Machine control and data collection was performed externally (ADM version 3.5, A. Wassermann Röntgenanalytik-Meßsysteme-Software, Kempten, Germany). The collected raw data were transformed into CSV files using a self-written program and evaluated using Microsoft Excel 2003.

Samples of set cement were ground in a mortar, put on a sample holder and mounted into the diffractometer. Spectra were collected at angles from 4° to 40° using a step size of 0.02° and a collection time of one second per data point.

2.2.3 Time-resolved powder x-ray diffractometry of the setting reaction of a DCPD-forming calcium phosphate cement

2.2.3.1 Cement preparation

MCPM was ground in a mortar to a mean particle size of approximately 80 µm prior to use. This powder was mixed with an equimolar amount of β-TCP (mean particle size approx. 2 µm). Particle sizes were obtained by dry powder laser diffractometry (Helos BF, Sympatec GmbH, Clausthal, Germany). The premixed powder was stored under dry conditions in a desiccator and used on the same day.

2.2.3.2 Time-resolved PXRD measurements

Time-resolved powder x-ray diffractometry was performed with the following equipment: PW2273/20 copper anode (PANalytical B.V., Almelo, The Netherlands), PW 1830 x-ray generator, PW 1710 diffraction control unit and PW 1820 vertical goniometer (Philips Industrial and Electro-acoustic Systems Division, Almelo, The Netherlands). Acceleration voltage was 40 kV and the current 25 mA.
External machine control and data collection was performed by a connected personal computer running the ADM software (version 3.5, A. Wassermann Röntgenanalytik-Meßsysteme-Software, Kempten, Germany). The collected raw data were transformed into the CSV file format using a self-written program. These data files were analyzed with Microsoft Excel 2003 (Microsoft Corporation, Redmond, WA, USA) or OriginPro 7.5 (OriginLab Corporation, Northampton, MA, USA) depending on the intended visualization.
Samples consisted of approximately 1 g either freshly mixed cement powder or the pure substances as controls.
Full x-ray diffraction spectra were collected at angles from 4° to 40° using a step size of 0.02° and a collection time of one second per data point. X-ray spectra for the kinetic measurements

were obtained by scanning the range of 27.5° to 30.5° at a step size of 0.05° and a collection time of 0.5 s per data point.
The setting reaction was started by manually adding 0.5 ml of either water or sodium citrate solutions of concentrations of 62.5, 125, 250, 500, 750 and 1000 mmol/l after the collection of the first spectrum, approximately 10 s before the collection of the second. Ten scans could be automatically taken within one series. After that, a new series was initiated manually, causing a delay of < 10 s between each series of 10 scans.

2.2.3.3 Isothermal DSC measurements

The kinetics of the setting reaction was observed via isothermal differential scanning calorimetry (iDSC) at 30 °C. The slightly elevated temperature was chosen as a supposed mean value for the effective temperature of the XRD samples which where run at room temperature and allowed to heat up during the setting reaction, autocatalyzing the reaction.
25 – 40 mg of freshly mixed calcium phosphate cement powder were accurately weighed into 40 µl aluminum crucibles using a Mettler M3 precision balance (Mettler Toledo GmbH, Gießen, Germany). The pans were placed in a DSC apparatus (DSC 821e, Mettler Toledo GmbH, Gießen, Germany) running Star^e Software (version 8.10, Mettler Toledo GmbH, Gießen, Germany) for machine control and basic thermogram evaluation. Further thermogram evaluation on the exported data was performed via Microsoft Excel.
The samples were tempered for 2 min to the desired temperature in the closed sample chamber, which was then opened for approximately 5 – 10 s to initiate the setting reaction by adding 20 µl of deionized water or aqueous sodium citrate solution (62.5 – 1000 mmol/l) with a micropipette (Research 10 – 100 µl, Eppendorf AG, Hamburg, Germany). The sample chamber was immediately reclosed and the energy required to keep the sample at the preset temperature was recorded. This energy was used as measure for the heat flux from the sample due to the exothermic setting reaction.

2.2.3.4 ATR-FTIR measurements

Cement samples consisting of equimolar amounts of MCPM and β-TCP were mixed with either pure water or the sodium citrate solutions. The cement slurries were immediately placed on the diamond ATR crystal (Pike MIRacle, Pike Technologies, Madison, WI, USA)

of an FT-IR spectrometer (Varian Excalibur 3100 FT-IR Varian Inc., Palo Alto, CA, USA). Scans were taken every 2 min over 30 min using the Resolutions Pro Software (Version 4.0, Varian Inc., Palo Alto, CA, USA). Data were exported to Microsoft Excel for further evaluation.

2.2.4 Storage stability of a DCPD-forming calcium phosphate cement for bone tissue engineering monitored by iDSC, DVS, FTIR, XRD and mechanical testing

2.2.4.1 Preparation of cement powder and tablet samples

A DCPD-forming calcium phosphate cement was prepared by mixing equimolar amounts of MCPM and β-TCP. MCPM was ground with a mortar and pestle to a mean particle size of approx. 80 µm. β-TCP was used as received (mean particle size approx. 2 µm). The particle size data were obtained by dry powder laser diffractometry (Helos BF, Sympatec GmbH, Clausthal, Germany).

The cement powder was stored in closed containers (room temperature and -70 °C, no desiccant) and in open containers (room temperature) over a desiccant, saturated $MgCl_2$ solution (approx. 33 % RH), saturated NaCl solution (approx. 75 % RH) and deionized water (approx. 100 % RH).

Cement tablets (containing 0.5 % w/w magnesium stearate as lubricant, diameter 9 mm, height 3 mm, weight 300 mg, hardness 8 N) were compressed on a single punch tablet press (EK0, Korsch AG, Berlin, Germany) and stored in open containers as described above.

2.2.4.2 Isothermal DSC measurements (iDSC)

The stored premixed calcium phosphate cement powder (25 – 40 mg) was accurately weighed (Mettler M3, Mettler Toledo GmbH, Gießen, Germany) into 40 µl aluminum crucibles. The pans were placed in a DSC apparatus (DSC 821e, Mettler Toledo GmbH, Gießen, Germany) and equilibrated to the desired temperature (30 °C) in the closed sample chamber. The setting of the cement was initiated by opening the chamber for approximately 5 to 10 s and adding 20 µl deionized water. The sample chamber was immediately reclosed. The energy required to keep the sample at the preset temperature was recorded to determine the heat flux from the

sample due to the exothermic setting reaction (Star^e Software, version 8.10, Mettler Toledo GmbH, Gießen, Germany).
All samples for the zero day values were measured within 3 h after cement preparation. Values from the stored samples were recorded up to day 46 after cement preparation ($n \geq 3$).

2.2.4.3 Mechanical testing

Mechanical tests on the set cement samples were performed with a texture analyzer (TA.XTplus, Stable Micro Systems Ltd., Godalming, United Kingdom). A cylindrical plunger attached to a 50 kg load cell was used for indirect tensile strength tests[157] on the tablet samples, while a modified needle intrusion test using a 5 kg load cell was used for the samples obtained by the iDSC measurements or from cement slurries.
Values of the needle test will are given in Newton. For the indirect tensile strength measurement, the applied forces were converted into MPa to indicate their nature as pressure/tension. Tablet samples were tested either with or without induced setting. Samples with induced setting were immersed in approx. 1 – 2 ml deionized water for 24 h to allow the setting and then dried in a desiccator for at least 24 h prior to testing. Samples without induced setting were used as obtained from the storage container.
Cement slurries were prepared by mixing the premixed CPC powder with water (powder-to-liquid ratio, 1:1) for around 20 s. The slurries were then allowed to harden and dry under room conditions for 24 h prior to testing.

2.2.4.4 Dynamic vapor sorption (DVS) measurements

Water vapor uptake studies were done with a DVS-1000 system (Surface Measurement Systems Ltd., Alperton, United Kingdom) controlled via DVSWin 2.16 beta (same manufacturer).
Approximately 20 mg of premixed fresh or stored cement powder were placed in the sample chamber, equilibrated at 30 °C, and dried at 0 % relative humidity (RH) for 10 h before running the humidity programs. Data evaluation employed Microsoft Excel (Microsoft Corporation, Redmond, WA, USA) and the DVS Analysis Suite (version 3.5, Surface Measurement Systems Ltd., Alperton, United Kingdom).

Humidity programs started at 50 % RH, which was then raised in steps of 10 % every 6 h. The maximum RH was 98 %, which was kept for 10 h. Finally, RH was set to 0 % for 10 h to dry the sample again and allow the quantification of irreversibly bound water.
For comparison, also a mixture of anhydrous MCP (MCPA) and β-TCP was prepared and tested. MCPA was prepared by drying MCPM in an oven at 105 °C for several days followed by quenching in a desiccator and immediate sample preparation.

2.2.4.5 ATR-FTIR measurements

IR measurements were performed on a FTIR spectrophotometer (Excalibur 3100 FT-IR Varian Inc., Palo Alto, CA, USA) equipped with a diamond crystal ATR unit (Pike MIRacle, Pike Technologies, Madison, WI, USA). Computer-based processing of the collected data was performed with the spectrometer software (Resolutions Pro, version 4.0, Varian Inc., Palo Alto, CA, USA) and Microsoft Excel.

2.2.4.6 X-ray diffractometry (XRD)

X-ray diffractometry was performed with a powder x-ray diffractometer (PW2273/20 copper anode, PANalytical B.V., Almelo, The Netherlands; PW 1830 x-ray generator, PW 1710 diffraction control unit and PW 1820 vertical goniometer, Philips Industrial and Electro-acoustic Systems Division, Almelo, The Netherlands). Machine control and data collection was performed externally (ADM version 3.5, A. Wassermann Röntgenanalytik-Meßsysteme-Software, Kempten, Germany). The collected data were evaluated with Microsoft Excel.
Samples of the set cement were ground in a mortar, put on a sample holder and mounted into the diffractometer. Spectra were collected at angles from 4° to 40° using a step size of 0.02° and a collection time of one second per data point. The acceleration voltage was 40 kV and the current 25 mA.

3 Results and discussion

3.1 DCPD-forming calcium phosphate cements containing polycaprolactone microparticles for controlled protein drug delivery: Release behavior and mechanical properties

3.1.1 Introduction

Bone has the unique ability to heal completely even after very large injuries. However, without external help, healing is limited to a certain so-called "critical" defect size. This size depends on factors like age or species, as well as on the location of the defect[34-41]. The critical size for adult humans is around 5 – 8 mm[42, 43]. Larger defects, e.g. after the resection of bone tumors, therefore need to be treated by filling the void with a suitable filler preventing the ingrowth of other tissues and therefore a permanent loss of bone function. The void filler has to be biocompatible and should be biodegradable, i.e. it should degrade as newly formed bone tissue grows in. The implant should also provide some mechanical strength, reducing the time of patient immobilization. Various bone void fillers have been described in the literature[244, 311, 340, 353-358].

Calcium phosphate cements forming hydroxylapatite (HA) are one of the most promising systems. Cements forming dicalcium phosphate dihydrate (DCPD) upon setting share their easy preparation and good biocompatibility. However, DCPD-forming cements have much lower mechanical strengths[290]. DCPD degrades faster than HA because of its higher water solubility at physiological pH-conditions. This is undesirable, if the degradation of the implant is faster than bone ingrowth; a gap between implant and surrounding bone could be formed. A weakening of the implantation site during the healing process and increased risk of fractures would be the consequences. As it is not possible to reduce the degradation rate of the implant, the ingrowth of bone has to be increased to avoid such a situation.

Bone morphogenetic proteins like BMP-2 have been proposed and tested as effective factors to increase the formation of new bone[66]. Their combination with DCPD-forming calcium phosphate cements could therefore effectively close the gap between implant dissolution and bone formation.

The release of the growth factor from the cement should be controlled and mimic physiological profiles to reduce possible adverse side effects and cost[64].

The introduction of the growth factor in the cement without a separate drug delivery system appears not promising for long term drug release. The amount of water permeating bone, mainly from the endosteal to the periosteal side, is quite large and thus would result in a rapid release through the bone matrix[80, 81].

Biodegradable polymeric microparticles have been used for controlled drug delivery for many decades and are promising delivery systems for drugs/growth factors to be combined with the cement product.

In this study, polycaprolactone (PCL) was chosen as biodegradable and biocompatible polymer[226, 227, 236]. Its slow degradation rate appeared promising for the desired long term release because polymer degradation effects on drug release could be avoided, thus simplifying the design of a proper release system. In contrast to the widely used poly(lactide-co-glycolide), PCL forms only slightly acidic degradation products upon degradation, which means that possible negatively effects of the degradation products on the stability of the encapsulated protein are reduced.

Lysozyme was chosen as model protein to replace BMP-2 in this study because of its comparable molecular weight and isoelectric point. To enable an easier quantification of the drug release, the applied lysozyme loadings were much higher than required for a final formulation using BMP-2.

The mechanical strength of DCPD-forming cements is usually much lower than that of HA-forming cements[84]. Any further weakening is therefore unwanted. Therefore, a compression of the cement-microparticle composite prior to setting was evaluated to compensate possible negative effects of the microparticle addition on the mechanical strength of the cement.

The use of predefined compression forces required the application of the cement as dry powder. This technique may also help to solve working-time issues otherwise often addressed by chemical setting modifiers[119, 345, 359].

3.1.2 Results and discussion

In order to develop a biodegradable bone void filler with controlled drug release properties, the proposed microparticle-containing cement system was compared to a system in which the protein drug was just mixed with the cement powder. This conventional cement system was prepared in the form of tablets to obtain defined sample geometry.

The lysozyme release from these cement tablets was rapid (approximately 40 % released within 4 h) and incomplete with a leveling off after around 24 h (approx. 85 % released) (Figure 7). This is consistent with reports on the release of vancomycin from a DCPD-forming cement[293].

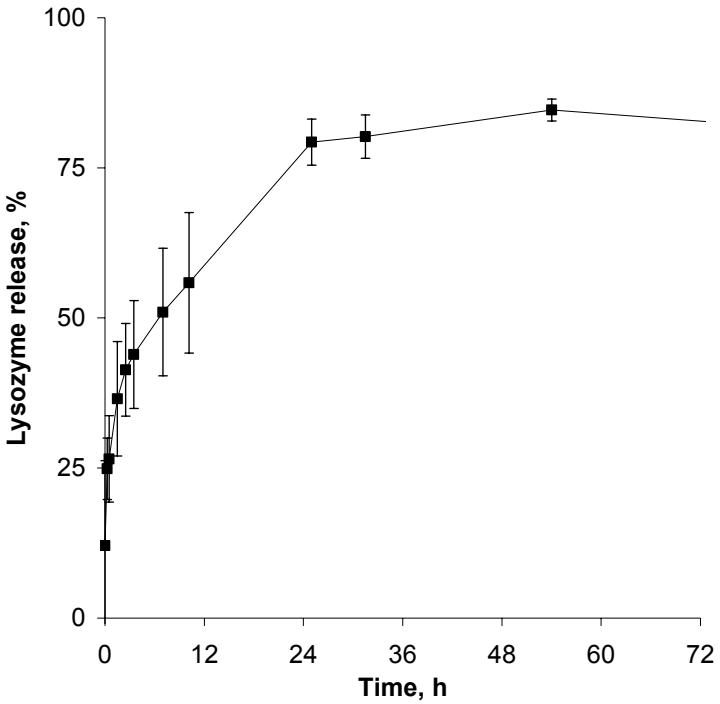

Figure 7: Lysozyme release from CPC tablets.

The rapid initial release could be explained with the high porosity of the CPC matrix, leading to a fast diffusion of the highly water-soluble protein through the water-filled matrix structure. The incomplete release most likely resulted from interactions between the polar protein and the polar CPC surfaces. Hence, around 15 % of the protein was adsorbed to the CPC. As the adsorbed protein covers the surface of the CPC, the remaining 85 % of the protein could

diffuse freely through the pores of the CPC matrix without further diffusion limiting interactions with the cement.

In order to prolong the protein release from the cement to the desired release periods of at least two weeks[59], protein-containing PCL microparticles to be incorporated into the cement were prepared with the w/o/w-solvent evaporation method.

The mean particle sizes could be controlled by the polymer content of the polymer solution and the stirring speed of the outer emulsion (250 – 1000 rpm). For the desired purpose, the mean particle size was adjusted to 250 – 400 µm to allow optimal bone ingrowth after microparticle degradation[249, 250]. Encapsulation efficiencies of 55 – 75 % were achieved with most batches, as some of the highly soluble lysozyme was lost during the emulsification process to the external aqueous PVA phase, probably because of a too large size of the inner water droplets. The encapsulation efficiency of water-soluble compounds can be close to 100 % and correlates clearly with the dispersion intensity of the primary w/o emulsion formation[360, 361]. The activity of the encapsulated lysozyme was checked with a *Micrococcus lysodeikticus* assay. The protein activity was > 95 % compared to a fresh protein solution. The protein did also not degrade during storage of the microparticles for 6 months (room temperature, desiccator).

The microparticles retarded the lysozyme release to more than 10 days (Figure 8).

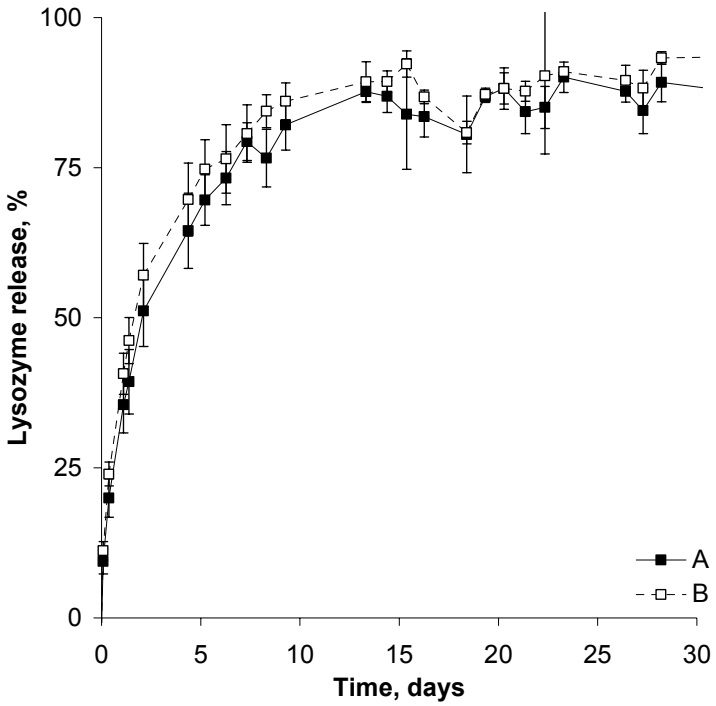

Figure 8: Lysozyme release from two PCL microparticle batches (800 mg PCL, 40 mg lysozyme).

The protein release occurred by diffusion through media-filled pores. Diffusion through the intact polymer matrix was not possible because of the high molecular weight of the protein. The release was also not controlled by the degradation of PCL, as the degradation time of PCL is much longer than the observed release period. The incomplete release could not be attributed to strong or irreversible interactions between PCL and lysozyme, because the recovery from mass balance studies revealed approx. 100 % protein recovery. The incomplete release thus resulted from protein trapped in pores of the PCL-matrix not connected to the particle surface.

The protein release was affected by the amount of PCL in the organic phase (Figure 9). The higher polymer content resulted in a higher viscosity of the polymer solution, thicker walls around each droplet of the inner aqueous phase and – after evaporation of the solvent – reduced interconnections between the pores. In addition, the protein loading also decreased with increasing polymer content in the organic polymer solution because of a constant composition of the inner aqueous protein phase. Therefore, the release of microparticles prepared from higher concentrated organic phases was slower and more prolonged.

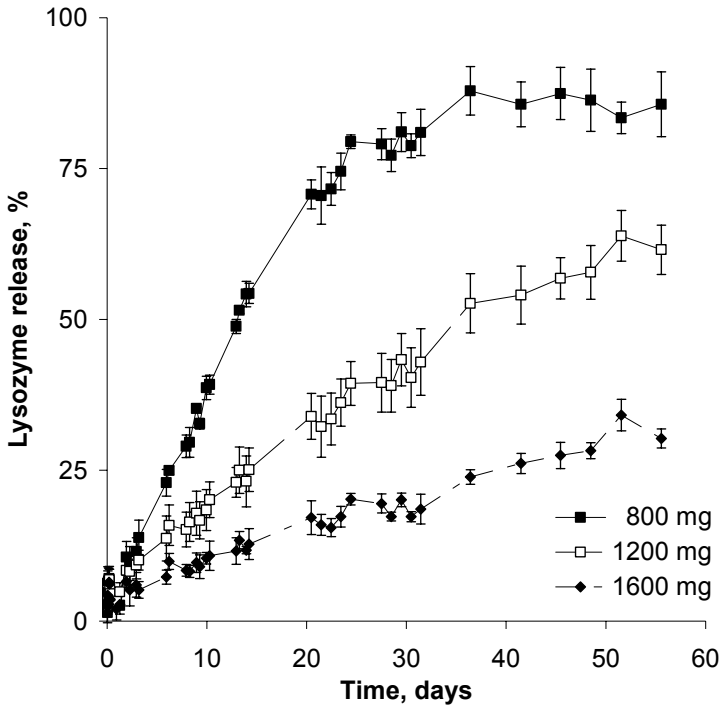

Figure 9: Effect of PCL amount used during microparticle preparation on the release of lysozyme.

SEM images of the microparticles and their surface revealed a spherical shape and a surface with increased roughness and reduced amount of pores with increasing polymer content in the batch (Figure 10 A, B). Cross-sections showed a highly porous inner structure with most pores in the size range of 25 to 75 μm (Figure 10 C, D). The pores were interconnected by small ports (Figure 10 D). Higher magnification of the pores showed a thin, partially fragmented layer on the inner surface of some of the pores (Figure 10 E, F).

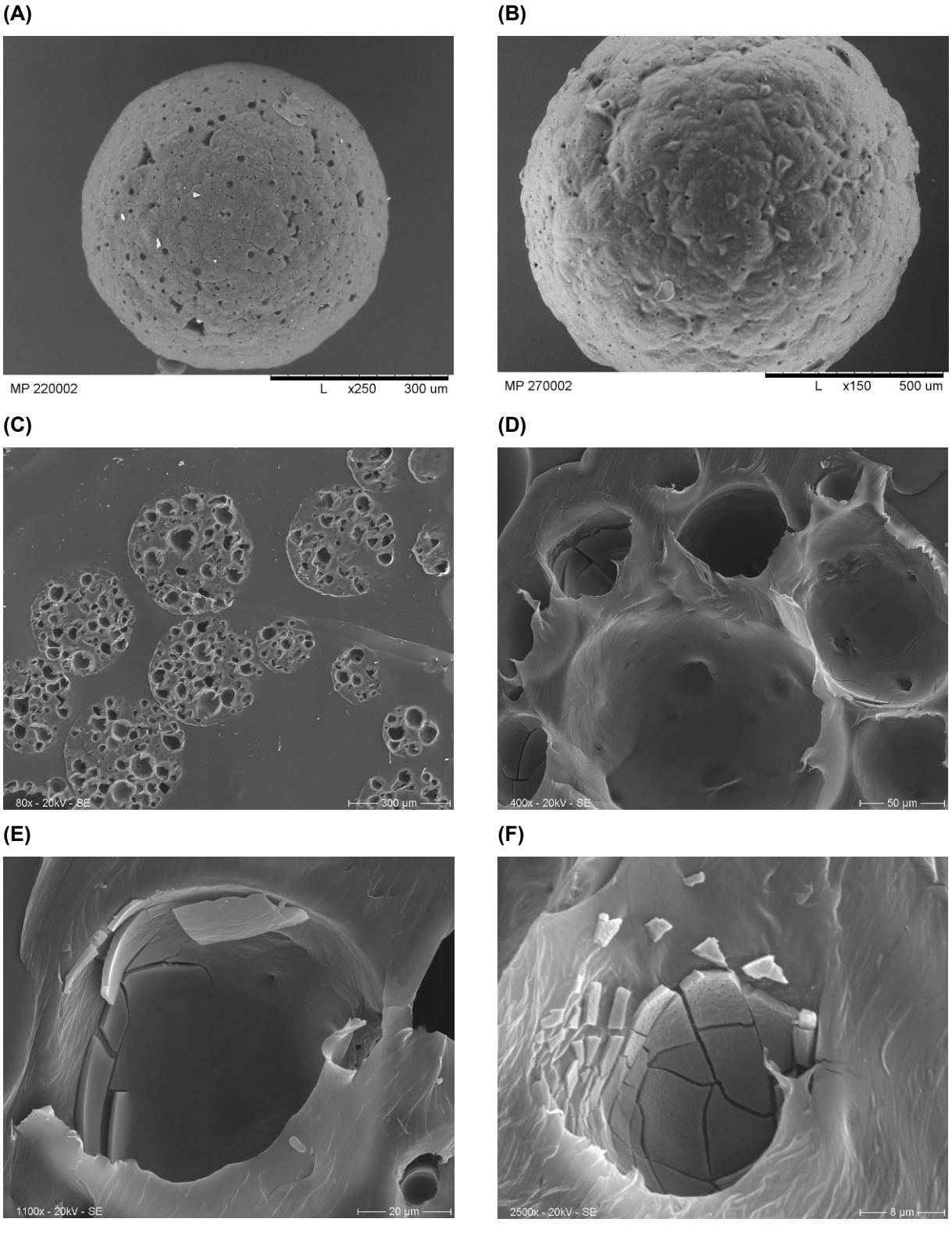

Figure 10: SEM images of PCL microparticles: (A) Microparticle surface (800 mg PCL in batch); (B) microparticle surface (1600 mg PCL in batch); (C) microparticle cross-sections; (D) detailed view of the pores with interconnections; (E, F) platelet-like structures/thin film on the inner surface of some pores.

Energy dispersive x-ray analysis (EDX) of these platelet-like layer structures revealed two pronounced peaks for sulfur and chlorine (Figure 11 A), while no signals for these two elements were detected within pores without the layer structures (Figure 11 B) or on other parts of the cross-sections.

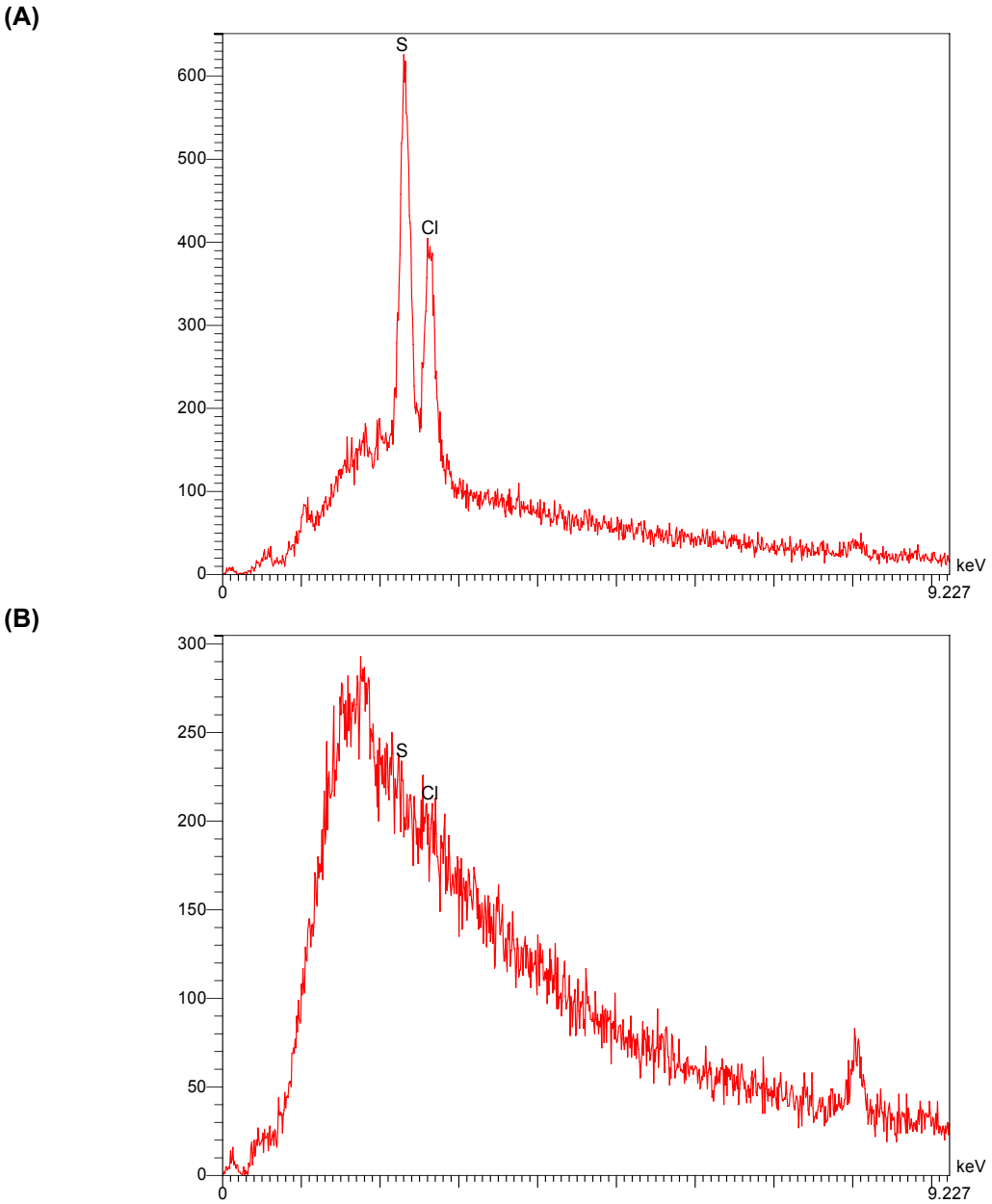

Figure 11: EDX spectra of (A) the plate-like/film structure within a pore of lysozyme-loaded PCL microparticles and (B) the inner surface of a pore without this structure.

The peaks could be clearly attributed to lysozyme hydrochloride as no other excipient in the formulation contains either of these elements. Lysozyme was initially dissolved in the

aqueous droplets emulsified into the organic PCL solution. Upon removal/drying of the organic solvent and of the water from the inner aqueous phase, lysozyme could not diffuse with the water molecules through the polymer matrix but only through interconnected pores. Upon drying, lysozyme precipitated from a highly concentrated solution on the inner surface of some (not all) pores. The partially fragmented nature of the formed lysozyme layers/films can be explained with the brittle nature of the protein salt.

Next, these microparticles were incorporated into cement to create the composites. Tablets were used to increase sample throughput, while implants were used to simulate the proposed system. The release rates of the protein from the tested systems increased in the following order: CPC-microparticle implants ≤ pure microparticles < CPC-microparticle tablets (Figure 12).

The release from the non-disintegrating implants was only slightly slower than from the pure microparticles. Longer diffusion pathways between the microparticles and the release medium and a lower total protein content of the implants due to their preceding setting in aqueous medium account for that. While this was expected, the release of the CPC-microparticle tablets was faster than from the pure microparticles.

Therefore, the increased release had to be attributed to the high mechanical stress applied to the microparticles in the cement powder during tableting. The high compression forces exerted by the tablet press apparently damaged the incorporated microparticles, altering their release behavior possibly by the introduction of small cracks, acting as additional pores.

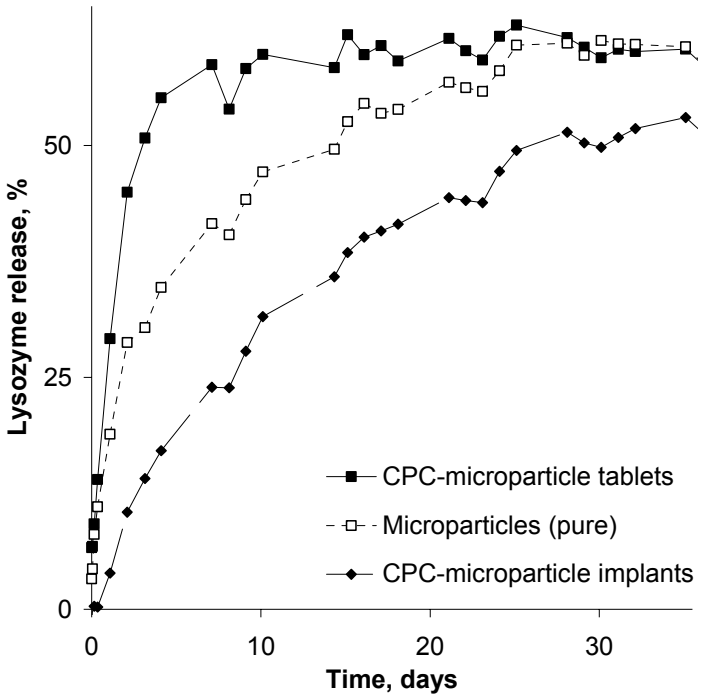

Figure 12: Lysozyme release from microparticles and CPC-microparticles implants or tablets.

The effect of different compression forces during preparation was investigated by applying forces of 0, 10, 20, 40, 80 or 160 N on cement-microparticle implants during their preparation. Two opposing effects of the used compression force on the release rate of the implant samples were found (Figure 13 A, B).

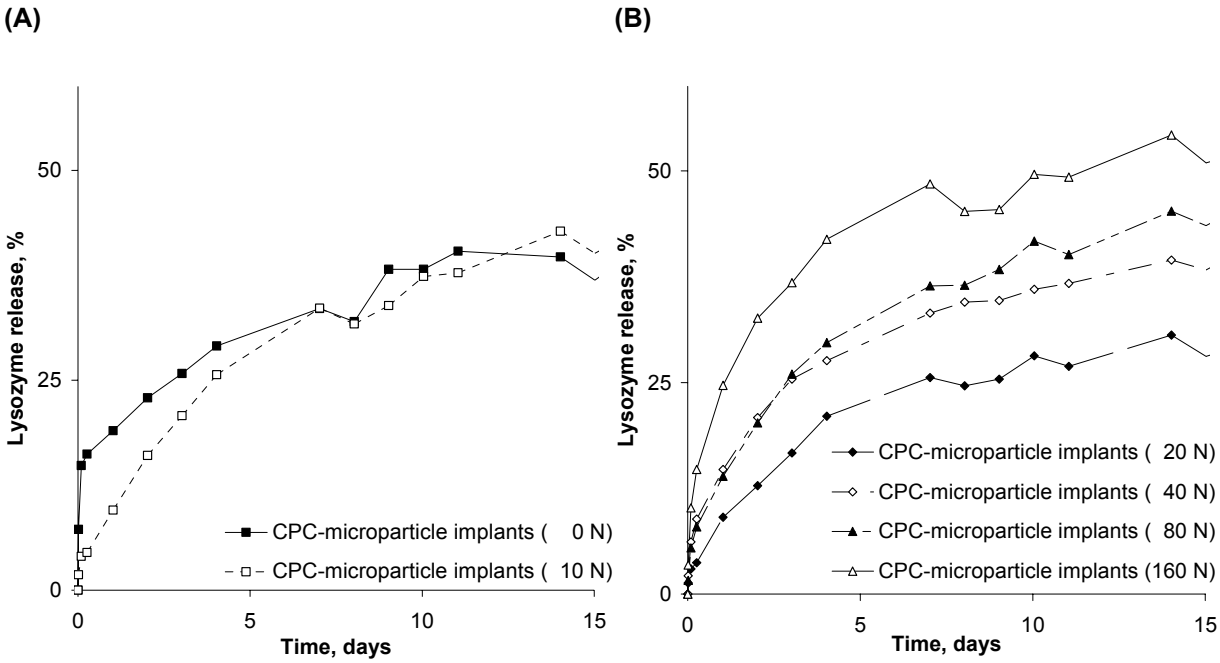

Figure 13: Comparison of the release profiles of PCL microparticles containing lysozyme, compressed into a CPC-microparticle implant at different maximum pressures. (A) Basic values; (B) values for different, higher compression forces.

Implants without any compression prior to setting partially disintegrated upon release, while implants compressed with ≥ 10 N did not. With increasing compression force, the release rate first decreased, likely due to a distortion of the ports between the pores of the microparticles. With higher compression forces, this effect is overcompensated by the formation of new cracks acting as ports between the pores. This would explain the different release rates as well as the different total releases.

The ultimate tensile strength (compressive strength) of the set CPC implant could be increased by a factor two by the compression of the unset CPC powder prior to initiation of the setting reaction (Figure 14).

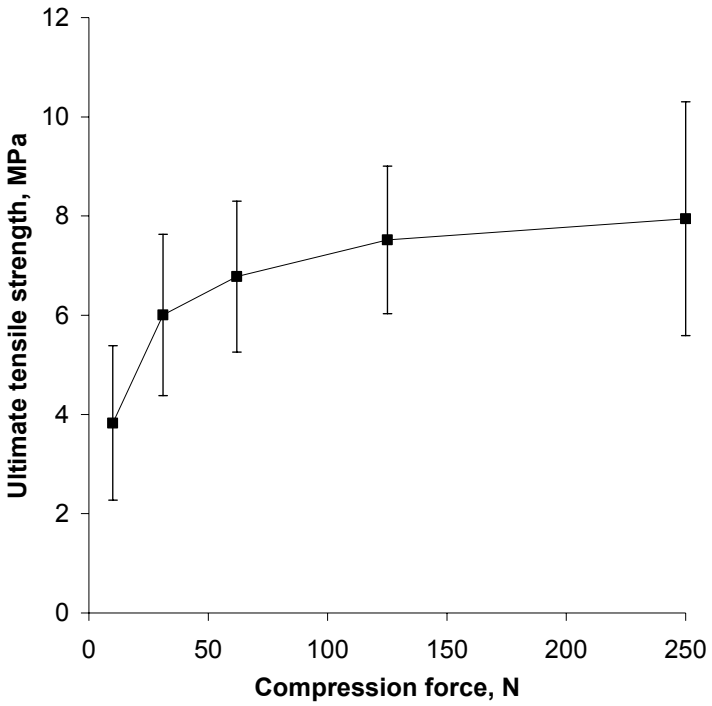

Figure 14: Effect of compression force prior to induced setting on the ultimate tensile strength of set microparticle-free CPC implants.

The observed effect was slightly higher and required much lower maximum forces than previously reported[294].

Higher compression forces and therefore higher densities of the unset samples resulted in a higher mechanical strength of the set cement. Within the denser samples, the amount of water available during setting is lower, thus local supersaturation is reached sooner and DCPD precipitation has to take place in a smaller volume, resulting in a denser and therefore more stable crystal network. Comparable effects for cement slurries are also described as effects of the powder-to-liquid ratio[296] and have also been reported for slurries being continuously compressed during their setting[295].

CPCs are usually applied as aqueous slurries/pastes. In this study, the cement was used as dry powder. Working with cement powder in drained cavities may also overcome issues of short working times of DCPD-forming cements. However, handling of the pure CPC powder mixture was inconvenient. Due to the very fine particle size of the used β-TCP, its flowability was extremely poor. The cement workability was significantly improved by the incorporation of the microparticles, visible by the increasing smoothness of the compression curves (Figure 15).

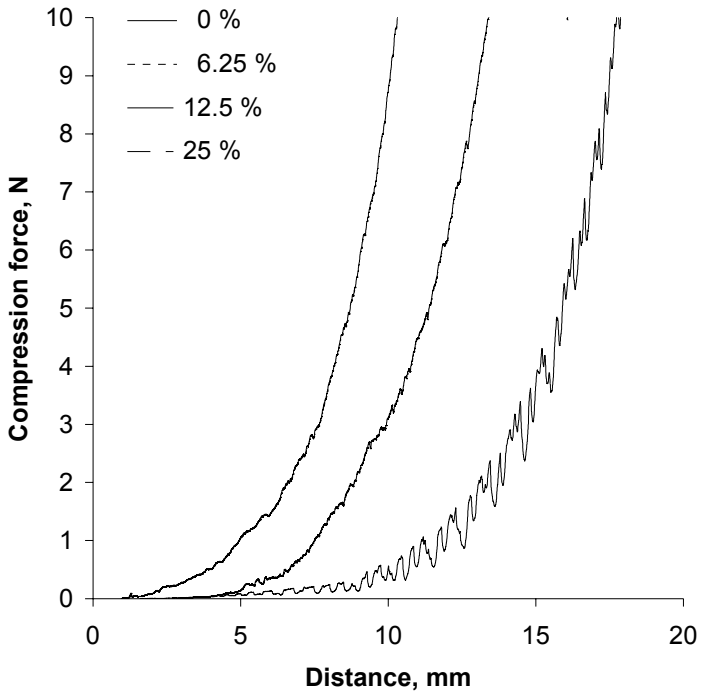

Figure 15: Effect of microparticle content (w_{MP}/w_{total}) on the flow behavior of the CPC powder expressed as force distance curve recorded while compressing the powder prior to initiated setting.

Increasing the microparticle content decreased the density of the cement blend (indicated by a left shift of the compression curves) and the ultimate tensile strength of the set composites. Ultimate tensile strength was reduced by more than 50 % with just 6.25 % (w/w) microparticles added (Figure 16).

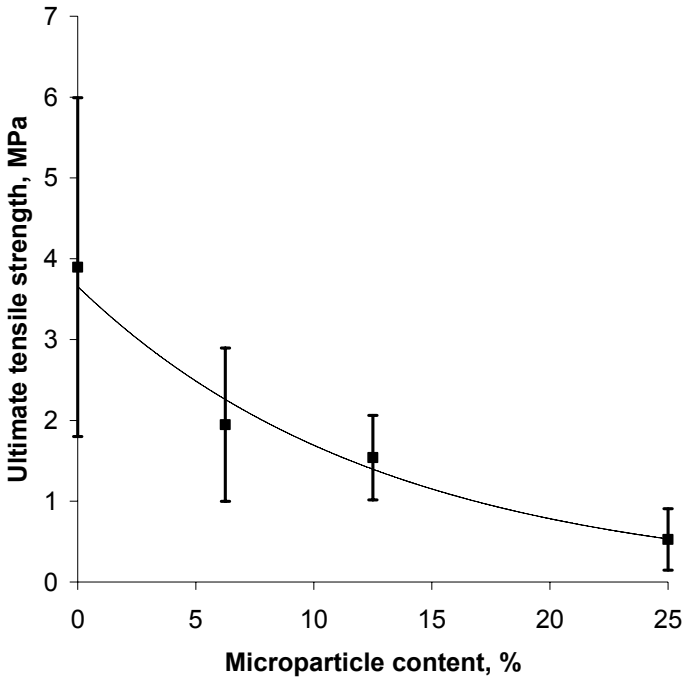

Figure 16: Mechanical strength, expressed as ultimate tensile strength, of set CPC implants compressed with 10 N prior to setting after their hardening vs. microparticle content (w_{MP}/w_{total}) of the samples.

Although microparticle addition did not really influence the density of the cement parts of the composite, the addition caused a pronounced loss in mechanical strength comparable to a general decrease in cement density. SEM images (Figure 17 A - D) indicated that the microparticle surface at lines of breakage was still covered by larger amounts of cement crystals. However, the interactions between cement and microparticles were much weaker than between the cement crystals themselves.

The mentioned compression prior to setting could not compensate the loss in mechanical strength, due to the observed sensitivity of the porous microparticles' release profiles to mechanical stress. However, it should allow a compensation of mechanical strength for composites using compact microparticles.

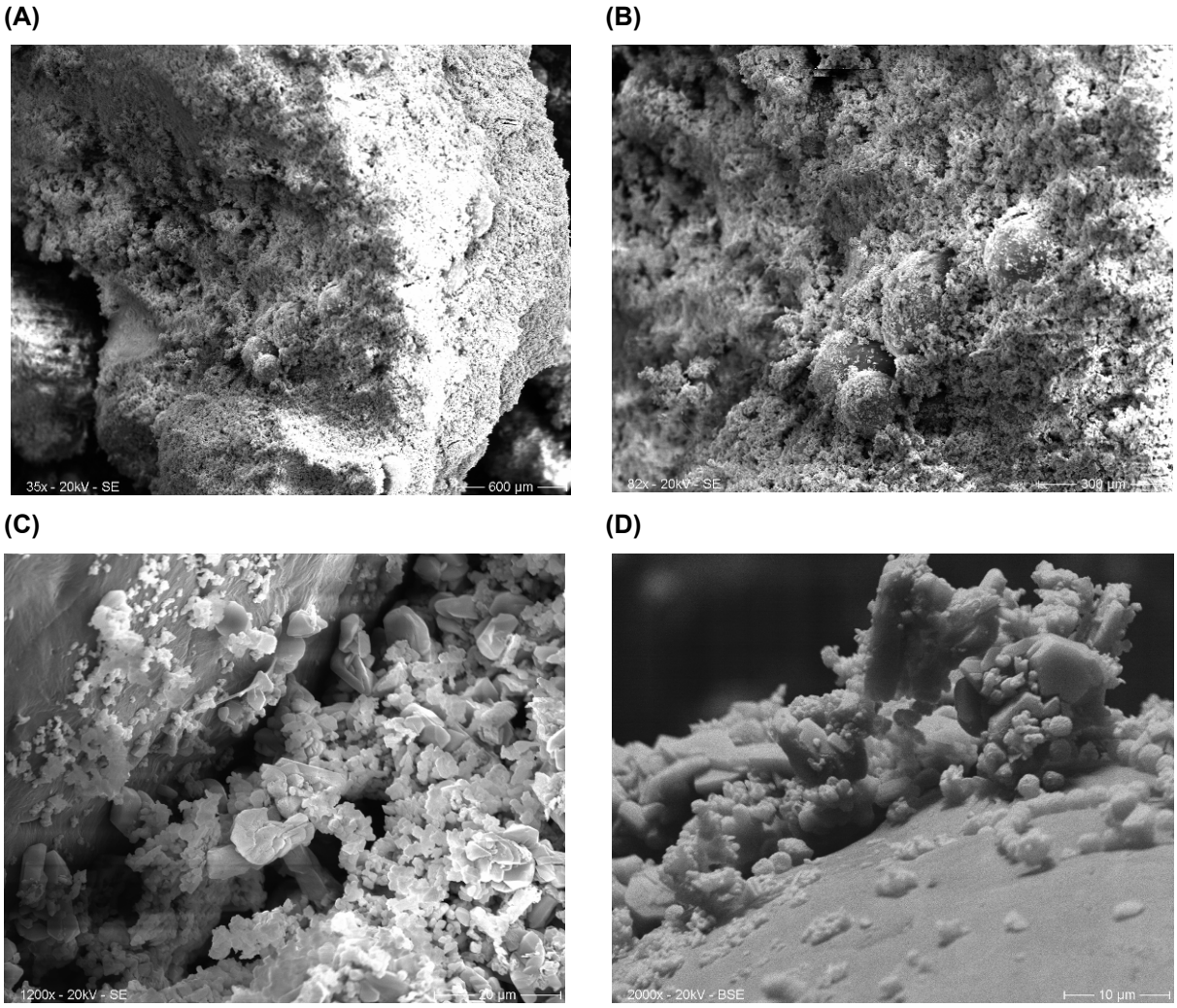

Figure 17: SEM images of broken CPC-microparticle implants. (A) CPC-microparticle cement after breaking; (B) view of the surface of the line of breakage with four still cement covered microparticles in the center; (C, D) DCPD crystals on the surface of PCL microparticles.

3.1.3 Conclusions

A composite system consisting of calcium phosphate cement (CPC) and polycaprolactone (PCL) microparticles intended as void filler and drug delivery system for super critical-sized bone defects was prepared. The release of lysozyme as model protein from the pure cement, pure microparticles and the composite was tested. The effect of compressive stress prior to setting on the release profiles was evaluated by compressing the composites into tablets or by applying predefined compression forces (10 – 160 N) using a texture analyzer.

Lysozyme release from the pure cement very fast, whereas microparticles and CPC-microparticle composites provided controlled release of active protein for several weeks. A sensitivity of the release profile to high mechanical forces prior to the initiation of the setting reaction was found. The release from samples prepared with high compression forces was significantly increased. Microparticle addition to the cement powder improved its handling properties but led to impaired mechanical strength after setting. A compensation of this weakening by a short compression prior to initiated setting was critical due to the mentioned effect on the release profile. Therefore, the presented CPC-microparticle composite was an effective controlled delivery system for protein drugs but should just be applied to non-load-bearing areas of bone.

3.2 Effect of temperature and citrate-addition on the setting time of a DCPD-forming calcium phosphate cement and on the mechanical properties of DCPD

3.2.1 Introduction

While smaller bone defects usually completely heal without scar formation, bone defects above a certain size require special treatment to provide a healing *ad integrum* [34-41]. These "super critical-size" defects are the main targets of bone tissue engineering. One of the most common approaches to treat these defects is to fill them with a degradable implant, acting as void filler, which is then replaced by ingrowing new bone tissue. For the purpose of pure void filling, the mechanical strength of the filler is not essential. However, mechanical support by the implant is often wanted to minimize immobilization of the patient.

Different types of void fillers have been proposed, including polymeric scaffolds, sintered hydroxylapatite scaffolds and self-setting calcium phosphate cements[12, 223, 240, 293, 340, 362]. The latter have the advantages of being moldable in virtually any shape directly at the implantation site, while still providing mechanical strengths sufficient for most application sites after their setting. Although many different compositions for self-setting calcium phosphate cements (CPC) have been tested and proposed, the formed products are usually just two: Hydroxylapatite (HA) or calcium hydrogen phosphate dihydrate (dicalcium phosphate dihydrate, DCPD). Both compounds differ in physical and physicochemical properties like solubility, surface pH, mechanical strength of the set cement or setting speed[290].

DCPD-forming calcium phosphate cements using calcium dihydrogen phosphate monohydrate (monobasic calcium phosphate monohydrate, MCPM) and β-calcium phosphate (β-tricalcium phosphate, β-TCP) usually show a very fast reaction upon contact with water. This results in very fast cement setting (sometimes just 2 – 3 minutes) and even shorter and therefore clinically inappropriate working times.

The setting reaction of the described cement system is given below (Equation 6). The reaction takes place at slightly acidic pH, making DCPD the calcium salt with the highest crystal formation rate, although not being the least soluble[109, 110, 120].

$$\beta\text{-}Ca_3(PO_4)_2 + Ca(H_2PO_4)_2 \cdot H_2O + 7\ H_2O \rightarrow 4\ CaHPO_4 \cdot 2\ H_2O$$

Equation 6: Empirical formula of the setting reaction of a DCPD-forming CPC using MCPM and β-TCP as reactants.

Being a crystalline transformation reaction in acidic medium, the setting time can be controlled by modifications of the dissolution rate of the reactants or the crystallization rate of the product. A reduction in the dissolution rate could be obtained by using larger β-TCP particles with a smaller relative surface area. However, this may lead to unreacted β-TCP in the product.

Setting retardants reduce the reaction speed by keeping dissolved calcium and/or phosphate ions in solution. Thereby they reduce the crystallization rate of DCPD and subsequently the dissolution rate of the reactants. Several retarding agents have been described including pyrophosphates, sulfates[338] or citrates[345]. However, the addition of retardants also affects the chemical composition of the cement, which can affect biocompatibility and mechanical properties of the set cement.

These problems could potentially be avoided by a physicochemical retardation based on a pronounced cooling of the cement during setting. According to the Arrhenius equation, the speed of a chemical reaction can roughly be slowed down by a factor of two by a decrease in temperature of 10 K.

In addition, we propose the application of the cement in the form of a dry premixed powder into drained cavities instead of using premixed aqueous slurries. The slurry approach is usually preferred as it theoretically allows the injection of the cement through cannulas. However, injectability is usually quite poor[276, 280, 363, 364].

The application of the dry powder increased working times and allowed the monitoring of the complete setting process. In this study, the effect of different temperatures on the cement setting were observed and evaluated by isothermal DSC and mechanical tests. These results were compared with those of cement systems using the setting retardant sodium citrate (62.5 – 1000 mmol/l) in the setting medium instead of pure water.

3.2.2 Results and discussion

3.2.2.1 Definition of setting time

The term "setting time" is usually related to the development of mechanical strength of the setting cement. Often, it is not distinguished between initial and final setting time. Besides, initial setting time is not defined consistently. In this study, the term setting time will be defined "chemically" and applied to the time between the maximum initial endothermic deflection and the following exothermic curve maximum of the DSC curve (Figure 18).
This definition of setting time, being the "time to reach the maximum amount of reaction", is correlated with the "mechanical" setting time and the "real" setting time, which is the time of reaction completeness. It allows a very precise, non-destructive measurement of the setting rate and therefore reactivity of the cement.

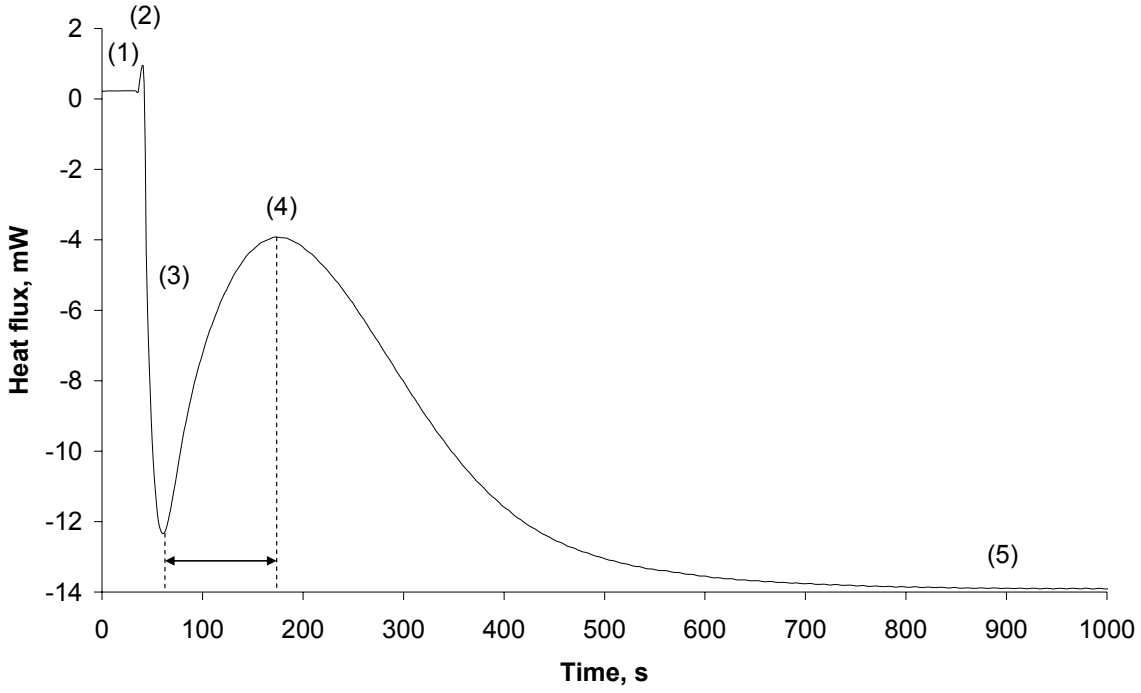

Figure 18: Full thermogram of the cement setting at 25 °C. The marked time between the dashed lines is the "setting time" as defined in this study. The curve can be divided into five parts: (1) Baseline of dry CPC powder; (2) small peak of the water addition; (3) endothermic dissolution of the reactants (MCPM); (4) exothermic peak of DCPD formation; (5) baseline of the set cement.

3.2.2.2 Effect of temperature on the setting time

The setting time of the unmodified cement at room temperature was only around 3 min as the particle size of the β-TCP was very small. This did not allow the preparation of premixed cement pastes; too much information would have been lost due to sample preparation before placement in the DSC equipment. The cement was therefore used as powder and the setting was initiated inside the DSC by the addition of setting liquid, thus enabling the monitoring of the complete setting process.

An exponential relationship between the cement temperature and setting time was obtained within the observed range of 4 °C to 40 °C (Figure 19 A, B).

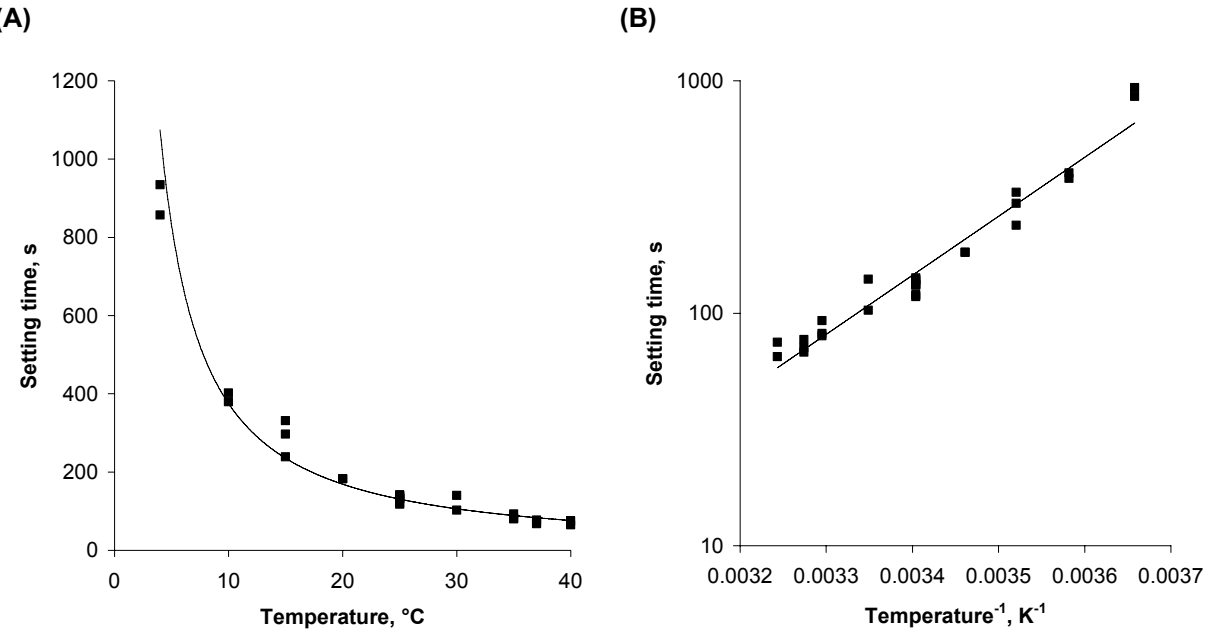

Figure 19: Time to reach the maximum heat flux during CPC setting vs. sample temperature. (A) Plot of the normalized values; (B) Arrhenius plot. (Dashed lines are trend indicators.)

This relationship was in very good agreement with the one expected from the Arrhenius equation. A decrease in temperature by 10 °C resulted in an increase of the setting time by a factor of approx. two. Therefore, a reduction in temperature from 30 °C to 10 °C prolonged the setting time from approx. 100 s to approx. 400 s. Cement cooling thus prolonged the setting time of the cement from not clinically applicable time periods into a well applicable time range.

At 4 °C, the setting time was longer than predicted from the Arrhenius function. The same was found with the highest observed temperature. Both may be explained by the dissolution processes of the reactants that are not explicitly given in the setting reaction (Equation 6). These dissolution processes limit the overall reaction rate at lower and higher temperatures. At lower temperatures, dilution may be retarded due to limited available energy required to break the crystal structure. At higher temperatures, phenomena like local supersaturation may prevent faster dissolution of the reactants.

3.2.2.3 Effect of citrate concentration on setting time

Increasing the citrate concentration increased the setting time in an exponential fashion within the investigated range of sodium citrate concentrations from 0 to 1000 mmol/l (Figure 20 A, B).

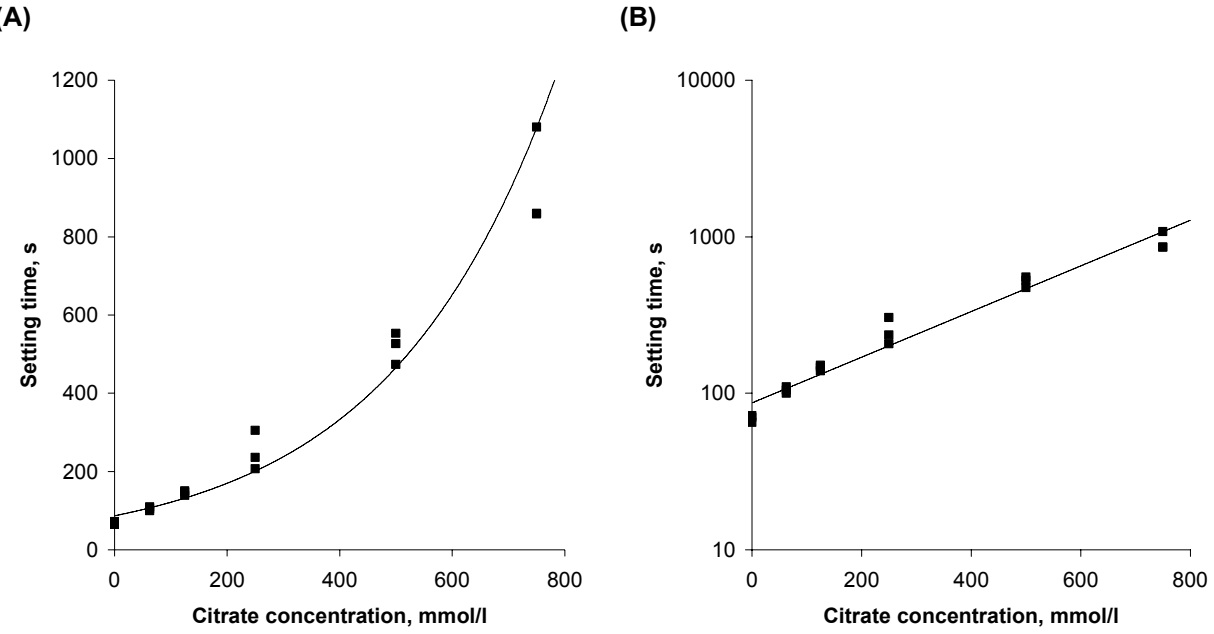

Figure 20: Time to reach the maximum heat flux (for 0 – 125 mmol/l) or the minimum slope of the heat flux curve (for 250 – 750 mmol/l) as indicator for the setting times vs. citrate concentration of the setting liquid. (A) Plot of the normalized values. (B) Plot of the same data with a semi-logarithmic time scale. (Dashed lines are trend indicators.)

The retardation has to be explained by the changed chemical system during cement setting. The rate-limiting step before the addition of citrate ions was the dissolution of the poorly soluble β-TCP. Within the new system, the formation of DCPD becomes rate-limiting, as its precipitation is hindered by citrate ions in solution.

A doubling of the setting time could be achieved with 250 mmol/l sodium citrate solution compared to pure water as setting liquid. An increase of the sodium citrate concentration to 500 and 750 mmol/l resulted in repeated doubling of the setting time. For a sodium citrate concentration of 1000 mmol/l, no setting time could be identified within 20 min.

3.2.2.4 Mechanical properties

The mechanical properties of the set cement were not affected by the setting temperature. Resistance to needle intrusion of the iDSC samples was 22.0 ± 4.5 N for 4 °C and 21.5 ± 1.7 N at 30 °C. Thus, setting temperature apparently did not affect the structure of the formed crystal network in the set cement.

In contrast, with sodium citrate-containing setting liquids, the mechanical strength of the cements strongly decreased even after the addition of small amounts of sodium citrate (Figure 21).

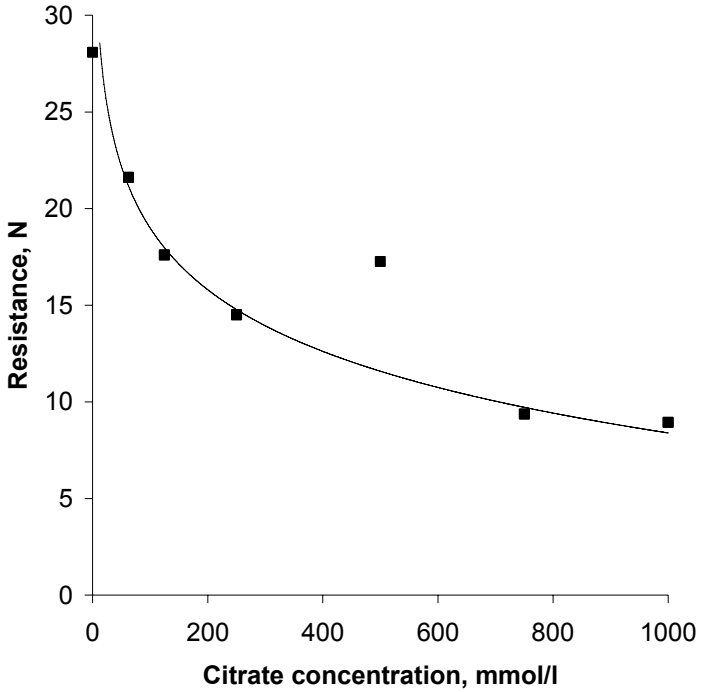

Figure 21: Resistance to needle intrusion of iDSC samples prepared with different concentrations of sodium citrate.

The reduction in the mechanical strength of the cement, expressed as resistance to needle intrusion, could be approximated with an exponential function; the detrimental effect of the same absolute additional amount of sodium citrate was highest at low total citrate concentrations.

The described detrimental effect of sodium citrate on the mechanical strength could be partially compensated by a short compression step of the cement powder prior to the addition of the setting liquid (Figure 22). This increased the density of the cement powder prior and after setting and therefore the mechanical strength of the set cement. Already relatively small compression forces of just 80 N doubled the ultimate tensile strength of the set cements. The effect of compression force leveled off at higher compression forces as the density did not increase proportionally to the applied force.

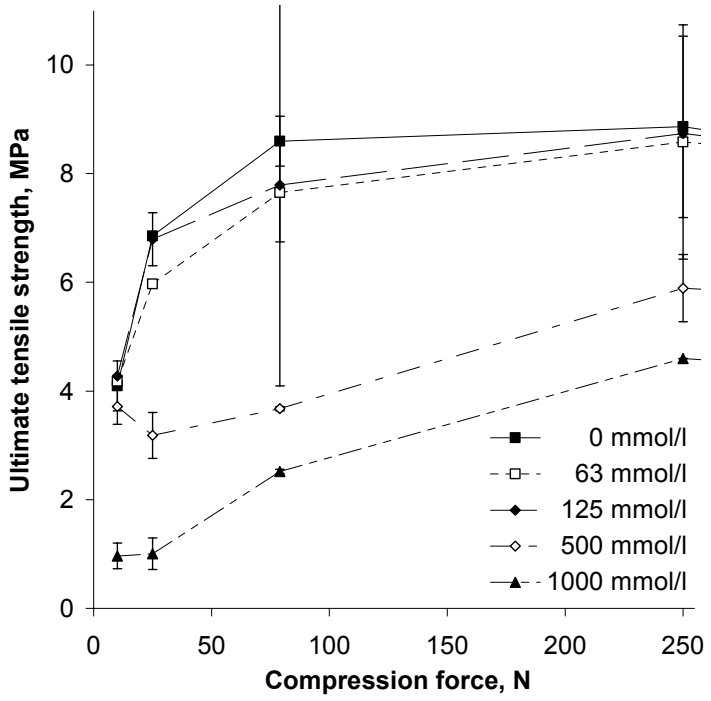

Figure 22: Effect of a compression force of the cement powder prior to setting on the ultimate tensile strength of the hardened cement set with sodium citrate solutions (0 – 1000 mmol/l).

The differences in mechanical strength could not be attributed to reduced crystallization and precipitation rates, as temperature lowering showed the same retardation effects but no effects on mechanical strength.

3.2.2.5 X-ray diffractometry (XRD)

XRD showed no differences in the spectra of cements set at 4 °C or 40 °C, indicating the formation of the same crystalline phases. This was expected, due to the same mechanical properties. XRD was then applied on cements set with sodium citrate, to evaluate the presence of any different crystalline compound that could explain the reduced mechanical strength.
No additional peaks from compounds like e.g. calcium citrate could be found (Figure 23).

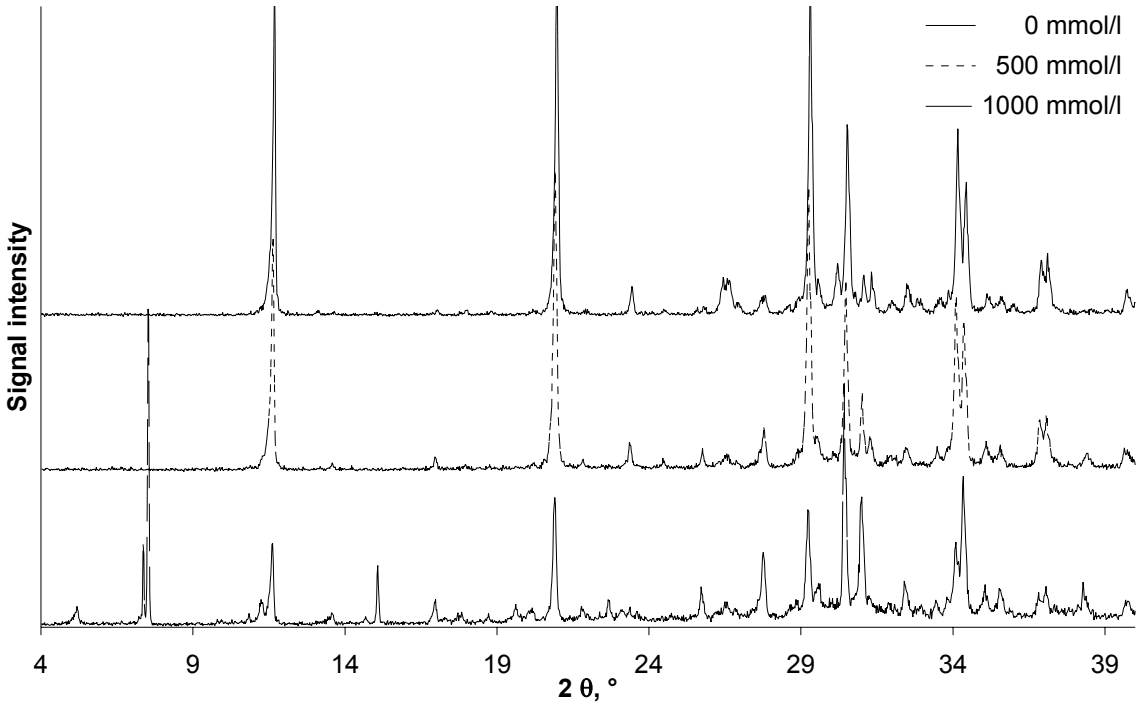

Figure 23: X-ray diffraction spectra of set CPCs prepared with different citrate concentrations in the setting liquid.

The only significantly different spectrum was obtained from samples set with 1000 mmol/l sodium citrate solution.

This spectrum was compared with the pure calcium citrate spectrum (Figure 24) to identify calcium citrate as the most likely foreign crystal substance. Since there were no superimposing peaks between the reference spectrum and the difference spectrum of cements prepared with and without sodium citrate, the amount of calcium citrate in the set cement had to be less than 2 %, which was the detection limit determined from spectra of physical mixtures of the expected compounds.

Finally, the additional peaks in the XRD spectrum of the 1000 mmol/l sample had to be attributed to unreacted MCPM, having a characteristic peak at around 7.5°. This is interesting as the cement samples were kept wet for at least 12 h, indicating an extreme retardation of the setting reaction.

The decrease in mechanical strength with samples prepared with the 1000 mmol/l sodium citrate solution may thus be partially explained by an incomplete setting. However, the reduction in mechanical strength at lower amounts of citrate had to be attributed to other effects. As it appears unlikely that foreign crystals in a concentration far below 2 % can have

such a negative effect of the mechanical strength, differences in the shape of the formed DCPD-crystals were the most likely explanation for the pronounced loss in mechanical strength. Bohner et al.[345] found more round DCPD crystals in a cement set with a 100 mmol/l citrate solution. This could explain a lower level of interaction within the crystal network, reducing the set cement's hardness. However, they reported no significant loss in tensile strength at 100 mmol/l, while this study suggests a pronounced loss already at this low citrate concentration.

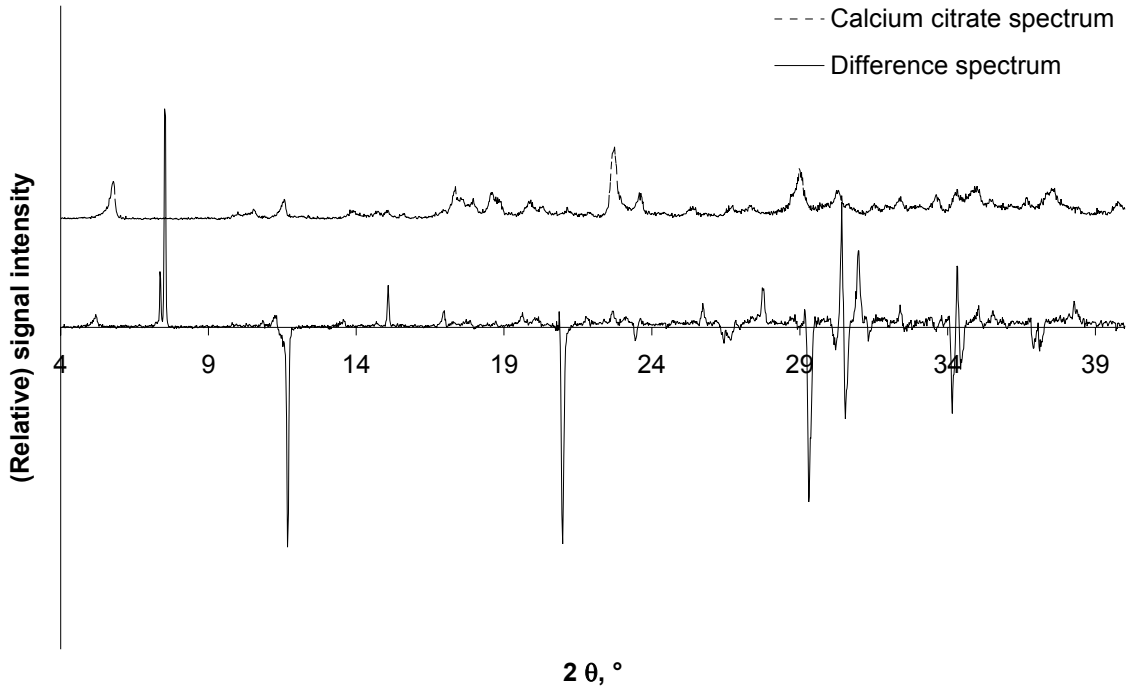

Figure 24: Difference spectrum of samples prepared with 1000 mmol/l and 0 mmol/l sodium citrate solutions in comparison with pure calcium citrate. The amount of crystalline calcium phosphate in the set cements is below the detection limit (< 2 %).

3.2.3 Conclusions

Calcium phosphate bone cements made of calcium dihydrogen phosphate (MCPM) and β-calcium phosphate (β-TCP) form calcium hydrogen phosphate dihydrate (DCPD) as their product. These cements usually have only very short working times, due to their very fast setting. Several chemical additives have been proposed to address this issue. However, their

use can alter chemical composition and mechanical properties of the set cement, eventually lowering biocompatibility and strength. In this study, we evaluated the effects of cooling on the reaction rate and the mechanical properties of the set cement by isothermal differential scanning calorimetry (iDSC), mechanical testing and x-ray diffractometry (XRD). The effects were compared with the effects of sodium citrate addition as chemical setting retardant. Cooling was as effective as high sodium citrate concentrations in the setting medium. It had no negative effects on the mechanical strength of the set cement, while citrate addition had a pronounced negative effect on the mechanical strength of the set cement.

Cooling is thus suggested as easy, predictable and highly effective method to reduce the reaction rate and increase the working time without negatively affecting chemical composition, biocompatibility or mechanical strength.

3.3 Time-resolved powder x-ray diffractometry of the setting reaction of a DCPD-forming calcium phosphate cement

3.3.1 Introduction

Self-setting calcium phosphate cements are promising candidates for the filling of bone defects. Their chemical composition, biocompatibility or mechanical properties have been widely investigated[87]. While many different reactants for the preparation of calcium phosphate cements have been proposed, the products of such cements are usually limited to either hydroxylapatite (HA) or calcium hydrogen phosphate dihydrate (DCPD).

HA-forming cements have gained more interest during the last years as HA is the major inorganic component of natural bone and therefore most likely highly biocompatible. HA-forming cements also possess high mechanical strengths with comparable strengths to cortical bone[84]. They usually harden quite slow and thereby do not increase in temperature during the setting process, minimizing the risk for thermally induced tissue necrosis as observed with PMMA bone cements[214]. As the setting speed of unmodified HA-forming cements is sometimes seen as too slow for clinical applications, several options to increase the setting speed have been proposed [299, 362].

In contrast, DCPD-forming cements have a setting speed, which is usually too fast. Therefore, chemical retardants including citrates have been added[338, 345].

Several analytical techniques including isothermal DSC[365, 366] and FTIR[367] have been used to monitor changes in the cement during setting with pure water or in combination with a chemical retardant. As all reactants and products of calcium phosphate cements are crystalline compounds, x-ray diffractometry (XRD) might offer a better insight in the cement setting process because of its specificity in identifying crystalline structures when compared to DSC or FTIR.

Although X-ray diffraction patterns of calcium phosphates have been recorded for decades[118], accompanying time resolution studies are generally not performed. Rau et al.[368] performed a time-resolved x-ray study on the setting of a hydroxylapatite-forming cement using chitosan as retardant. However, their time resolution was less than one hour. Fukase et al.[369] monitored the setting of a HA-forming cement with low time resolution by taking and preserving samples during the setting reaction.

We evaluated x-ray diffractometry for the real-time monitoring of the setting of a DCPD-forming cement. The much faster setting rate required several adaptations of the usual powder XRD methodology, e.g. a significant reduction of the scanned range. Due to limitations of the used equipment, the setting reaction could not be slowed down by reducing the temperature of the setting cement as proposed before. Therefore, a further increase in the time-resolution had to be achieved by the addition of the setting retardant sodium citrate. The results were compared with results obtained by the abovementioned techniques iDSC and FTIR to evaluate the possible advantages of the proposed XRD method.

3.3.2 Results and discussion

3.3.2.1 General x-ray results and development of the time-resolved method

As DCPD-forming calcium phosphate systems consist of crystalline reactants and form a crystalline product, XRD is an excellent technique to identify both reactants and product (Figure 25).

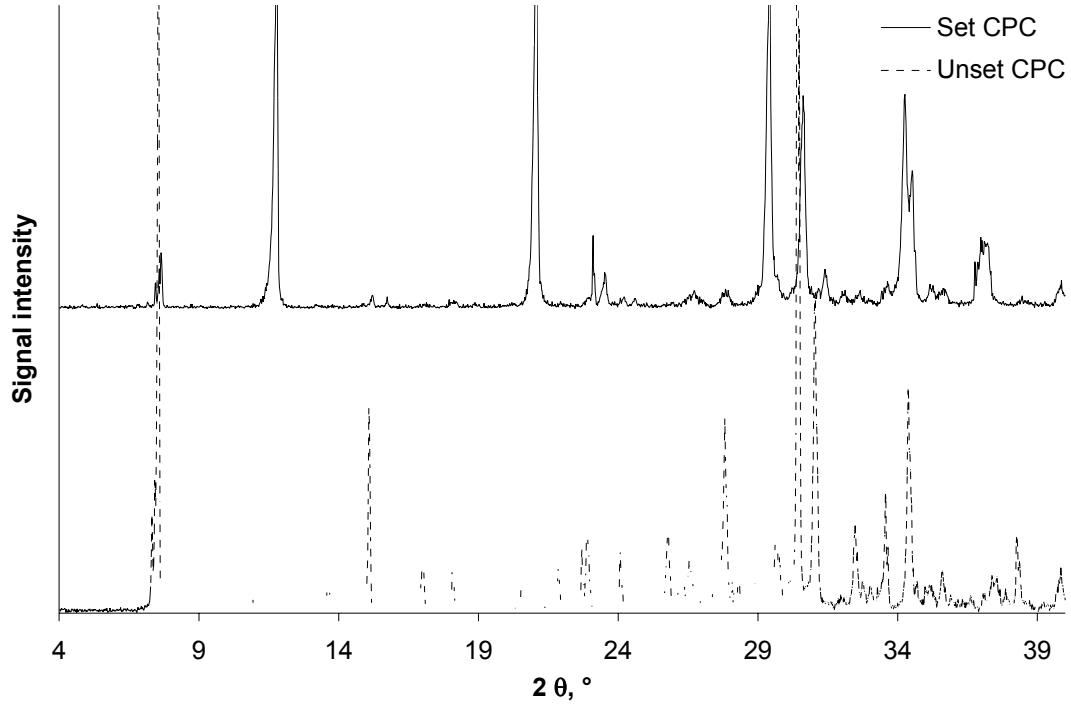

Figure 25: PXRD spectra of a DCPD-forming calcium phosphate cements (CPC) consisting of MCPM and β-TCP before and after setting.

To monitor processes with fast kinetics like the setting of DCPD-forming calcium phosphate cements, the time resolution of conventional PXRD equipment is often insufficient.
This drawback could be overcome by optimizing the measurement conditions. In a first step, the amount of recorded data points was minimized by reducing the observed angle range to a range limited to the characteristic peaks of reactants and product. Therefore, the spectra of the reactants calcium dihydrogen phosphate monohydrate (MCPM), β-calcium phosphate (β-

TCP) and the reaction product calcium hydrogen phosphate dihydrate (DCPD) were collected at a spatial resolution of 0.02° in the range of 4° to 40° (Figure 26).

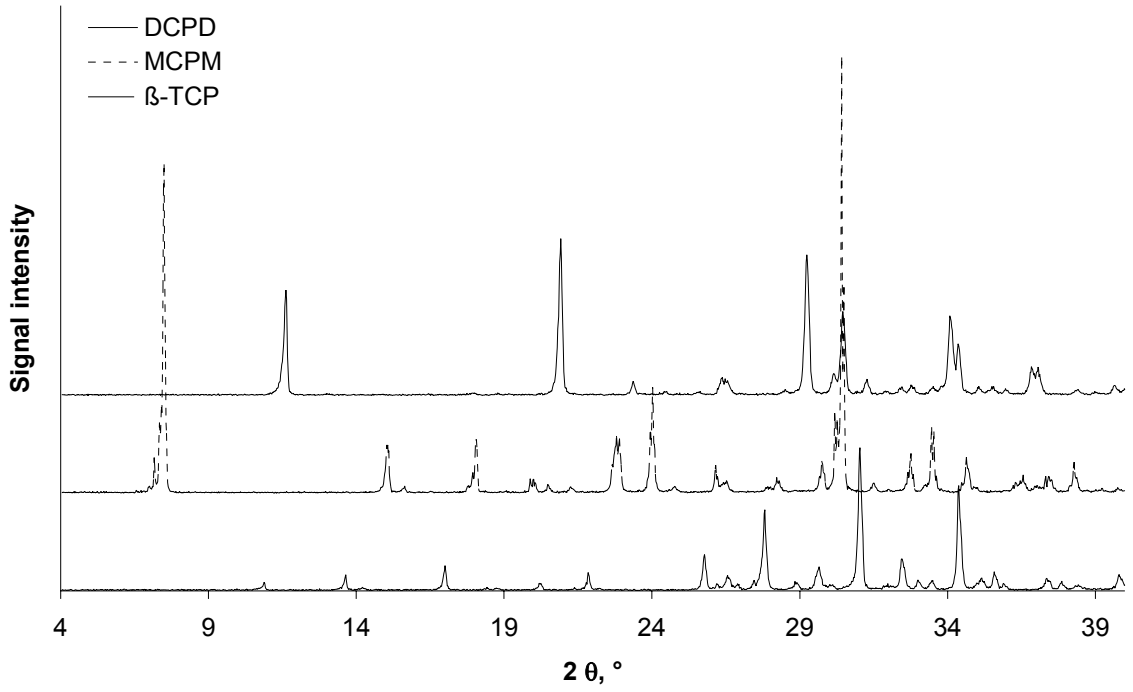

Figure 26: XRD spectra of dicalcium phosphate dihydrate (DCPD), calcium dihydrogen phosphate monohydrate (MCPM) and β -tricalcium phosphate (β -TCP).

MCPM showed two pronounced peaks at 7.50° and 30.42°. All other peaks were of much lower intensity and therefore not suitable for the intended application. The x-ray diffractometry spectrum of β-TCP was characterized by three major peaks at 27.82°, 31.04° and 34.38°. The reaction product DCPD showed three pronounced peaks at 11.62°, 20.92° and 29.24°. Two slightly smaller peaks at 30.46° and at 34.08° had also to be considered here. Based on these data, the smallest area of interest with strong characteristic peaks of each compound was identified between 27.5° and 30.5°. Within this range, MCPM, β-TCP and DCPD were identified by their peaks at 30.42°, 27.82° and 29.24°, respectively (Figure 27).

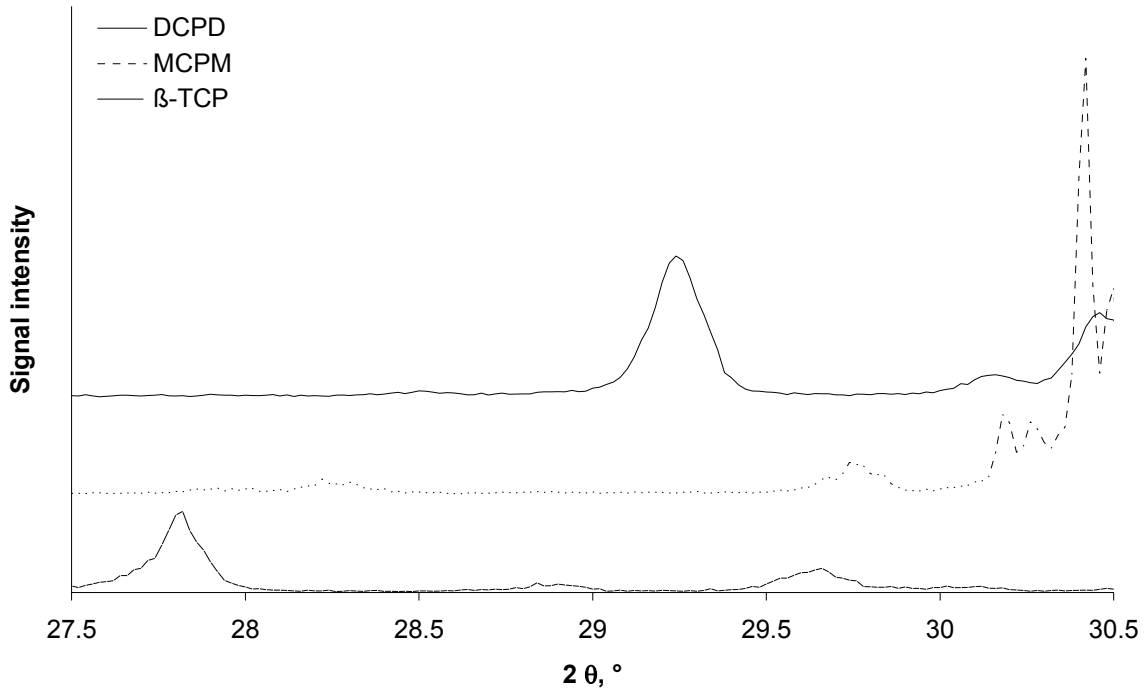

Figure 27: XRD spectra of DCPD, MCPM and β-TCP within the scanned range.

The step size was increased to 0.05° to enhance the time resolution of this method. The counting time was not decreased in order to keep the good signal-to-noise ratio. The lower spatial resolution could be tolerated as all chosen peaks had sufficiently separated positions.
The DCPD peak at 30.46° and the MCPM peak at 30.42° were very close to each other and may not be absolutely distinguishable at a spatial resolution of 0.05°. However, based on the following two considerations, it was feasible to clearly attribute any peak around 30.4° to either MCPM or DCPD. First, the intensity of the 30.4° peak is much higher for MCPM than for DCPD. Thus, a peak at around 30.4° larger than the 29.24° peak of DCPD had to be attributed to MCPM, while smaller peaks could be attributed to DCPD. Second, because of the high water solubility of MCPM, any fraction of a 30.4° peak caused by MCPM should diminish quite fast after the addition of water, while the growth of the peak due to the formation of new DCPD should be slower.
A time resolution of approximately 60 s could be achieved. This means there is a time difference of around 1 min between the same point in spectra A and B as well as between the data points at 27.5° and at 30.5°. This should be taken into consideration when evaluating the spectra as the cement is setting within just a few minutes under normal conditions.

The developed setup does not allow the absolute quantification of each compound, as factors like differences in the roughness of the sample surface – especially after the addition of the setting liquid – will affect the distinct peak signal intensity[370-372].

3.3.2.2 Cement setting with water as setting liquid

The setting of the cement was observed at room temperature with water as setting liquid (Figure 28). The measurements were limited to 10 min based on own preliminary studies which indicated a setting in less than this time.

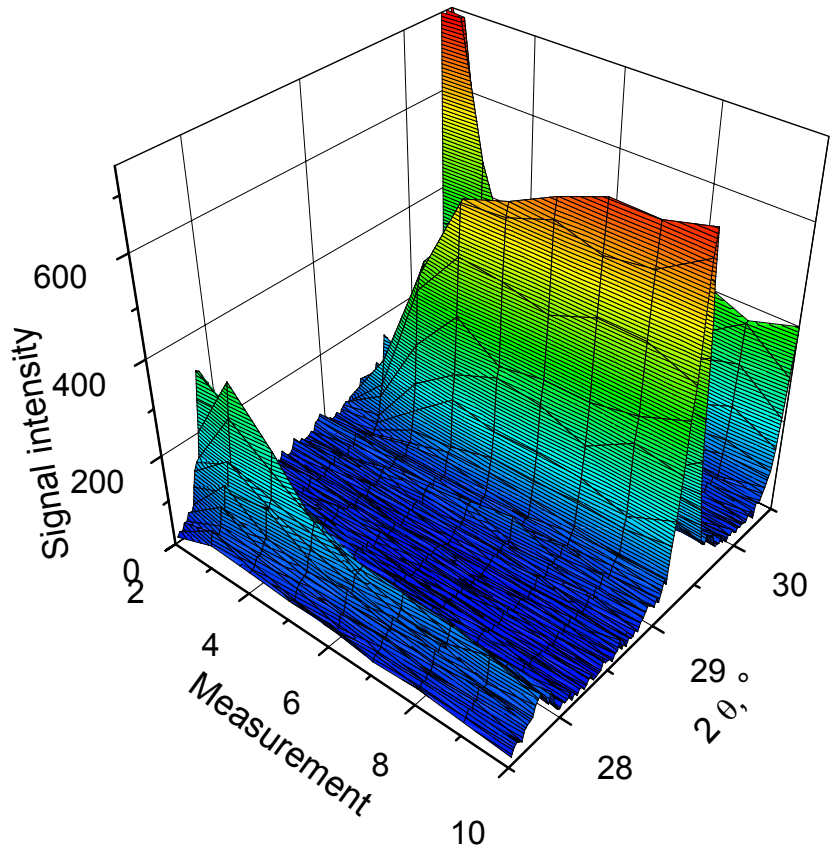

Figure 28: Changes in the XRD spectra within the first 9 min of the setting of a DCPD-forming CPC using water as setting liquid. Blue indicates low, green/yellow higher and red the highest signal intensity.

The first recorded spectrum represented the non-wetted CPC powder prior to the addition of the setting liquid. The following spectra were taken approximately every minute, beginning

approximately 10 s after the addition of the setting liquid. The strong MCPM signal at 30.4° decreased within less than 3 min to a level where it could not be clearly attributed to MCPM anymore, as at this time the DCPD signal slowly became prevailing. The signal change of the less soluble β-TCP was slower. A continuous decrease in its signal occurred during the first 5 min of the reaction. This decrease was accompanied by an increase of the DCPD signal showing the greatest slope during the first 3 min after addition of the setting medium prior to leveling off.

DCPD crystal formation only takes place from media supersaturated with calcium and phosphate ions in respect of the solubility limit of DCPD. Both ions have to be provided by the dissolution of the reactants MCPM and β-TCP. Based on broadly reported setting times of DCPD-forming CPCs, β-TCP dissolution is the rate-limiting reaction step for the setting the unmodified cement.

3.3.2.3 Cement setting with sodium citrate solutions

As the time resolution was still critical with water as setting liquid, the setting reaction was retarded with different amounts of sodium citrate. This retarding agent has proved to effectively slow down the setting reaction. Own studies showed a pronounced negative effect on the mechanical strength of the set cement, most likely caused by a different shape of the formed DCPD crystals[345], but revealed no change in the chemical entity of the reaction product. Therefore, sodium citrate concentrations of up to 1000 mmol/l could be employed as setting liquids. Kinetic measurements were performed for up to 60 min because of the expected retardation of the setting reaction (Figure 29).

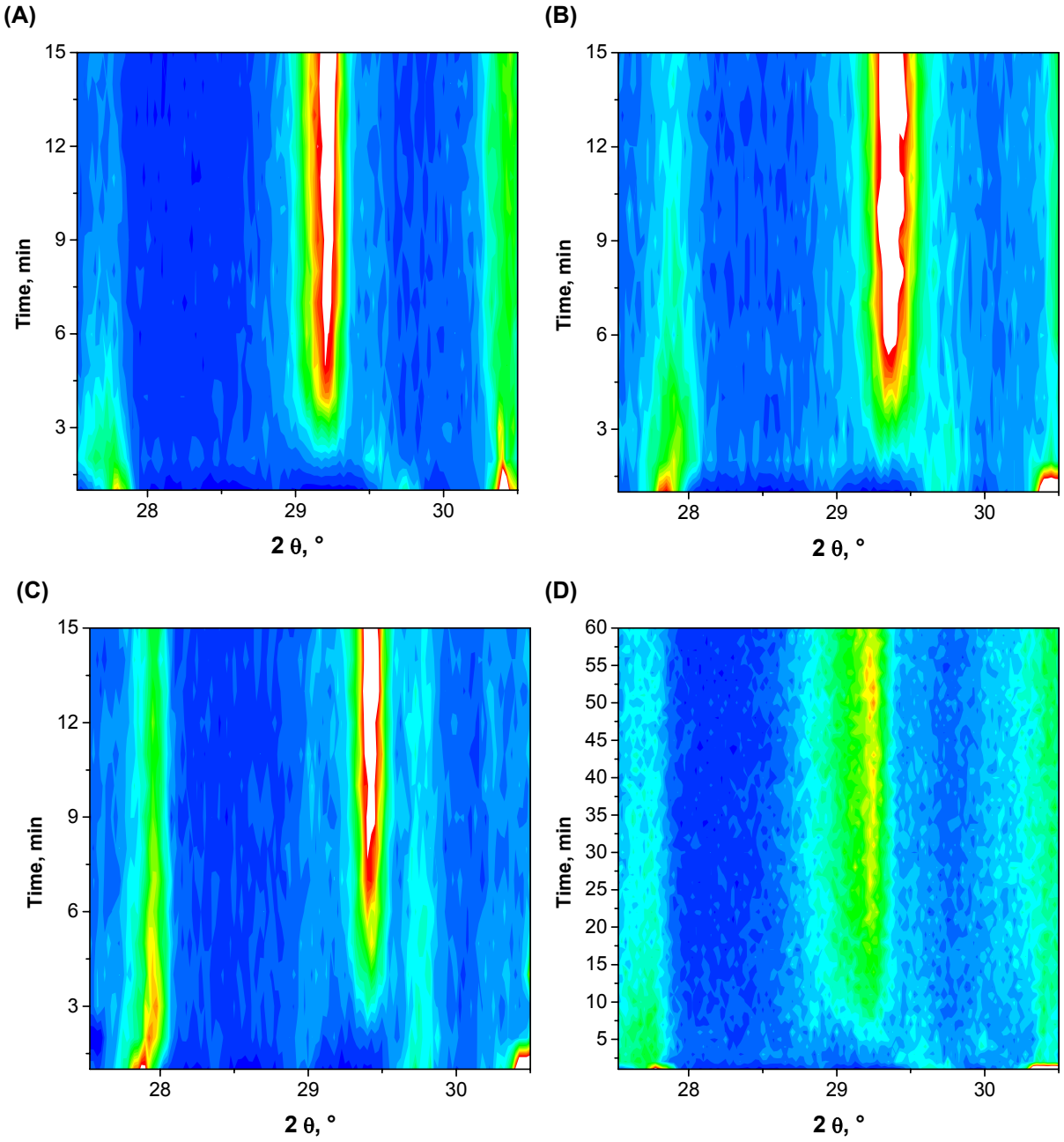
(A)
(B)
(C)
(D)
Time, min
2 θ, °
28
29
30
3
6
9
12
15
5
10
20
25
35
40
45
50
55
60

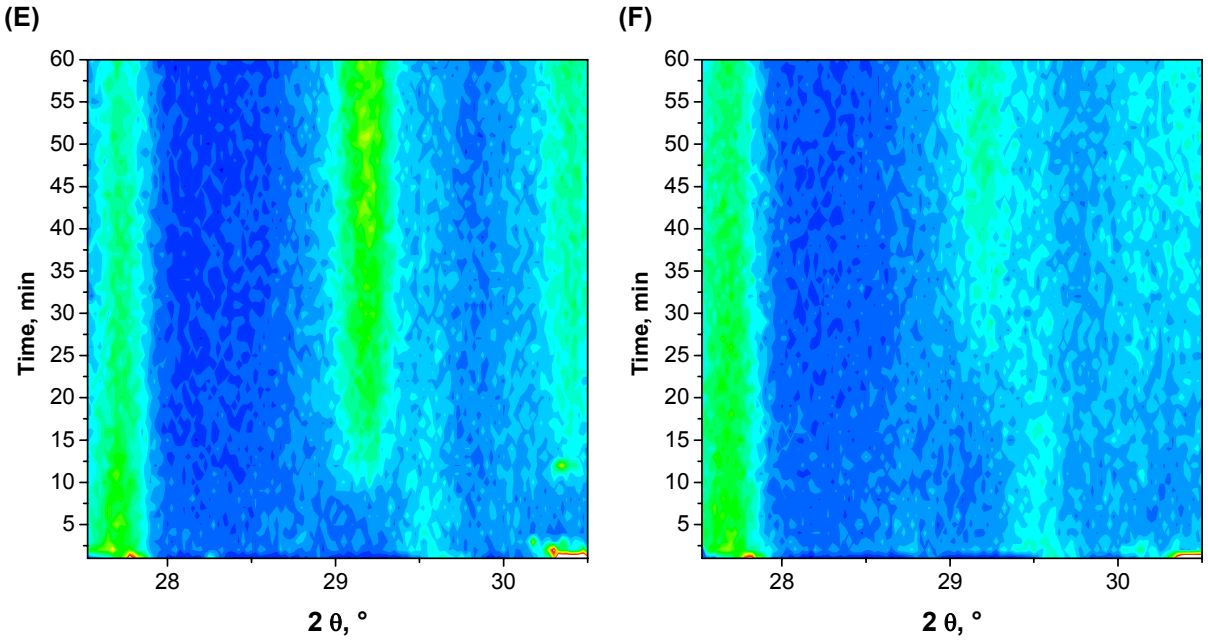

Figure 29: XRD spectra changes using sodium citrate-containing setting liquids of (A) 62.5 mmol/l, (B) 125 mmol/l, (C) 250 mmol/l, (D) 500 mmol/l, (E) 750 mmol/l, and (F) 1000 mmol/l. Blue indicates low, green/ yellow higher and red the highest signal intensity. Color scaling is constant for all spectra, therefore very high signal intensities may be expressed as white areas.

The addition of sodium citrate had no significant effect on the dissolution of MCPM. The initial reduction in the XRD signal at 30.4° was very fast for all citrate concentrations. On the other hand, the dissolution of β-TCP and the formation of DCPD were clearly slowed down in a citrate concentration-dependent way. With the addition of citrate ions, dissolved calcium is kept in solution and may therefore not react into DCPD. In consequence, new calcium phosphate from the β-TCP fraction cannot go into solution because the aqueous phase is still saturated with calcium ions. At higher citrate concentrations, the probability of calcium reacting with citrate instead of phosphate increased, thus decelerating the cement setting. The reduction rate of the β-TCP peak at 27.82° and the formation rate of the DCPD peak at 29.24° are significantly slowed down.

3.3.2.4 Comparison with isothermal DSC results

Isothermal DSC offers the possibility of monitoring endothermic and exothermic events of the setting reaction continuously by recording the heat flux from the sample (Figure 30). In this study, the freshly mixed cement was wetted directly in the DSC; the setting reaction could thus be monitored immediately. No time was lost as reported with other studies where the setting reaction was started externally prior to placement of the sample in the DSC[366].

Upon the addition of the setting medium and correlating with the XRD data, the pronounced endothermic peak reflects the fast dissolution of MCPM. The following exothermic peak indicates the crystallization of DCPD from the aqueous system. The peak maximum should be consistent with the maximum slope of a peak between two consecutive XRD spectra. While iDSC and XRD can support each other in the explanation of the aforementioned processes, only XRD can give information on the time-dependent chemical composition of the observed system. Isothermal DSC alone is not able to show which component is dissolved, how much is dissolved or what crystals are formed during the setting.

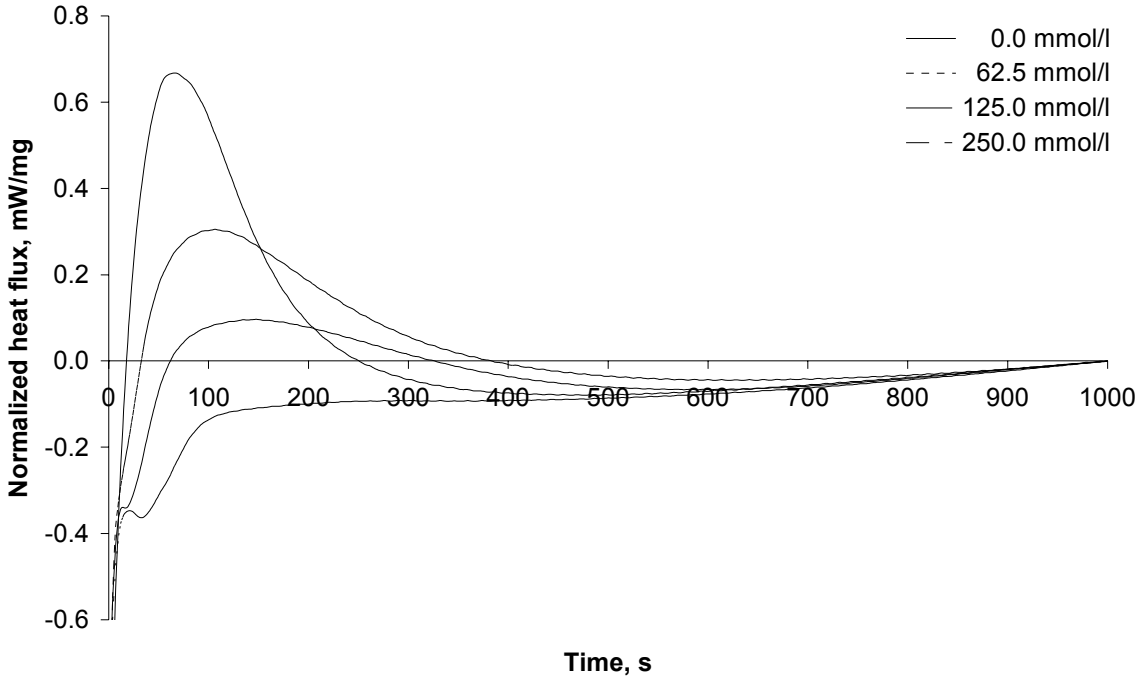

Figure 30: Normalized heat flux curves from isothermal DSC measurements taken on a CPC wetted with 20 µl sodium citrate solution of the given concentrations starting from the maximum endothermal deflection due to the dissolution of MCPM.

3.3.2.5 Comparison with FT-IR results

FTIR has been used to monitor the setting reaction[367, 373]. In our study, ATR-FTIR was only of limited use to monitor the kinetic of the setting reaction. The reaction of the cement using just water as setting liquid was too fast to obtain useful IR spectra. Too few scans resulted in quite high signal-to-noise ratios and an increase in the number of scans reduced the time resolution. These different findings to previous reports may be attributed to the different particle sizes of the β-TCP used in the cited and in this study. While Hoffmann et al.[366] reported a mean diameter of 11 µm, the β-TCP particles in this study had a mean diameter of approx. 2 µm. The smaller particle size resulted in a faster dissolution of the β-TCP particles, a faster supersaturation of the aqueous phase within the cement and a faster setting with the formation of DCPD crystals.

Spectra recorded with sodium citrate solutions as setting medium provided only limited information. The spectra recorded 20 s after the addition of a sodium citrate solution

(125 mmol/l) were almost identical to the ones recorded 10 min later. In both spectra, only DCPD could be clearly identified. The strongest peak of β-TCP at 1020 cm^{-1} was not found in any spectra during cement setting. However, a smaller peak at 947 cm^{-1} that showed a time-dependent decrease during setting may be attributed to β-TCP, which has a peak of less than a third of the intensity of the 1020 cm^{-1} peak at this position. While this peak showed a continuous decrease in intensity during the observed period of 10 min, the signal intensity for the formed DCPD reached its maximum already at 2 min and did not significantly change during the remaining measurement.

The limited use of ATR-FTIR can be explained by its small measuring depth, which is usually less than 2 μm[374] and can be even smaller for samples with low infrared transparency. Therefore, ATR-FTIR measures just within a very small volume above the ATR-crystal, which is rapidly filled by precipitating DCPD crystals.

In contrast, the presented XRD method measures with a much larger depth of several hundred micrometers, giving an overview of the chemical composition in large parts of the sample.

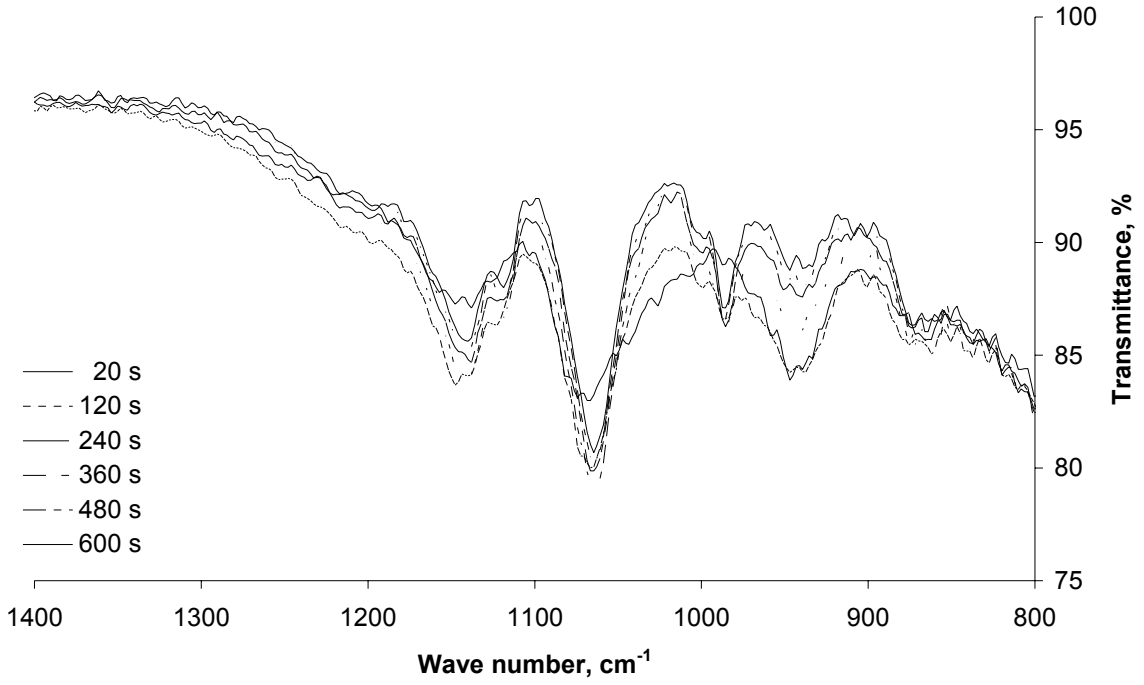

Figure 31: ATR-FTIR-spectra obtained from the setting of a DCPD-forming calcium phosphate cement, mixed directly on the ATR-crystal with 125 mmol/l sodium citrate solution (powder-to-liquid ratio 1:1).

3.3.3 Conclusions

The crystallographic changes during the setting of a calcium phosphate cement into calcium hydrogen phosphate dihydrate (DCPD) were monitored using conventional powder x-ray diffraction (PXRD) equipment. A time resolution of about 1 min was achieved by limiting the range of scanned angles to the major peaks of the reactants and the product, which was sufficient to track dissolution and crystallization processes of the cement components. The effective resolution was increased by the addition of sodium citrate as setting retardant. While the dissolution of calcium dihydrogen phosphate monohydrate (MCPM) was virtually not affected by the amount of citrate (0 – 1000 mmol/l) added, the dissolution of β-calcium phosphate (β-TCP) and the formation of DCPD were. The results of the presented PXRD technique were compared to those obtained from isothermal differential scanning calorimetry (iDSC) or Fourier-transformation infrared spectroscopy (FTIR). Time-resolved powder x-ray diffractometry was able to monitor the crystallographic changes during the setting of the DCPD-forming cement. While correlation with iDSC results was very good, correlation with FTIR was rather poor, mainly due to inherent limitations of FTIR.

3.4 Storage stability of a DCPD-forming calcium phosphate cement for bone tissue engineering monitored by iDSC, DVS, FTIR, XRD and mechanical testing

3.4.1 Introduction

Self-setting calcium phosphate cements (CPC) have been proposed as bone implants and drug delivery systems for the filling of larger bone defects, e.g. after the resection of bone tumors[87, 311]. Mainly, two types of cements can be distinguished based on the formed product, namely hydroxylapatite (HA) or calcium hydrogen phosphate dihydrate (DCPD, brushite). HA-forming cements have drawn much more attention than DCPD-forming cements due to their similarity to the chemical composition of natural bone[84]. In addition, their mechanical properties are inherently superior to those of the DCPD-forming cements[290]. However, DCPD-forming cements have advantages as bone void fillers, too. Their faster resorption in biological systems can provide shorter healing times than the poorly soluble HA implants, especially in combination with suitable drugs and drug delivery systems[66, 375]. Besides mechanical strength and resorption rate, HA- and DCPD-forming CPCs also differ in parameters such as surface pH and biocompatibility. However, these differences are of minor clinical interest.

From a chemical perspective, the major difference between the two types of cement is the role of water in the setting process. With HA-forming cements, consisting of tetracalcium phosphate (TTCP) and dicalcium phosphate (DCP), water just acts as dissolution medium for the reactants and as transport medium for the dissolved ions. The setting reaction is a crystalline transformation in aqueous media, in which no water is "consumed" (Equation 7).

$$Ca_4(PO_4)_2O + CaHPO_4 + H_2O \rightarrow Ca_5(PO_4)_3(OH) + H_2O \qquad \text{Equation 7}$$

(TTCP + DCPA + Water → HA + Water)

This is different to DCPD-forming cements, where the setting involves the "consumption" of water by binding it into the final product (Equation 8).

$$\beta\text{-}Ca_3(PO_4)_2 + Ca(H_2PO_4)_2 \cdot H_2O + 7\ H_2O \rightarrow 4\ CaHPO_4 \cdot 2\ H_2O \qquad \textbf{Equation 8}$$

(β-TCP + MCPM + Water → DCPD)

The different role of water may make premixed DCPD-forming cements look less sensitive to small amounts of moisture during storage than HA-forming cements, as these amounts would be bound in the reaction, while for the HA-forming cements the amount of available water would stay the same during storage. However, a pronounced loss in reactivity and mechanical strength with increasing storage time ("ageing") was reported for premixed DCPD-forming CPCs stored under humid conditions[120, 376, 377].

The objective of this study was to investigate/explain processes occurring during "ageing" of a premixed DCPD-forming calcium phosphate cement under different storage conditions with various analytical techniques.

3.4.2 Results and discussion

A combination of analytical techniques was used to identify the processes behind the cement "ageing". The proposed mechanisms will be discussed already with the iDSC measurements, other results will then be used to confirm the given explanations.

3.4.2.1 Isothermal DSC measurements (iDSC)

Isothermal DSC has been used to monitor the rate and extent of the setting reaction of aqueous CPC slurries by measuring the heat flux from the sample[366]. We applied this technique to monitor the changes in the reactivity of premixed cement powder samples stored under different conditions over time.

The total amount of released energy (reflected by the area under the curve) (Figure 32 A) and the maximum heat flux (Figure 32 B) during induced setting decreased with increasing storage time of the premixed cement. The maximum heat flux decreased in an exponential manner (Figure 32B) and thus suggests a first-order kinetic ageing process.

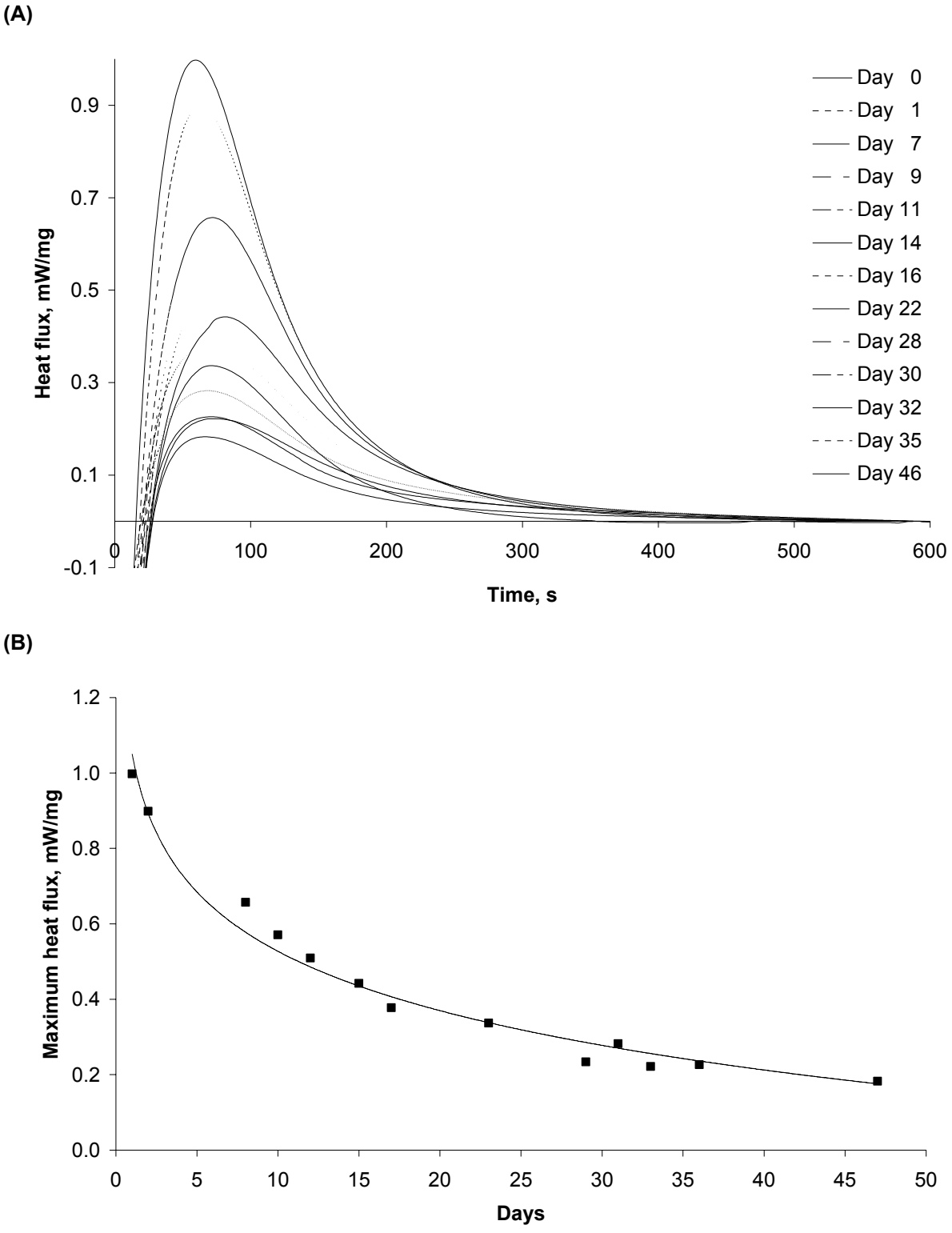

Figure 32: (A) Heat flux curves obtained by isothermal DSC during induced setting of premixed CPC powder as a function of storage time. (B) Maximum heat flux obtained by iDSC during induced setting of premixed CPC powder stored for up to 46 days. (Both: Room temperature, closed container)

The ageing had no significant effect on the time to reach the peak maximum (Figure 1A). The setting reaction itself therefore apparently was not affected by ageing. However, as setting time is usually defined by the acquired mechanical strength, a reduced total reaction will result in a prolonged setting time, as it takes longer to reach a certain amount of new crystal formations in the setting cement.

It is most likely that the process occurring during ageing of the cement is identical to the normal setting reaction. This assumption will be confirmed by the results of other analytical techniques later.

It could be speculated that the hygroscopic MCPM would draw water into the sample, enabling the reaction. However, DVS results will show that the hygroscopicity of MCPM cannot alone explain a water uptake causing local condensation and thereby reaction.

The used β-TCP powder has a very fine particle size, thus the surface of the β-TCP component is very large and the number of touch points and therefore also structures acting as small capillary structures is very high. As the vapor pressure in the small capillaries is reduced, this can facilitate local moisture condensation. The effective radius of the capillaries is extremely small, therefore the reduction of the vapor pressure can account for the condensation of small amounts of moisture even at very low humidity levels.

Even the formed small amounts of water can dissolve calcium and phosphate ions from the reactants, creating small spots of saturated calcium phosphate solution and subsequent precipitation of DCPD. Due to the very different solubility of MCPM and β-TCP, it is likely that MCPM dissolution is much more pronounced than β-TCP dissolution within these spots. Therefore, the precipitation of newly formed DCPD will take place preferably on the surface of β-TCP particles. While the ageing process proceeds, the surface of the cement particles will become increasingly covered by a thin layer of DCPD. The observed reduction of the “speed of ageing” and the conservation of some reactivity even after long storage times can be explained by this thin DCPD layer, acting as a protective coating for the underlying reactants. Larger amounts of water, as they are used in the induced setting reaction, can dissolve parts of the covering DCPD and react with the now uncovered reactants.

Due to the suggested model, the rate and extent of the ageing process will be affected by the particle size of the cement reactants. Cements consisting of larger particles should show slower and less pronounced ageing. However, β-TCP particles above a certain size may not

completely dissolve upon addition of water and therefore leave a significant amount of unreacted β-TCP in the set cement making the use of large β -TCP granules problematic.

3.4.2.2 Mechanical tests

A pronounced reduction in the resistance to needle intrusion was seen for the set cement samples obtained previously by the iDSC measurements. The reduction in mechanical strength occurred already within the first days, reaching a fairly stable plateau after around 14 days (Figure 33:).

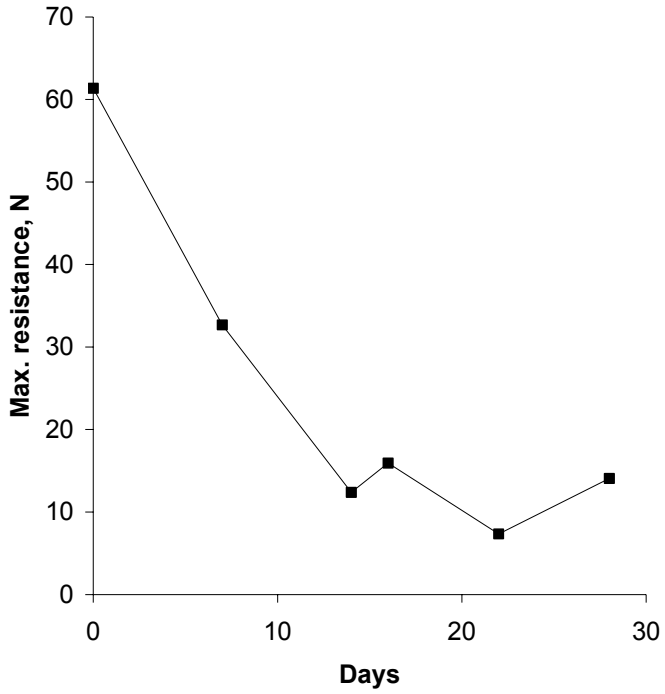

Figure 33: Maximum resistance to needle intrusion of premixed CPC powder samples stored up to 28 days after induced setting (room temperature, closed container).

The loss in mechanical strength after induced setting was higher for samples stored at higher RH levels. It was more pronounced with the hardened slurry samples tested with the needle test (Figure 34 A) than with set tablets measured with the indirect compression test (Figure 34 B). After one week of storage, only the slurries prepared from cement powder kept at 0 % RH still significantly hardened, whereas those from powders stored at higher humidity

failed to form stable crystal networks. Already the storage at only 33 % RH resulted in a decrease in mechanical resistance to less than one tenth of the value of samples stored under dry conditions.

The mechanical strength of the set samples from the slurries (Figure 3 A) was much lower than that of the set samples from the iDSC (Figure 2). This can be explained with the different preparation processes. While the samples from the iDSC were not agitated during the complete setting period, the samples prepared from the slurries were mixed during the first 20 s of setting. As the mechanical strength of the cement relies on a well-entangled crystal network, any stirring inhibits network formation and therefore impairs the mechanical properties of the set cement, as seen with the slurries.

(A)

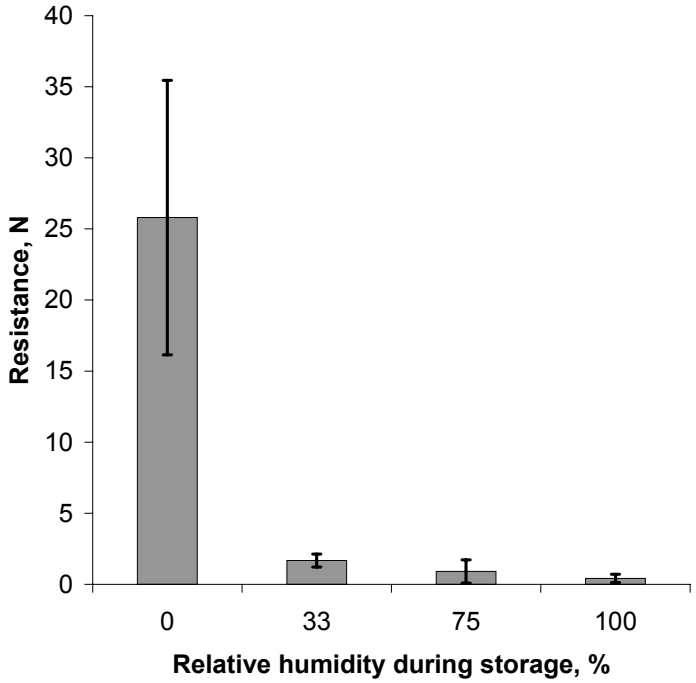

(B)

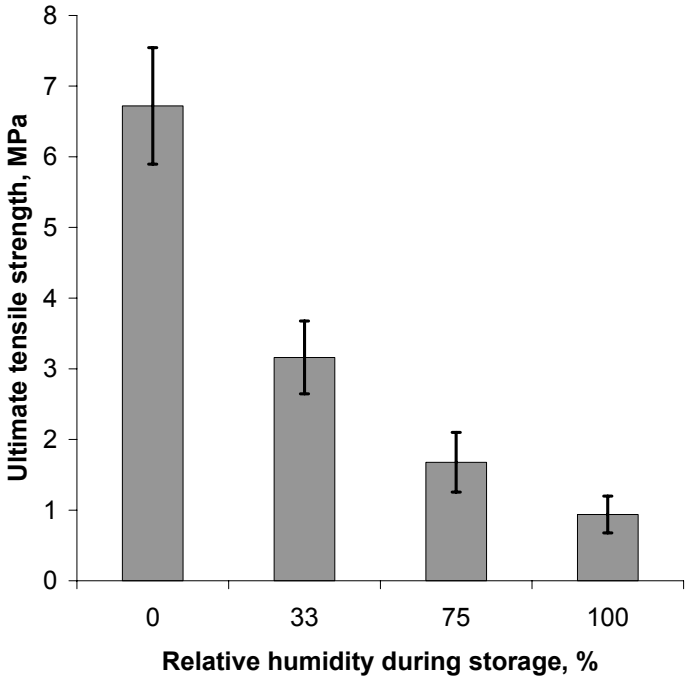

Figure 34: Mechanical strength of set CPC samples after storage of the unset cement at different relative humidities for one week. (A) Resistance to needle intrusion of a hardened CPC slurry prepared from loose premixed CPC powder. (B) Ultimate tensile strength of CPC tablets compressed before storage after induced setting.

Within the tablet samples, crystal network formation was undisturbed like in the iDSC samples. A better differentiation between ageing effects at different humidity levels was possible as the larger samples allowed the use of the more accurate testing method. The reduction in mechanical strength followed an exponential relationship, leveling off at higher storage humidities. This supports the assumption of larger parts of the cement being transformed into DCPD during storage but also of leaving some reactants still available for setting after the addition of larger amounts of water.

Mechanical tests on the unset tablets revealed a minor increase in hardness during storage with moisture exposure (Figure 35:). Interestingly, this increase was approximately the same for all humidity storage conditions and might be explained by the fusion of the cement particles at their surfaces caused by dissolution and precipitation processes in the presence of moisture. This process was independent of the formation of larger DCPD crystals and therefore not related to a real cement hardening.

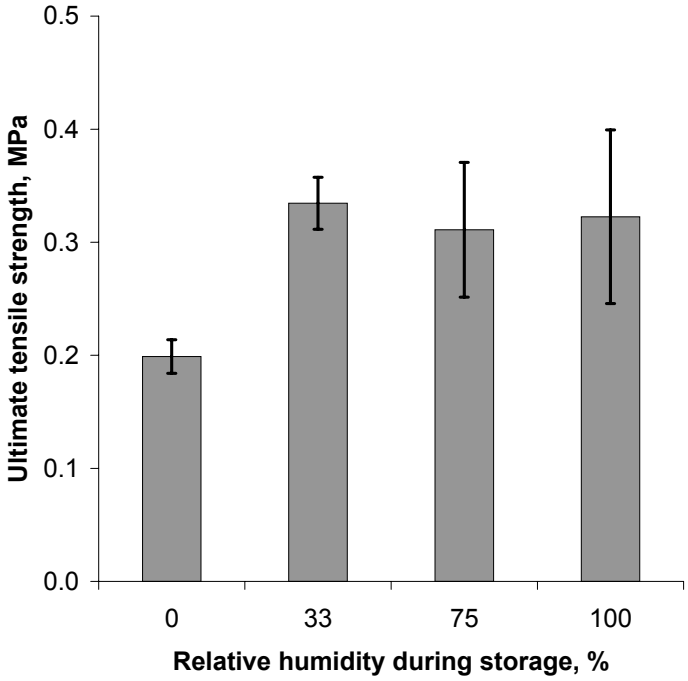

Figure 35: Ultimate tensile strength of unset CPC tablets stored in different humidity conditions at room temperature. Initial hardness was around 8 N (0.189 MPa) for all tablets.

3.4.2.3 Dynamic vapor sorption (DVS) measurements

DVS measurements were performed to quantify the amount of water within the cement system and to distinguish between chemically bound and free water. Adsorbed surface water completely desorbs upon drying, while water reacting with the cement does not, resulting in an irreversible mass gain. This mass gain can be used to quantify the fraction of cement powder reacting during the DVS measurement, as reaction stoichiometry, molecular weights of the reactants and initial weight of the sample are known (Equation 9). For the complete reaction of the cement, a mass gain of 18.3 % is expected.

$$\beta\text{-}Ca_3(PO_4)_2 + Ca(H_2PO_4)_2 \cdot H_2O + 7\ H_2O \rightarrow 4\ CaHPO_4 \cdot 2\ H_2O \quad \textbf{Equation 9}$$

$$(310.18 + 252.08 + 7 \cdot 18.02 = 4 \cdot 172.09 = 688.36)$$

In a first step, the water uptake of the pure compounds was tested. Neither MCPM (Figure 36 A), nor β-TCP (Figure 36 B) showed any irreversible water uptake as indicated by a return to the original mass upon drying.

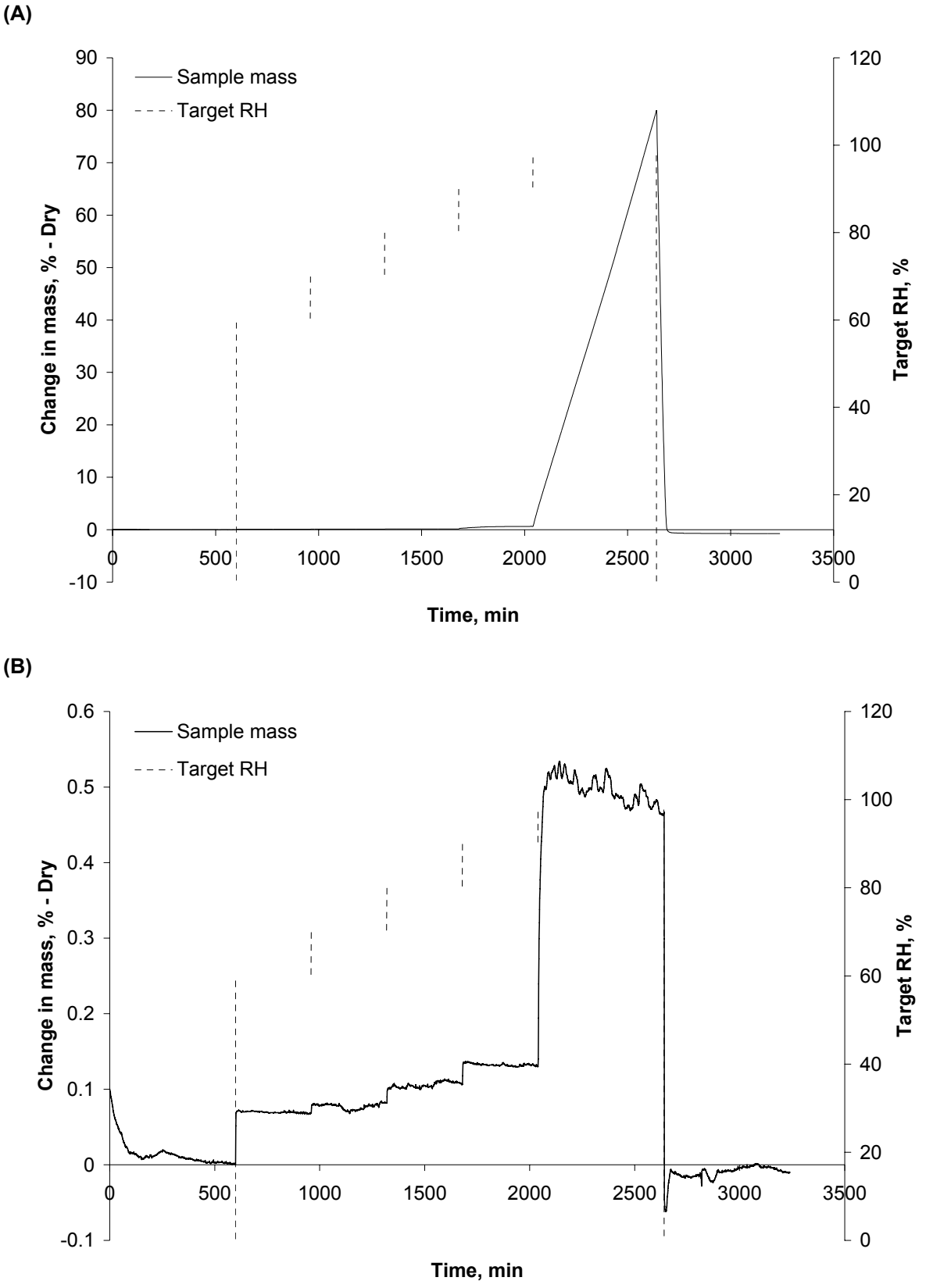

Figure 36: Changes in mass due to moisture uptake for (A) MCPM powder and (B) β-TCP powder at 30 °C.

At the highest humidity tested, the water uptake of MCPM was much higher than of β-TCP. This was expected, as MCPM is considered hygroscopic. However, up to a RH of 80 %, the sorption isotherms of MCPM and β-TCP were not significantly different; the moisture uptake of MCPM was 0.12 % w/w and 0.10 % w/w for β-TCP. The pronounced moisture uptake of MCPM starting from ≥ 90 % RH, resulted in a continuous linear mass increase that caused the formation of a concentrated MCPM solution at 98 % RH, as indicated from the appearance of recrystallized MCPM after the final drying step.

Next, the water uptake of the premixed cement powder stored in closed container at room temperature was evaluated as a function of storage times (Figure 37).

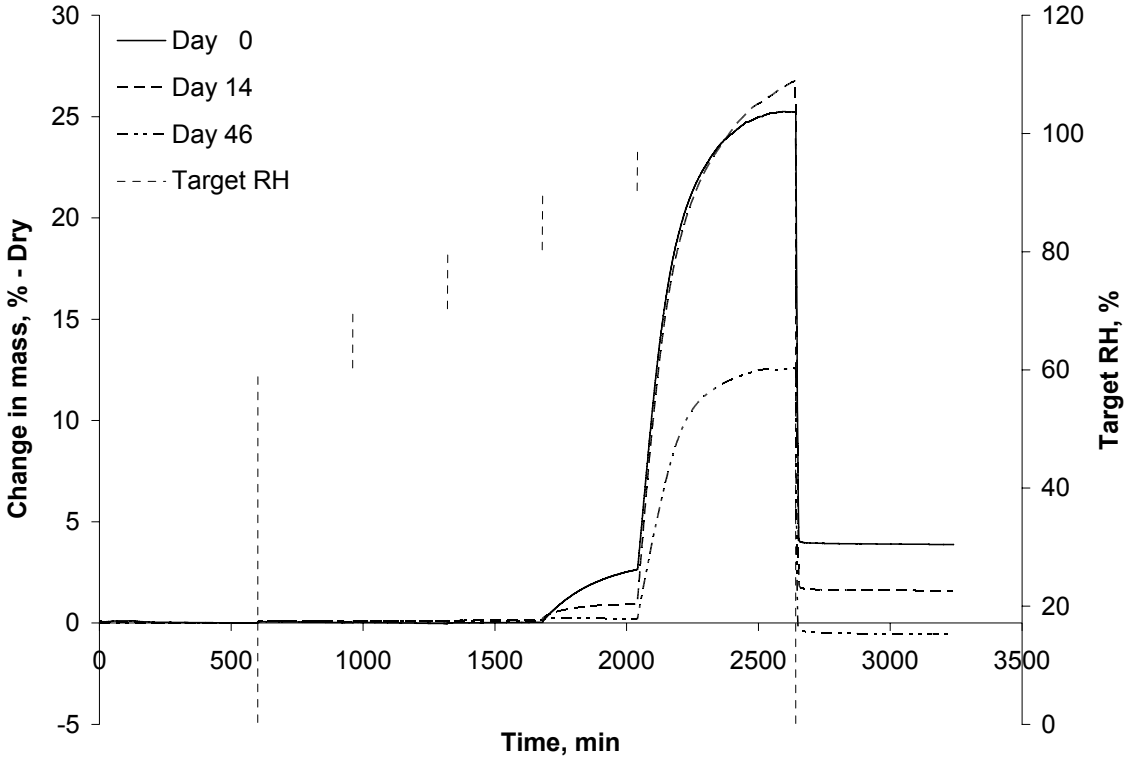

Figure 37: Changes in mass due to moisture uptake for a premixed CPC powder consisting of MCPM and β-TCP stored at room temperature for the given number of days (closed container).

In contrast to the pure calcium salts, the mass gain of the premixed cement powders was not completely reversible after drying. This irreversible mass gain resulted from the chemical binding of water, which took place during the cement setting. As expected, the amount of irreversible water uptake during the DVS measurement reduced with increasing storage times.

Moisture uptake was not limited to the presented high humidity conditions, but was also found with fresh cement samples exposed to just 5 % RH. The mass gain due to the absorption of water was small but clearly detectable (0.02 %). Around 0.005 % mass gain was irreversible, as it did not change during 6 h of subsequent drying (data not shown). Thus, the cement was very sensitive to moisture.

Some samples were stored at -70 °C. In the absence of moisture, the reactivity of the cement did not significantly change for at least 35 days (Figure 38).

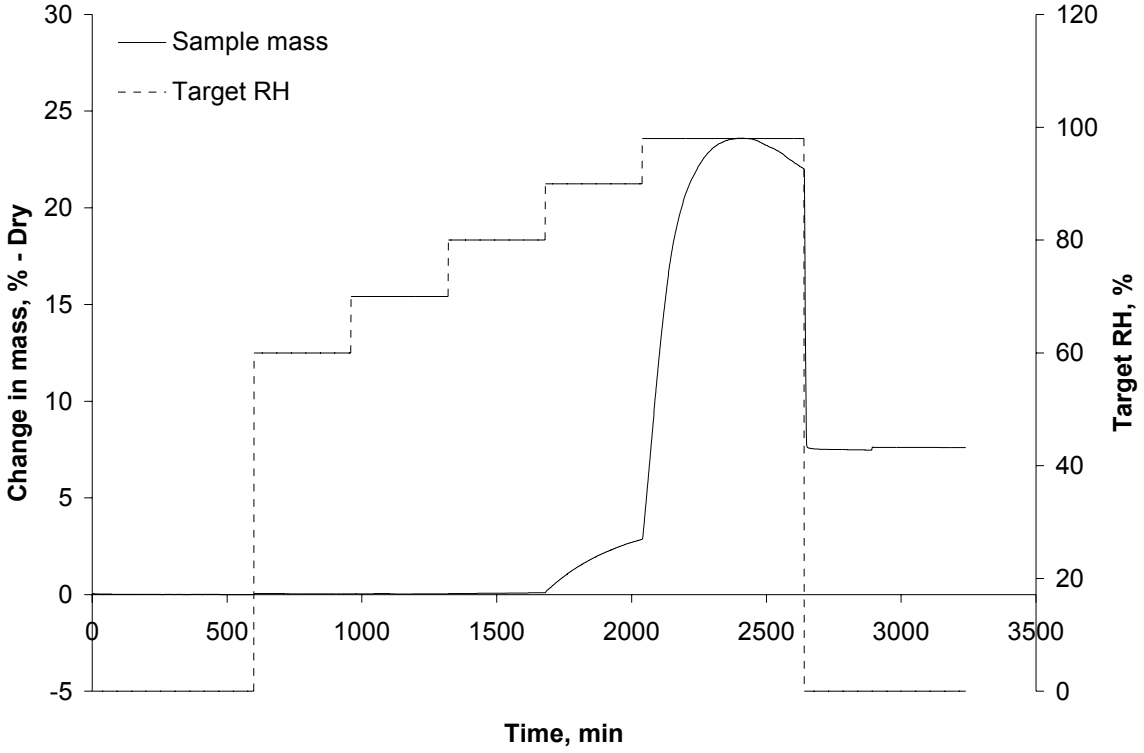

Figure 38: Change in mass due to moisture uptake during a DVS run for a premixed CPC powder stored at -70 °C for 35 days (closed container).

The cement stored at -70 °C showed a mass gain comparable to fresh cement. A mass gain of more than 5 % indicated that more than 30 % of the setting process had taken place under the given DVS conditions (calculations based on Equation 9).

Due to the small sample mass of just around 20 mg, already small inhomogeneities in the ratio between MCPM and β-TCP can have a significant result on reversible and irreversible water uptake. Therefore, the shape of the curve at 98 % RH was interesting. The strong increase could be attributed to the hygroscopic nature of MCPM, drawing high amounts of

water into the cement. The increase leveled off with most samples, or – for the cement stored at -70 °C – even turned into a decrease during the high humidity phase. This could be explained by the increasing conversion of the sample into non-hygroscopic DCPD. The amount of hygroscopic MCPM decreased, thus enabling some water to desorb from the sample. As this indicated that the reaction was already at a later stage for the presented cement sample stored at -70 °C, the total irreversible mass gain within the DVS run had to be higher than that of the room temperature sample presented before.

Freshly mixed CPCs using MCPA and β-TCP as reactants were also studied. The water uptake curves of these cements showed a fast initial water uptake, not present for samples using MCPM, followed by a comparable plateau and finally a larger total mass gain (Figure 39).

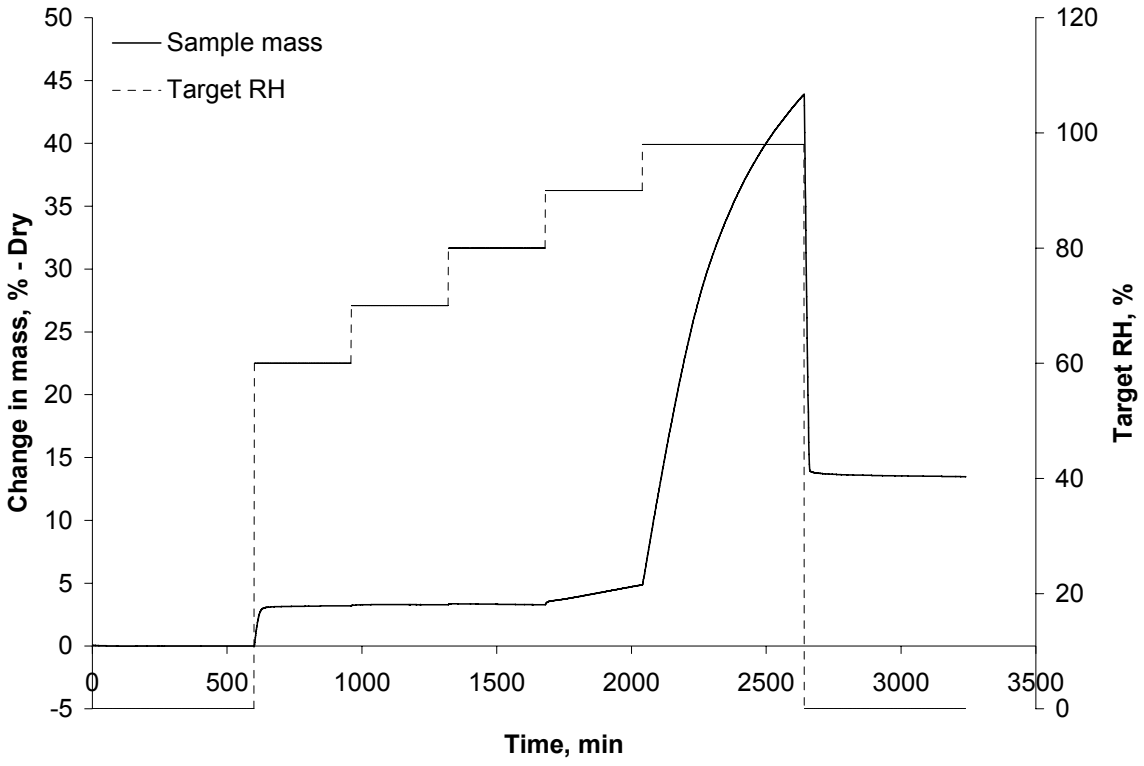

Figure 39: Change in mass due to moisture uptake for a CPC powder prepared from freshly prepared anhydrous MCP (MCPA) and β-TCP.

The mass gain for a complete conversion from MCPA into MCPM should be around 7.7 %. As only around 43.0 % w/w of the applied cement mixture consisted of MCPA, the effect of the conversion of MCPA into MCPM was expected to be around 3.3 %. The experimental

data of 3.1 % within 60 min at 60 % relative humidity, reaching 3.3 % at the time of the 70 % relative humidity step, are in very good agreement with this assumption. This test confirmed the presence of pure MCPM in former experiments and the validity of the method.
For this last DVS run, a total mass gain of approx. 13.5 % was observed, leaving a mass gain of 10.2 % for the setting of the cement. Thus, more than 55 % of the cement powder had reacted after the run although no liquid water was added.

3.4.2.4 ATR-FTIR measurements

ATR-FTIR revealed a complete transformation of the cement powder into DCPD during storage under humid conditions (Figure 40). While the sample stored under dry conditions showed the characteristic peaks of β-TCP (947, 972, 1020 cm^{-1}), the samples stored under humid conditions showed only peaks at positions characteristic for DCPD (989, 1059, 1124 cm^{-1}). The "complete" conversion of the cement into DCPD has to be attributed to the small sampling depth (< 2 μm[374]) of the ATR-FTIR method, which will reflect information mostly from within the DCPD-surface layer and thus accounts for the missing MCPM signals in the cement stored under dry conditions.

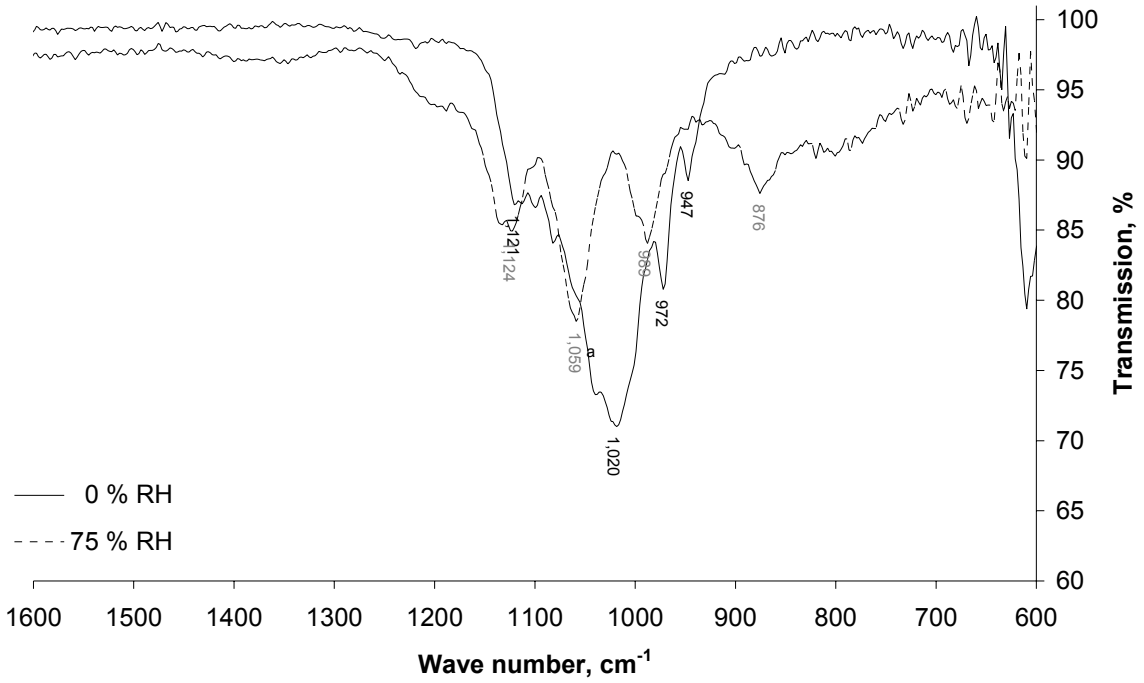

Figure 40: IR spectra of premixed DCPD-forming CPC powders stored at room temperature at either 0 % RH or 75 % RH for one month.

3.4.2.5 Powder x-ray diffractometry (PXRD) measurements

In contrast to ATR-FTIR measurements, PXRD has a sampling depth of more than one hundred micrometers, depending on material, angle and other factors[378-380]. Like with ATR-FTIR, quantification is theoretically possible but has to take care of several limitations[371].

PXRD showed virtually no conversion into DCPD for the cement stored at 0 % RH but comparable signal levels of conversion for cements stored at 33 %, 75 % or 100 % RH (Figure 41). Besides, it revealed the presence of unreacted MCPM and β-TCP in all samples confirming the surface coating theory.

Additionally, some signals for DCPA could be identified with samples stored in humid conditions. This is consistent with other reports on the transformation of DCPD into the thermodynamically more stable DCPA during storage[120].

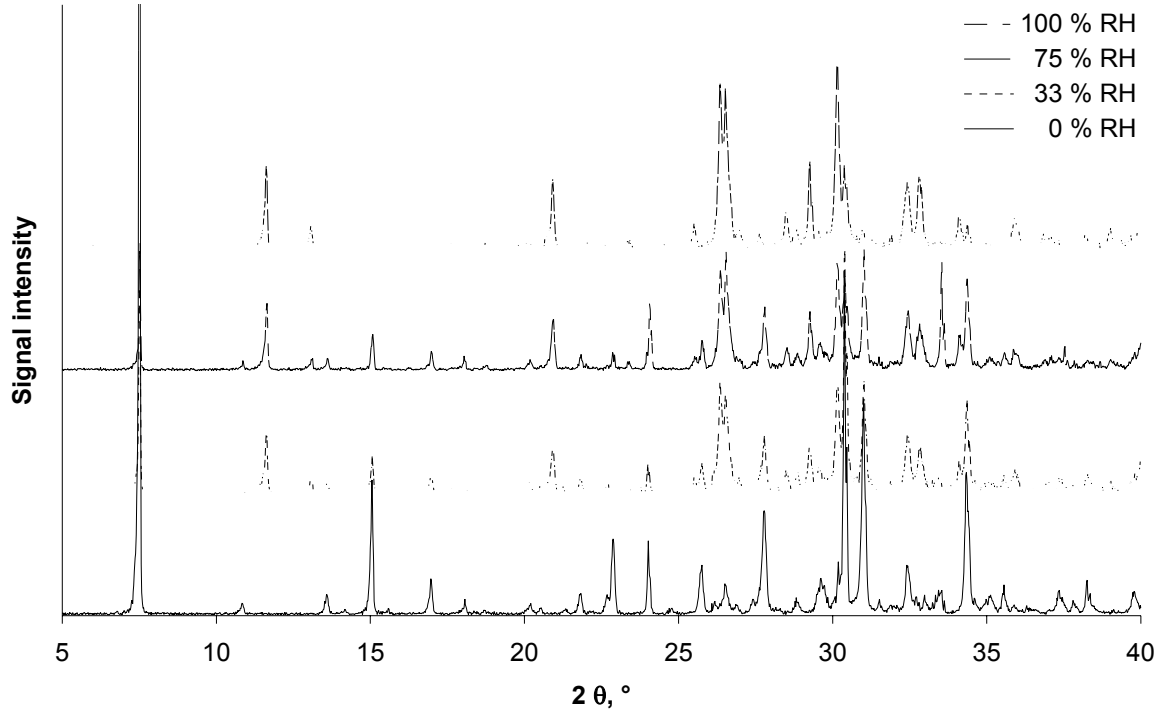

Figure 41: PXRD spectra of premixed CPC powders stored under different humidity conditions for one month.

X-ray irradiation offered an interesting option to semi-quantify the amount of DCPD formed during storage, which was more sensitive than PXRD or FTIR. Among the tested compounds (MCPM, DCPA, DCPD, β-TCP, HA), only DCPD showed a change in color when exposed to x-rays (Figure 42). This yellowish to brownish color change could be visually observed for samples containing less than 2 % of DCPD in a matrix of β-TCP. With colorimetric approaches, an even higher sensitivity should be feasible. The color change correlated with the DCPD concentration but not with the duration of x-ray irradiation in the investigated range; 25 min resulted visually in the same coloring as 180 min. The color change was reversible resulting in white samples after a few days.

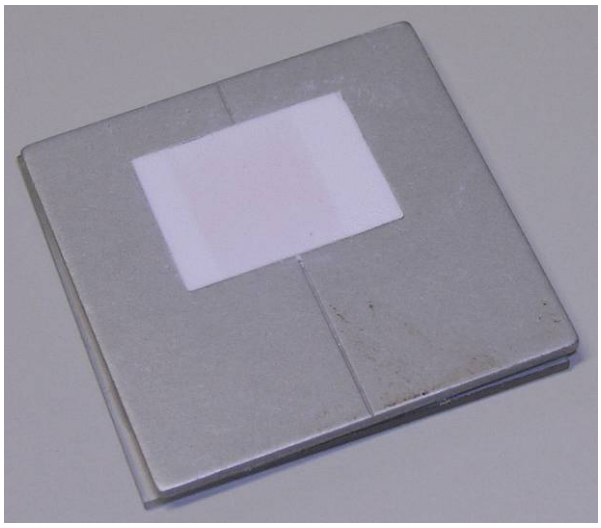

Figure 42: Reversible color change of DCPD after x-ray irradiation. Reddish-brown areas indicate areas irradiated with x-rays, while white parts at the sides consist of non-irradiated DCPD powder.

3.4.3 Conclusions

Calcium phosphate cements, consisting of equimolar blends of calcium dihydrogen phosphate monohydrate (MCPM) and β-tricalcium phosphate (β-TCP) form calcium hydrogen phosphate dihydrate (DCPD) upon contact with water. The cements are not storage stable under ambient conditions, since a pronounced loss in the mechanical properties of the set cements takes place. The underlying processes and the resulting chemical and structural changes of cement ageing were characterized by isothermal differential scanning calorimetry (iDSC), dynamic vapor sorption (DVS), Fourier-transformation infrared spectroscopy (FT-IR), x-ray diffractometry (XRD) and mechanical testing (texture analyzer). Ageing could be attributed to moisture uptake during storage. Already small amounts of available and absorbed moisture result in a pronounced loss in cement reactivity and mechanical strength, while leaving the normalized reaction rate unaffected. A consequent storage of the premixed cement in moisture free environment, e.g. at temperatures below 0 °C is therefore necessary. The ageing process was identified as transformation of the outer surface of the reactant particles into a thin layer of DCP. This coating explains the observed slowing down of the ageing effect and the existence of at least some reactivity even with quite old cements.

4 Summary

In order to develop a biodegradable bone void filler that could withstand at least moderate loads and increase the healing process after a larger bone damages, first, a self-setting calcium phosphate cement (CPC) consisting of calcium dihydrogen phosphate monohydrate (MCPM) and β-calcium phosphate (β-TCP) was developed. The product of this cement was calcium hydrogen phosphate dihydrate (DCPD).

The fine particle size of the β-TCP (approx. 2 µm) resulted in very fast setting when mixed with water. The effective working times were less than one minute when prepared with reasonable powder-to-liquid ratios (< 1:2). This was much too short for any clinical application. Higher powder-to-liquid ratios increased the working time to some extent but reduced the mechanical strength of the set cement significantly. A retardation of the setting reaction without effects on the mechanical strength of the cement thus had to be found. The addition of sodium citrate as setting retardant is widely reported in the literature. Different to the findings usually described there, sodium citrate had a pronounced negative effect on the mechanical strength of the set cement. These effects were quantified by mechanical testing. Test on compressive and tensile strengths were performed using uniaxial direct compression and indirect compression tests. Providing adequate sample geometry was very hard for uniaxial direct compression tests resulting in high variations of the obtained results. Indirect compression tests showed more consistent results and were therefore used as standard method. For measurements on very small samples, a needle intrusion method was developed.

An exponential trend in the loss of the mechanical strength with increasing citrate concentrations used in the applied setting liquids was found.

This was accompanied by an exponential trend in the loss of the reaction rate. Isothermal differential scanning calorimetry (DSC) measurements, performed on conventional DSC equipment, revealed an exponential trend in the increase of the time to reach the maximum heat flux from the samples with increasing citrate concentrations. With very high citrate concentrations in the setting medium (1000 mmol/l), setting was still incomplete after 12 h. The effects of citrate addition on the cement setting were additionally observed by ATR-FTIR and powder x-ray diffractometry (PXRD). In contrast to previously reported results, the use of ATR-FTIR on monitoring the setting reaction of fast setting DCPD-forming calcium phosphate cements was low. This had to be attributed to inherent limitations of ATR-FTIR. New formed DCPD crystals from the cement slurry sedimented on the ATR-crystal. In

combination with the small measuring depth, ATR-FTIR thus indicated a much faster reaction than other analytical methods.

To observe the setting reaction with powder x-ray diffractometry (PXRD), a method providing sufficient time and spatial resolution for the dissolution and crystallization processes during setting had to be developed. A time-resolution of around 1 min could be achieved, which was sufficient to distinguish between the effects of different citrate concentrations. The kinetic results obtained by this time-resolved PXRD method, which could be deduced from the slopes of the formed peaks, were in very good agreement with data on the setting reaction obtained by isothermal DSC. Additionally, time-resolved PXRD revealed semi-quantitative information about the undissolved reactants and on the formed crystalline reaction product.

As the mechanical strength of DCPD-forming calcium phosphate cements is an overall issue, methods to increase the working time without impairing mechanical properties had to be found.

Temperature is known to have significant effects on virtually all chemical reactions. A decrease in temperature thus should prolong the setting time of a calcium phosphate cement. The effects of different temperatures, ranging from 4 – 40 °C were tested. Isothermal DSC revealed the expected temperature-reaction rate relationship over most of the observed temperature range. At the lower and upper end of the range, deviations were observed, most likely caused by effects of temperature also on the dissolution of the reactants. In total, temperature decrease proved very predictable and, despite some complexity, practicable to increase the setting time without weakening the set cement.

As the issue of short working times arises from the immediate start of the setting reaction after wetting the cement, working with dry cement would not have to face this issue at all. Thus, the cement was applied as powder and wetted at the final “setting site”. This allowed the application of predefined forces prior to setting to increase the cement’s density and thus mechanical strength. The observed effects for the compression of the dry powder prior to initiating the setting reaction by the addition of water were more pronounced and developed at lower forces than previously reported.

Due to the low particle size of the β-TCP, the flowability of the prepared calcium phosphate cement was very poor. This could be overcome by the addition of polycaprolactone (PCL) microparticles. The microparticles adsorbed the fine cement particles on their surface and thus partially transferred the fine powder into a sphere-shaped granulate material. However, the

addition of the microparticles, originally intended as drug delivery system for proteins drugs and as pore formers for the set cement, had a pronounced negative effect the mechanical strength of the set CPC. The effect was correlated to the added amount of microparticles.

Being intended as bone void filler for large bone defects, the prepared cement should have the capability of stimulating bone regeneration. This could be accomplished by the addition of growth factors to the final cement formulation. Within this work, lysozyme was used as model protein. Lysozyme was incorporated in porous PCL microparticles as the quite large protein drug required diffusion through pores as release mechanism. Continuous release for at least one week could be obtained. The release rates could be controlled by the amount of polymer used for the organic phase of the applied w/o/w double emulsion/solvent evaporation technique. While providing adequate drug release profiles for the desired application, the cement-microparticle composite had to face the drawback of changes in its release profile after exposition to even moderate compressive forces. Increasing the compression force first reduced release rate and total release but increased both parameters with higher forces.

Intended as premixed calcium phosphate cement-protein drug containing microparticle composite, the storage stability of the system was evaluated. It was found, that under the given conditions, lysozyme stability was no issue as well as changes of the release profile due to polymer degradation. However, the cements did not set properly after storing in closed containers without additional desiccants.

Storage stability was addressed by isothermal DSC, mechanical testing, ATR-FTIR, PXRD and dynamic vapor sorption (DVS) studies. The latter revealed a significant loss in moisture uptake for aged cements during the DVS runs. In combination with isothermal DSC, which revealed a reduced total heat flux, the reaction of the cement with already small amounts of moisture was identified as solely cause of the ageing. Extremely slow ageing could even be detected at 5 % relative humidity, suggesting consequent storage of the cement-microparticle composite at temperatures below 0 °C. This would also increase the stability of the protein drugs in the final product.

5 Zusammenfassung

Aufgrund des Ziels einen bioabbaubaren Knochenfüller zu entwickeln, der moderaten Lasten widerstehen und zudem die Heilung von Knochendefekten beschleunigen kann, wurde zunächst ein selbsthärtender Calciumphosphatzement aus Calciumdihydrogenphosphat, Monohydrat (MCPM) und der β-Modifikation von Calciumphosphat (β-TCP) entwickelt. Beim Aushärten dieses Zements entstand Calciumhydrogenphosphat, Dihydrat (DCPD).
Die geringe mittlere Partikelgröße des verwendeten β-TCP (etwa 2 µm) führte zu einer sehr schnellen Aushärtung des Zements nach dem Anmischen mit Wasser. Die Verarbeitungszeit betrug nur etwa eine Minute, was deutlich zu kurz für eine Anwendung in der Praxis war. Eine Erhöhung des Flüssigkeitsanteils in der hergestellten Zementsuspension erhöhte zwar die mögliche Verarbeitungszeit, reduzierte jedoch auch die mechanische Festigkeit des ausgehärteten Zements.
Eine in der Literatur beschriebene Methode zur Verzögerung der Aushärtung ist der Einsatz von Citrationen. Im Unterschied zu den meisten dort gemachten Angaben, hatte die Zugabe von Citrat jedoch einen deutlichen, negativen Effekt auf die mechanischen Eigenschaften des ausgehärteten Zements. Einaxiale direkte Druckfestigkeitsversuche wurden ebenso durchgeführt wie indirekte Zugfestigkeitsversuche. Letztere waren vorteilhaft, da sie eine geringere Empfindlichkeit für kleinere Unterschiede in der Geometrie der Proben aufwiesen. Zur Messung der mechanischen Eigenschaften sehr kleiner Proben wurde eine Nadelintrusionsmethode entwickelt. Mit allen Methoden wurde eine exponentielle Abnahme der Endfestigkeit des Zements mit zunehmender Citratkonzentration festgestellt. Diese Abnahme wurde von einer gleichartigen Reduktion der Reaktionsgeschwindigkeit begleitet. Zur Datenaufnahme wurde vor allem die isotherme dynamische Differenzkalorimetrie (iDSC) eingesetzt. Citratkonzentrationen von 1000 mmol/l führten dazu, dass selbst nach 12 h die Reaktion nicht vollständig abgeschlossen war.
Die Effekte von Citrationen auf das Aushärteverhalten des Zements wurden auch per ATR-FTIR und Pulver-Röntgendiffraktometrie (PXRD) untersucht. Im Gegensatz zu veröffentlichen Daten, war ATR-FTIR nur von begrenztem Nutzen. Dies war mit inhärenten Einschränkungen der ATR-FTIR-Technik zu erklären. Die neu entstandenen DCPD-Partikel sedimentierten auf dem ATR-Kristall. Zusammen mit der geringen Messtiefe der Technik (< 2 µm), führte die Sedimentation dazu, dass bereits deutlich rascher, als aus den

Ergebnissen mit anderen analytischen Methoden erwartet, praktisch nur noch Signale für DCPD aufgefangen wurden.

Um die Aushärtung des Zements mit Hilfe der PXRD beobachten zu könnten, musste eine Methode mit ausreichender Zeit- und Ortsauflösung entwickelt werden. Mit der verwendeten PXRD-Anlage konnte schließlich eine Zeitauflösung von etwa 1 min erreicht werden. Dies war ausreichend um die Unterschiede im Aushärtevorgang bei unterschiedlichen Citratkonzentrationen eindeutig nachzuweisen.

Aus den Steigungen der einzelnen Signalmaxima konnten Daten zur Reaktionskinetik gewonnen werden, die sehr gut mit denen der isothermen DSC übereinstimmten. Darüber hinaus lieferte die zeitaufgelöste PXRD-Technik Informationen über Art und Menge der kristallinen Bestandteile der Probe.

Da die mechanische Festigkeit ein generelles Problem DCPD-bildender Calciumphosphatzemente darstellt, wurde der Einsatz von Citrat als Reaktionsverzögerer schließlich verworfen. Zwei Methoden, um dennoch die Verarbeitungszeit zu verlängern, wurden stattdessen erprobt.

Es ist bekannt, dass die Temperatur einen ausgeprägten Effekt auf chemische Reaktionen hat. Eine Verminderung der Zementtemperatur während des Aushärtens sollte somit das Aushärten verlangsamen und damit die Verarbeitungszeit verlängern.

Für den betrachteten Bereich (4 – 40 °C) wurde mittels isothermer DSC der erwartete Einfluss der Temperatur bestätigt. Am unteren und oberen Ende des Bereichs waren leichte Abweichungen zu erkennen, die mit Einflüssen der Temperatur auf die der Aushärtereaktion vorangehenden Auflösungsprozesse erklärt werden. Trotz eines gewissen Aufwands, wäre das Kühlen des Zements während des Anrührens und der Verarbeitung ein relativ einfacher Weg die Verarbeitungszeit zu erhöhen, ohne die mechanischen Eigenschaften der Probe zu verschlechtern.

Da das Problem der kurzen Verarbeitungszeit dadurch entsteht, dass der Zement unmittelbar mit der Zugabe von Wasser auszuhärten beginnt, könnte das Problem durch Anwendung des trockenen Pulvers in zuvor drainierten Defekten weitgehend umgangen werden. Die Verarbeitung des trockenen Zements würde zudem eine Kompression des Zements vor Beginn des Aushärteprozesses ermöglichen. Die beobachteten Effekte der Kompression auf die mechanische Festigkeit des Zements waren stärker ausgeprägt und traten bereits bei niedrigeren Kräften auf, als zuvor berichtet.

Aufgrund der geringen Partikelgröße des verwendeten β-TCP war das Fließverhalten des Zementpulvers sehr schlecht und somit die gesamte Verarbeitbarkeit stark eingeschränkt. Dieses Problem konnte durch Zugabe von Mikropartikeln aus Polycaprolacton (PCL) gelöst werden. Diese adsorbierten die feinen Zementpartikel auf ihrer Oberfläche und führten so zu einer weitgehenden Umwandlung des schlecht fließenden Pulvers in ein gut verarbeitbares Granulat. Die Zugabe der Mikropartikel, die eigentlich als Vehikel zur kontrollierten Arzneistofffreisetzung (DDS) und als Porenbildner gedacht waren, hatte jedoch deutliche, mit dem Anteil der Mikropartikel in der Formulierung korrelierte, negative Auswirkungen auf die mechanischen Eigenschaften des Zement-Mikropartikel-Komposits.

Um die Knochenheilung nach Einbringen des Zements in einen Defekt zu beschleunigen, sollte dieser in der Lage sein, z.B. Wachstumsfaktoren über eine längere Zeit kontrolliert freigeben zu können. Lysozym diente als Modellprotein. Die Substanz wurde in poröse PCL-Mikropartikel verkapselt, da aufgrund der Molekülgröße nur eine Freisetzung durch Poren als Freisetzungsmechanismus möglich erschien. Kontrollierte Freisetzungen von zum Teil deutlich über einer Woche konnten erzielt werden, was physiologischen Erfordernissen entsprach. Die entstandenen Zement-Mikropartikel-Komposite zeigten jedoch einen unvorteilhaften Einfluss mechanischer Lasten während ihrer Herstellung auf das spätere Freisetzungsverhalten. Mit zunehmender Belastung verminderten sich zunächst Freisetzungsgeschwindigkeit und insgesamt freigesetzte Menge, um dann beide anzusteigen.

Da das Zement-Mikropartikel-Komposit als vorgefertigte Mischung verfügbar sein sollte, musste die Lagerstabilität des Systems nachgewiesen werden. Es zeigte sich hierbei, dass weder die Stabilität des Modellproteins, noch ein verändertes Freisetzungsverhalten der Mikropartikel aufgrund evt. Abbauprozesse ein Problem darstellten. Jedoch ließen Reaktivität und erreichte Endhärte bei Lagerung im verschlossenen Behälter und Raumtemperatur rasch nach. Die Lagerstabilität wurde daher mittels isothermer DSC, mechanischer Tests, ATR-FTIR, PXRD und dynamischer Wasserdampfsorption (DVS) untersucht. Damit konnte gezeigt werden, dass es sich bei der beobachteten Alterung des Zements allein um eine vorzeitige Aushärtung handelte. Diese trat bereits bei sehr geringen Luftfeuchtigkeiten von nur 5 % auf. Für ein späteres Marktprodukt bedeutete dies, dass eine konsequente Lagerung des Zements unter 0 °C zu empfehlen ist, was zudem auch die Stabilität der dann enthaltenen Arzneistoffe und Wachstumsfaktoren erhöhen würde.

6 References

1. Carano, R. A. D.; Filvaroff, E. H., Angiogenesis and bone repair. *Drug Discovery Today* **2003,** 8, (21), 980-989.
2. Murugan, R.; Ramakrishna, S., Development of nanocomposites for bone grafting. *Composites Science and Technology* **2005,** 65, (15-16), 2385-2406.
3. Braddock, M.; Houston, P.; Campbell, C.; Ashcroft, P., Born again bone: tissue engineering for bone repair. *News in Physiological Sciences* **2001,** 16, (Oct.), 208-213.
4. Dorozhkin, S., Calcium orthophosphates. *Journal of Materials Science* **2007,** 42, (4), 1061-1095.
5. Cremers, S.; Sparidans, R.; den Hartigh, J.; Hamdy, N.; Vermeij, P.; Papapoulos, S., A pharmacokinetic and pharmacodynamic model for intravenous bisphosphonate (pamidronate) in osteoporosis. *European Journal of Clinical Pharmacology* **2002,** 57, (12), 883-890.
6. Weigert, P.; Fischer, H., Heavy metals in human tissues. *Wissenschaft und Umwelt* **1979**, (2), 99-101.
7. Iguchi, H.; Sano, S., Occupational bone, skin and eye diseases. Effect of cadmium or other heavy metals on bone collagen metabolism. *Journal of UOEH* **1982,** 4, Suppl., 205-14.
8. Bone. In *Encyclopædia Britannica*, 2009.
9. Biltz, R. M.; Pellegrino, E. D., The chemical anatomy of bone. I. A comparative study of bone composition in sixteen vertebrates. *The Journal of bone and joint surgery American volume* **1969,** 51, (3), 456-66.
10. Bone. In *Wikipedia*, 2009.
11. Misch, C. E.; Qu, Z.; Bidez, M. W., Mechanical properties of trabecular bone in the human mandible: implications for dental implant treatment planning and surgical placement. *Journal of oral and maxillofacial surgery : official jour* **1999,** 57, (6), 700-6; discussion 706-8.
12. Rezwan, K.; Chen, Q. Z.; Blaker, J. J.; Boccaccini, A. R., Biodegradable and bioactive porous polymer/inorganic composite scaffolds for bone tissue engineering. *Biomaterials* **2006,** 27, (18), 3413-3431.
13. Zioupos, P.; Currey, J. D., Changes in the stiffness, strength, and toughness of human cortical bone with age. *Bone* **1998,** 22, (1), 57-66.
14. Reilly, D. T.; Burstein, A. H., The elastic and ultimate properties of compact bone tissue. *Journal of biomechanics* **1975,** 8, (6), 393-405.
15. Rincon-Kohli, L.; Zysset Philippe, K., Multi-axial mechanical properties of human trabecular bone. *Biomechanics and modeling in mechanobiology* **2009,** 8, (3), 195-208.
16. Rohl, L.; Larsen, E.; Linde, F.; Odgaard, A.; Jorgensen, J., Tensile and compressive properties of cancellous bone. *Journal of biomechanics* **1991,** 24, (12), 1143-9.
17. Goldstein, S. A., The mechanical properties of trabecular bone: dependence on anatomic location and function. *Journal of biomechanics* **1987,** 20, (11-12), 1055-61.
18. Hamdy, N. A. T., Bone remodeling in health and disease. *Nederlands Tijdschrift voor Klinische Chemie* **2000,** 25, (5), 311-313.
19. Mosekilde, L.; Ebbesen, E. N.; Tornvig, L.; Thomsen, J. S., Trabecular bone structure and strength - remodelling and repair. *Journal of musculoskeletal & neuronal interactions* **2000,** 1, (1), 25-30.
20. Heino Terhi, J.; Kurata, K.; Higaki, H.; Vaananen, H. K., Evidence for the role of osteocytes in the initiation of targeted remodeling. *Technology and health care : official journal of the European Society for Engineering an* **2009,** 17, (1), 49-56.
21. Smith, I. O.; Baumann, M. J.; Case, E. D., Induced microcracking affects osteoblast attachment on hydroxyapatite scaffolds for tissue engineering. *American Journal of Biochemistry and Biotechnology* **2006,** 2, (3), 105-110.
22. Martin, R. B., Is all cortical bone remodeling initiated by microdamage? *Bone* **2002,** 30, (1), 8-13.
23. Fukada, E.; Yasuda, I., *J Phys SOC Jpn* **1957,** 12, 1158-1162.
24. Gross, D.; Williams, W. S., Streaming potential and the electromechanical response of physiologically-moist bone. *Journal of biomechanics* **1982,** 15, (4), 277-95.
25. Hassler, C. R.; Rybicki, E. F.; Diegle, R. B.; Clark, L. C., Studies of enhanced bone healing via electrical stimuli. Comparative effectiveness of various parameters. *Clinical orthopaedics and related research* **1977**, (124), 9-19.
26. Hartig, M.; Joos, U.; Wiesmann, H.-P., Capacitively coupled electric fields accelerate proliferation of osteoblast-like primary cells and increase bone extracellular matrix formation in vitro. *European Biophysics Journal* **2000,** 29, (7), 499-506.
27. Ercan, B.; Webster, T. J., Greater osteoblast proliferation on anodized nanotubular titanium upon electrical stimulation. *International Journal of Nanomedicine* **2008,** 3, (4), 477-485.

28. Supronowicz, P. R.; Ullmann, K. R.; Ajayan, P. M.; Arulanandam, B. P.; Metzger, D. W.; Bizios, R., Cellular/molecular responses of electrically stimulated osteoblasts cultured on novel polymer/carbon nanophase substrates. *Carbon'01, An International Conference on Carbon, Lexington, KY, United* **2001**, 1-2.
29. Goldenberg, D. M.; Hansen, H. J., Electric enhancement of bone healing. *Science (New York, NY)* **1972,** 175, (26), 1118-20.
30. Lienau, J.; Schmidt-Bleek, K.; Peters, A.; Weber, H.; Bail, H. J.; Duda, G. N.; Perka, C.; Schell, H., Insight into the molecular pathophysiology of delayed bone healing in a sheep model. *Tissue Engineering, Part A* **2010,** 16, (1), 191-199.
31. Axelrad, T. W.; Einhorn, T. A., Bone morphogenetic proteins in orthopaedic surgery. *Cytokine & Growth Factor Reviews* **2009,** 20, (5-6), 481-488.
32. Baldini, N.; Cenni, E.; Ciapetti, G.; Granchi, D.; Savarino, L., Bone repair and regeneration. *Bone Repair Biomaterials* **2009**, 69-105.
33. Sandberg, M. M.; Aro, H. T.; Vuorio, E. I., Gene expression during bone repair. *Clinical orthopaedics and related research* **1993**, (289), 292-312.
34. Prolo, D. J.; Pedrotti, P. W.; Burres, K. P.; Oklund, S., Superior osteogenesis in transplanted allogeneic canine skull following chemical sterilization. *Clinical orthopaedics and related research* **1982**, (168), 230-42.
35. Einhorn, T. A.; Lane, J. M.; Burstein, A. H.; Kopman, C. R.; Vigorita, V. J., The healing of segmental bone defects induced by demineralized bone matrix. A radiographic and biomechanical study. *The Journal of bone and joint surgery American volume* **1984,** 66, (2), 274-9.
36. Johnson, E. E.; Urist, M. R.; Schmalzried, T. P.; Chotivichit, A.; Huang, H. K.; Finerman, G. A., Autogeneic cancellous bone grafts in extensive segmental ulnar defects in dogs. Effects of xenogeneic bovine bone morphogenetic protein without and with interposition of soft tissues and interruption of blood supply. *Clinical orthopaedics and related research* **1989**, (243), 254-65.
37. Collier, M. A.; Brighton, C. T.; Norrdin, R.; Twardock, A. R.; Rendano, V. T., Direct current stimulation of bone production in the horse: preliminary study with a "gap healing" model. *American journal of veterinary research* **1985,** 46, (3), 610-21.
38. Frame, J. W., A convenient animal model for testing bone substitute materials. *Journal of oral surgery (American Dental Association : 1965)* **1980,** 38, (3), 176-80.
39. Kaban, L. B.; Glowacki, J.; Murray, J. E., Repair of experimental mandibular bony defects in rats. *Surgical forum* **1979,** 30, 519-21.
40. Lange, T. A.; Zerwekh, J. E.; Peek, R. D.; Mooney, V.; Harrison, B. H., Granular tricalcium phosphate in large cancellous defects. *Annals of clinical and laboratory science* **1986,** 16, (6), 467-72.
41. Toombs, J. P.; Wallace, L. J.; Bjorling, D. E.; Rowland, G. N., Evaluation of Key's hypothesis in the feline tibia: an experimental model for augmented bone healing studies. *American journal of veterinary research* **1985,** 46, (2), 513-8.
42. Hollinger, J. O.; Kleinschmidt, J. C., The critical size defect as an experimental model to test bone repair materials. *The Journal of craniofacial surgery* **1990,** 1, (1), 60-8.
43. Roesgen, M.; Hierholzer, G., Standard method for the investigation of bone transplants, ceramics, or other material in a human bony layer. *Archives of orthopaedic and traumatic surgery Archiv fur orthopadische und Unfall-Chi* **1988,** 107, (2), 117-9.
44. Jowsey, J., Symposium on equine bone and joint diseases. Age and species differences in bone. *The Cornell veterinarian* **1968,** 58, Suppl:74-94.
45. Maus, U.; Andereya, S.; Gravius, S.; Ohnsorge, J. A. K.; Niedhart, C.; Siebert, C. H., BMP-2 incorporated in a tricalcium phosphate bone substitute enhances bone remodeling in sheep. *Journal of Biomaterials Applications* **2008,** 22, (6), 559-576.
46. Link, D. P.; van den Dolder, J.; van den Beucken, J. J.; Wolke, J. G.; Mikos, A. G.; Jansen, J. A., Bone response and mechanical strength of rabbit femoral defects filled with injectable CaP cements containing TGF-beta 1 loaded gelatin microparticles. *Biomaterials* **2008,** 29, (6), 675-682.
47. Rueger, D. C., Biochemistry of bone morphogenetic proteins. *Bone Morphogenetic Proteins* **2002**, 1-18.
48. Watabe, T.; Miyazono, K., Roles of TGF-beta family signaling in stem cell renewal and differentiation. *Cell Research* **2009,** 19, (1), 103-115.
49. Guo, X.; Wang, X.-F., Signaling cross-talk between TGF-beta /BMP and other pathways. *Cell Research* **2009,** 19, (1), 71-88.
50. Matthews, S. J. E., Biological activity of bone morphogenetic proteins (BMP's). *Injury* **2005,** 36 Suppl 3, S34-7.
51. Lee, M. B., Bone morphogenetic proteins: background and implications for oral reconstruction. A review. *Journal of clinical periodontology* **1997,** 24, (6), 355-65.

52. Reddi, A. H., Initiation of fracture repair by bone morphogenetic proteins. *Clinical orthopaedics and related research* **1998**, (355 Suppl), S66-72.
53. Miyazono, K.; Kusanagi, K.; Inoue, H., Divergence and convergence of TGF-beta /BMP signaling. *Journal of Cellular Physiology* **2001,** 187, (3), 265-276.
54. Buxton, P.; Edwards, C.; Archer, C. W.; Francis-West, P., Growth/differentiation factor-5 (GDF-5) and skeletal development. *The Journal of bone and joint surgery American volume* **2001,** 83-A Suppl 1, (Pt 1), S23-30.
55. Zeng, S.; Chen, J.; Shen, H., Controlling of bone morphogenetic protein signaling. *Cellular Signalling* **2010,** 22, (6), 888-893.
56. Miyazono, K.; Kamiya, Y.; Morikawa, M., Bone morphogenetic protein receptors and signal transduction. *Journal of Biochemistry* **2010,** 147, (1), 35-51.
57. Sebald, W.; Nickel, J.; Zhang, J.-L.; Mueller, T. D., Molecular recognition in bone morphogenetic protein (BMP)/receptor interaction. *Biological Chemistry* **2004,** 385, (8), 697-710.
58. Cheng, H.; Jiang, W.; Phillips Frank, M.; Haydon Rex, C.; Peng, Y.; Zhou, L.; Luu Hue, H.; An, N.; Breyer, B.; Vanichakarn, P.; Szatkowski Jan, P.; Park Jae, Y.; He, T.-C., Osteogenic activity of the fourteen types of human bone morphogenetic proteins (BMPs). *The Journal of bone and joint surgery American volume* **2003,** 85-A, (8), 1544-52.
59. Cho, T.-J.; Gerstenfeld, L. C.; Einhorn, T. A., Differential temporal expression of members of the transforming growth factor b superfamily during murine fracture healing. *Journal of Bone and Mineral Research* **2002,** 17, (3), 513-520.
60. Spector, J. A.; Luchs, J. S.; Mehrara, B. J.; Greenwald, J. A.; Smith, L. P.; Longaker, M. T., Expression of bone morphogenetic proteins during membranous bone healing. *Plastic and reconstructive surgery* **2001,** 107, (1), 124-34.
61. Kidd, L. J.; Stephens, A. S.; Kuliwaba, J. S.; Fazzalari, N. L.; Wu, A. C. K.; Forwood, M. R., Temporal pattern of gene expression and histology of stress fracture healing. *Bone* **2010,** 46, (2), 369-78.
62. Campisi, P.; Hamdy Reggie, C.; Lauzier, D.; Amako, M.; Rauch, F.; Lessard, M.-L., Expression of bone morphogenetic proteins during mandibular distraction osteogenesis. *Plastic and reconstructive surgery* **2003,** 111, (1), 201-8; discussion 209-10.
63. Schilephake, H., Bone growth factors in maxillofacial skeletal reconstruction. *International journal of oral and maxillofacial surgery* **2002,** 31, (5), 469-84.
64. King, G. N., The importance of drug delivery to optimize the effects of bone morphogenetic proteins during periodontal regeneration. *Current Pharmaceutical Biotechnology* **2001,** 2, (2), 131-142.
65. Woo, B. H.; Fink, B. F.; Page, R.; Schrier, J. A.; Jo, Y. W.; Jiang, G.; DeLuca, M.; Vasconez, H. C.; DeLuca, P. P., Enhancement of bone growth by sustained delivery of recombinant human bone morphogenetic protein-2 in a polymeric matrix. *Pharmaceutical research* **2001,** 18, (12), 1747-53.
66. Ohura, K.; Hamanishi, C.; Tanaka, S.; Matsuda, N., Healing of segmental bone defects in rats induced by a beta -TCP-MCPM cement combined with rhBMP-2. *Journal of Biomedical Materials Research* **1999,** 44, (2), 168-175.
67. Lavery, K.; Swain, P.; Falb, D.; Alaoui-Ismaili, M. H., BMP-2/4 and BMP-6/7 Differentially Utilize Cell Surface Receptors to Induce Osteoblastic Differentiation of Human Bone Marrow-derived Mesenchymal Stem Cells. *Journal of Biological Chemistry* **2008,** 283, (30), 20948-20958.
68. Wozney, J. M., Bone morphogenetic proteins. *Progress in growth factor research* **1989,** 1, (4), 267-80.
69. Lane, J. M.; Yasko, A. W.; Tomin, E.; Cole, B. J.; Waller, S.; Browne, M.; Turek, T.; Gross, J., Bone marrow and recombinant human bone morphogenetic protein-2 in osseous repair. *Clinical orthopaedics and related research* **1999**, (361), 216-27.
70. Laub, M.; Chatzinikolaidou, M.; Rumpf, H.; Jennissen, H. P., Modelling of Protein-Protein Interactions of Bone Morphogenetic Protein-2 (BMP-2) by 3D-Rapid Prototyping. *Materialwissenschaft und Werkstofftechnik* **2002,** 33, (12), 729-737.
71. Tabata, Y.; Yamamoto, M.; Ikada, Y., Comparison of release profiles of various growth factors from biodegradable carriers. *Materials Research Society Symposium Proceedings* **1998,** 530, (Biomaterials Regulating Cell Function and Tissue Development), 13-18.
72. Chen, F.-M.; Chen, R.; Wang, X.-J.; Sun, H.-H.; Wu, Z.-F., In vitro cellular responses to scaffolds containing two microencapulated growth factors. *Biomaterials* **2009,** 30, (28), 5215-24.
73. Uludag, H.; Friess, W.; Williams, D.; Porter, T.; Timony, G.; D'Augusta, D.; Blake, C.; Palmer, R.; Biron, B.; Wozney, J., rhBMP-collagen sponges as osteoinductive devices: effects of in vitro sponge characteristics and protein pI on in vivo rhBMP pharmacokinetics. *Annals of the New York Academy of Sciences* **1999,** 875, (Bioartificial Organs II), 369-378.
74. Ruppert, R.; Hoffmann, E.; Sebald, W., Human bone morphogenetic protein 2 contains a heparin-binding site which modifies its biological activity. *European Journal of Biochemistry* **1996,** 237, (1), 295-302.
75. Seliger, W. G., Tissue fluid movement in compact bone. *The Anatomical record* **1970,** 166, (2), 247-55.

76. Dillaman, R. M., Movement of ferritin in the 2-day-old chick femur. *The Anatomical record* **1984,** 209, (4), 445-53.
77. Montgomery, R. J.; Sutker, B. D.; Bronk, J. T.; Smith, S. R.; Kelly, P. J., Interstitial fluid flow in cortical bone. *Microvascular Research* **1988,** 35, (3), 295-307.
78. Johnson, M. W.; Chakkalakal, D. A.; Harper, R. A.; Katz, J. L.; Rouhana, S. W., Fluid flow in bone in vitro. *Journal of Biomechanics* **1982,** 15, (11), 881-885.
79. Kelly, P. J.; Bronk, J. T., Venous pressure and bone formation. *Microvascular Research* **1990,** 39, (3), 364-75.
80. Hillsley, M. V.; Frangos, J. A., Bone tissue engineering: the role of interstitial fluid flow. *Biotechnology and bioengineering* **1994,** 43, (7), 573-81.
81. Dillaman, R. M.; Roer, R. D.; Gay, D. M., Fluid movement in bone: theoretical and empirical. *Journal of biomechanics* **1991,** 24 Suppl 1, 163-77.
82. Athanasiou, K. A.; Zhu, C.; Lanctot, D. R.; Agrawal, C. M.; Wang, X., Fundamentals of biomechanics in tissue engineering of bone. *Tissue engineering* **2000,** 6, (4), 361-81.
83. Currey, J. D., Mechanical properties of vertebrate hard tissues. *Proceedings of the Institution of Mechanical Engineers Part H, Journal of engineering* **1998,** 212, (6), 399-411.
84. Dorozhkin, S. V.; Epple, M., Biological and medical significance of calcium phosphates. *Angewandte Chemie, International Edition* **2002,** 41, (17), 3130-3146.
85. Chow, L. C., Next generation calcium phosphate-based biomaterials. *Dental Materials Journal* **2009,** 28, (1), 1-10.
86. Fernandez, E.; Gil, F. J.; Ginebra, M. P.; Driessens, F. C. M.; Planell, J. A.; Best, S. M., Calcium phosphate bone cements for clinical applications. Part II: Precipitate formation during setting reactions. *Journal of Materials Science: Materials in Medicine* **1999,** 10, (3), 177-183.
87. Chow, L. C., Calcium phosphate cements: chemistry, properties, and applications. *Materials Research Society Symposium Proceedings* **2000,** 599, (Mineralization in Natural and Synthetic Biomaterials), 27-37.
88. Fernandez, E.; Gil, F. J.; Ginebra, M. P.; Driessens, F. C. M.; Planell, J. A.; Best, S. M., Calcium phosphate bone cements for clinical applications. Part I: solution chemistry. *Journal of Materials Science: Materials in Medicine* **1999,** 10, (3), 169-176.
89. Kalita, S. J.; Bhardwaj, A.; Bhatt, H. A., Nanocrystalline calcium phosphate ceramics in biomedical engineering. *Materials Science & Engineering, C: Biomimetic and Supramolecular Systems* **2007,** 27, (3), 441-449.
90. Gregory, T. M.; Moreno, E. C.; Brown, W. E., Solubility of dicalcium phosphate dihydrate in the system calcium hydroxide--orthophosphoric acid--water at 5, 15, 25, and 37.5.deg. *Journal of Research of the National Bureau of Standards, Section A: Physi* **1970,** 74, (4), 461-75.
91. McDowell, H.; Brown, W.; Sutter, J., Solubility Study of Calcium Hydrogen Phosphate: Ion Pair Formation. *Inorg Chem* **1971,** 10, 1638-1643.
92. Onuma, K.; Ito, A., Cluster Growth Model for Hydroxyapatite. *Chemistry of Materials* **1998,** 10, (11), 3346-3351.
93. Tung, M. S.; Eidelman, N.; Sieck, B.; Brown, W. E., Octacalcium phosphate solubility product from 4 to 37 DegC. *Journal of Research of the National Bureau of Standards (United States)* **1988,** 93, (5), 613-24.
94. Fowler, B. O.; Kuroda, S., Changes in heated and in laser-irradiated human tooth enamel and their probable effects on solubility. *Calcified Tissue International* **1986,** 38, (4), 197-208.
95. Gregory, T. M.; Moreno, E. C.; Patel, J. M.; Brown, W. E., Solubility of beta -tricalcium phosphate in the system calcium hydroxide-phosphoric acid-water at 5, 15, 25, and 37.deg. *Journal of Research of the National Bureau of Standards, Section A:* **1974,** 78A, (6), 667-74.
96. McDowell, H.; Gregory, T. M.; Brown, W. E., Solubility of hydroxyapatite (Ca5(PO4)3OH) in the system calcium hydroxide-phosphoric acid-water at 5, 15, 25, and 37 DegC. *Journal of Research of the National Bureau of Standards, Section A:* **1977,** 81A, (2-3), 273-81.
97. Matsuya, S.; Takagi, S.; Chow, L. C., Hydrolysis of tetracalcium phosphate in H3PO4 and KH2PO4. *Journal of Materials Science* **1996,** 31, (12), 3263-3269.
98. Bermudez, O.; Boltong, M. G.; Driessens, F. C. M.; Planell, J. A., Development of some calcium phosphate cements from combinations of alpha -TCP, MCPM and CaO. *Journal of Materials Science: Materials in Medicine* **1994,** 5, (3), 160-3.
99. Han, B.; Ma, P.-W.; Zhang, L.-L.; Yin, Y.-J.; Yao, K.-D.; Zhang, F.-J.; Zhang, Y.-D.; Li, X.-L.; Nie, W., [beta]-TCP/MCPM-based premixed calcium phosphate cements. *Acta Biomaterialia* **2009,** In Press, Corrected Proof.
100. Bohner, M.; Lemaitre, J.; Ohura, K.; Hardouin, P., Effects of sulfate ions on the in vitro properties of b-TCP - MCPM - water mixtures. Preliminary in vivo results. *Ceramic Transactions* **1995,** 48, 245-59.

101. Driessens, F. C.; Planell, J. A.; Boltong, M. G.; Khairoun, I.; Ginebra, M. P., Osteotransductive bone cements. *Proceedings of the Institution of Mechanical Engineers Part H, Journal of enginee* **1998,** 212, (6), 427-35.
102. Driessens, F. C. M.; De Maeyer, E. A. P.; Fernandez, E.; Boltong, M. G.; Berger, G.; Verbeeck, R. M. H.; Ginebra, M. P.; Planell, J. A., Amorphous calcium phosphate cements and their transformation into calcium deficient hydroxyapatite. *Bioceramics, Proceedings of the International Symposium on Ceramics* **1996,** 9, 231-234.
103. Termine, J. D.; Eanes, E. D., Comparative chemistry of amorphous and apatitic calcium phosphate preparations. *Calcified Tissue International* **1972,** 10, (1), 171-197.
104. LeGeros, R. Z., Formation and transformation of calcium phosphates: relevance to vascular calcification. *Zeitschrift fuer Kardiologie* **2001,** 90, (Suppl. 3), iii/116-iii/124.
105. LeGeros, R. Z.; Mijares, D.; Park, J.; Chang, X. F.; Khairoun, I.; Kijkowska, R.; Dias, R.; LeGeros, J. P., Amorphous calcium phosphates (ACP): formation and stability. *Key Engineering Materials* **2005,** 284-286, 7-10.
106. Greenfield, D. J.; Eanes, E. D., Formation chemistry of amorphous calcium phosphates prepared from carbonate containing solutions. *Calcified Tissue International* **1972,** 9, (1), 152-162.
107. Bachra, B. N.; Trautz, O. R.; Simon, S. L., Precipitation of calcium carbonates and phosphates. I. Spontaneous precipitation of calcium carbonates and phosphates under physiological conditions. *Archives of Biochemistry and Biophysics* **1963,** 103, (1), 124-38.
108. Termine, J. D.; Posner, A. S., Calcium phosphate formation in vitro. I. Factors affecting initial phase separation. *Archives of Biochemistry and Biophysics* **1970,** 140, (2), 307-17.
109. Pan, H. B.; Darvell, B. W., Calcium Phosphate Solubility: The Need for Re-Evaluation. *Crystal Growth & Design* **2009,** 9, (2), 639-645.
110. Miyazaki, T.; Sivaprakasam, K.; Tantry, J.; Suryanarayanan, R., Physical characterization of dibasic calcium phosphate dihydrate and anhydrate. *Journal of pharmaceutical sciences* **2009,** 98, (3), 905-16.
111. Clarkin, O. M.; Towler, M. R.; Insley, G. M.; Murphy, M. E., Phase transformations of calcium phosphates formed in wet field environments. *Journal of Materials Science* **2007,** 42, (19), 8357-8362.
112. Hesse, A.; Heimbach, D., Causes of phosphate stone formation and the importance of metaphylaxis by urinary acidification: a review. *World journal of urology* **1999,** 17, (5), 308-15.
113. LeGeros, R. Z., Calcium phosphates in oral biology and medicine. *Monographs in oral science* **1991,** 15, 1-201.
114. Brown, W. E.; Patel, P. R.; Chow, L. C., Formation of calcium hydrogen phosphate dihydrate from enamel mineral and its relation to caries mechanism. *Journal of Dental Research* **1975,** 54, (3), 475-81.
115. Brown, W. E.; Eidelman, N.; Tomazic, B., Octacalcium phosphate as a precursor in biomineral formation. *Advances in dental research* **1987,** 1, (2), 306-13.
116. Bohner, M.; Theiss, F.; Apelt, D.; Hirsiger, W.; Houriet, R.; Rizzoli, G.; Gnos, E.; Frei, C.; Auer, J. A.; von Rechenberg, B., Compositional changes of a dicalcium phosphate dihydrate cement after implantation in sheep. *Biomaterials* **2003,** 24, (20), 3463-3474.
117. Tovborg-Jensen, A.; Rathlev, J., Calcium hydrogen orthophosphate 2-hydrate and calcium hydrogen orthophosphate. *Inorganic Syntheses (McGraw-Hill Book Co, New York, NY)* **1953,** 4, 19-22.
118. McIntosh, A. O.; Jablonski, W. L., X-ray diffraction powder patterns of the calcium phosphates. *Anal Chem* **1956,** 28, 1424-7.
119. Bohner, M.; Merkle, H. P.; Van Landuyt, P.; Trophardy, G.; Lemaitre, J., Effect of several additives and their admixtures on the physicochemical properties of a calcium phosphate cement. *Journal of Materials Science: Materials in Medicine* **2000,** 11, (2), 111-116.
120. Gbureck, U.; Dembski, S.; Thull, R.; Barralet, J. E., Factors influencing calcium phosphate cement shelf-life. *Biomaterials* **2005,** 26, (17), 3691-3697.
121. Gregory, T. M.; Moreno, E. C.; Patel, J. M.; Brown, W. E., Solubility of b-tricalcium phosphate in the system calcium hydroxide-phosphoric acid-water at 5, 15, 25, and 37.deg. *Journal of Research of the National Bureau of Standards, Section A: Physi* **1974,** 78A, (6), 667-74.
122. Pochon, J. P.; Schwobel, M.; Illi, O.; Weihe, W. H., Bone replacement using beta-tricalcium phosphate--results of experimental studies and initial clinical case examples. *Zeitschrift fur Kinderchirurgie* **1986,** 41, (3), 171-3.
123. Wada, T.; Wu, C. H.; Sugita, H.; Sugita, N.; Katagiri, S.; Shimizu, M.; Hara, K., Autogenous, allogenic, and beta-TCP grafts: comparative effectiveness in experimental bone furcation defects in dogs. *The Journal of oral implantology* **1989,** 15, (4), 231-6.
124. Meadows Gilbert, R., Adjunctive use of ultraporous beta-tricalcium phosphate bone void filler in spinal arthrodesis. *Orthopedics* **2002,** 25, (5 Suppl), s579-84.
125. Burke, E. A. J., Tidying up mineral names: an IMA-CNMNC scheme for suffixes, hyphens and diacritical marks. *The Mineralogical Record* **2008,** 39, (2), 131 - 135.

126. Barth, E.; Ronningen, H.; Solheim, L. F., Bone fixation of ceramic-coated and fiber titanium implants. A study in weight-bearing rats. *Acta orthopaedica Scandinavica* **1986,** 57, (1), 25-9.
127. Huang, G. K.; Cao, M. J., Experimental study of metallic bone and joint prostheses with plasma-sprayed ceramic coating. *Zentralblatt fur Chirurgie* **1992,** 117, (3), 171-7.
128. Oonishi, H.; Yamamoto, M.; Ishimaru, H.; Tsuji, E.; Kushitani, S.; Aono, M.; Ukon, Y., The effect of hydroxyapatite coating on bone growth into porous titanium alloy implants. *The Journal of bone and joint surgery British volume* **1989,** 71, (2), 213-6.
129. Furlong, R. J.; Osborn, J. F., Fixation of hip prostheses by hydroxyapatite ceramic coatings. *The Journal of bone and joint surgery British volume* **1991,** 73, (5), 741-5.
130. Mueller-Mai, C. M.; Voigt, C.; Gross, U., Incorporation and degradation of hydroxyapatite implants of different surface roughness and surface structure in bone. *Scanning Microscopy* **1990,** 4, (3), 613-24.
131. Laschtschenko, P., Über die keimtötende und entwicklungshemmende Wirkung Hühnereiweiß. *Z Hyg infekt Krankh* **1909,** 64, 419-427.
132. Fleming, A., On a remarkable becteriolytic element found in tissues and secretion. *Proceedings of the Royal Society, Series B* **1922,** 93, 306-317.
133. Lysozyme. In 2010.
134. Jolles, P., From the discovery of lysozyme to the characterization of several lysozyme families. *EXS* **1996,** 75, (Lysozymes: Model Enzymes in Biochemistry and Biology), 3-5.
135. Hernandez-Hernandez, A.; Rodriguez-Navarro, A. B.; Gomez-Morales, J.; Jimenez-Lopez, C.; Nys, Y.; Garcia-Ruiz, J. M., Influence of model globular proteins with different isoelectric points on the precipitation of calcium carbonate. *Crystal Growth & Design* **2008,** 8, (5), 1495-1502.
136. Wetter, L. R.; Deutsch, H. F., Immunological studies on egg white proteins. IV. Immunochemical and physical studies of lysozyme. *Journal of Biological Chemistry* **1951,** 192, 237-42.
137. Kierzek, A. M.; Pokarowski, P.; Zielenkiewicz, P., Microscopic model of protein crystal growth. *Biophysical Chemistry* **2000,** 87, (1), 43-61.
138. Haliloglu, T.; Bahar, I., Structure-based analysis of protein dynamics: comparison of theoretical results for hen lysozyme with X-ray diffraction and NMR relaxation data. *Proteins: Structure, Function, and Genetics* **1999,** 37, (4), 654-667.
139. Paillard-Giteau, A.; Tran, V. T.; Thomas, O.; Garric, X.; Coudane, J.; Marchal, S.; Chourpa, I.; Benoit, J. P.; Montero-Menei, C. N.; Venier-Julienne, M. C., Effect of various additives and polymers on lysozyme release from PLGA microspheres prepared by an s/o/w emulsion technique. *European Journal of Pharmaceutics and Biopharmaceutics* **2010,** 75, (2), 128-136.
140. Kluge, J.; Fusaro, F.; Casas, N.; Mazzotti, M.; Muhrer, G., Production of PLGA micro- and nanocomposites by supercritical fluid extraction of emulsions: I. Encapsulation of lysozyme. *Journal of Supercritical Fluids* **2009,** 50, (3), 327-335.
141. Wilson, T.; Viitala, R.; Puska, M.; Jalonen, H.; Penttinen, R.; Jokinen, M., The release and bioactivity of lysozyme from selected sol-gel derived SiO2 matrices. *Key Engineering Materials* **2009,** 396-398, (Bioceramics 21), 547-550.
142. Li, Y.; Jiang, H.; Zhu, K., Encapsulation and controlled release of lysozyme from electrospun poly(e-caprolactone)/poly(ethylene glycol) non-woven membranes by formation of lysozyme-oleate complexes. *Journal of Materials Science: Materials in Medicine* **2008,** 19, (2), 827-832.
143. Miyazawa, M., Information of protein structure in NIR spectra. *Useful and Advanced Information in the Field of Near Infrared Spectroscopy* **2003**, 237-241.
144. Spenlehauer, G.; Spenlehauer-Bonthonneau, F.; Thies, C., Biodegradable microparticles for delivery of polypeptides and proteins. *Progress in Clinical and Biological Research* **1989,** 292, (Biol. Synth. Membr.), 283-91.
145. Pitt, C. G., The controlled parenteral delivery of polypeptides and proteins. *International Journal of Pharmaceutics* **1990,** 59, (3), 173-96.
146. Chang, T. M. S., Biodegradable semipermeable microcapsules containing enzymes, hormones, vaccines, and other biologicals. *Journal of Bioengineering* **1976,** 1, (1), 25-32.
147. Wischke, C.; Schwendeman Steven, P., Principles of encapsulating hydrophobic drugs in PLA/PLGA microparticles. *International journal of pharmaceutics* **2008,** 364, (2), 298-327.
148. Van de Weert, M.; Hennink, W. E.; Jiskoot, W., Protein instability in poly(lactic-co-glycolic acid) microparticles. *Pharmaceutical Research* **2000,** 17, (10), 1159-1167.
149. Zambaux, M. F.; Bonneaux, F.; Gref, R.; Dellacherie, E.; Vigneron, C., Preparation and characterization of protein C-loaded PLA nanoparticles. *Journal of Controlled Release* **1999,** 60, (2-3), 179-188.
150. Oliva, A.; Santovena, A.; Farina, J.; Llabres, M., Effect of high shear rate on stability of proteins: kinetic study. *Journal of Pharmaceutical and Biomedical Analysis* **2003,** 33, (2), 145-155.

151. Faisant, N.; Akiki, J.; Siepmann, F.; Benoit, J. P.; Siepmann, J., Effects of the type of release medium on drug release from PLGA-based microparticles: Experiment and theory. *International Journal of Pharmaceutics* **2006,** 314, (2), 189-197.
152. Xu, Q.; Crossley, A.; Czernuszka, J., Preparation and characterization of negatively charged poly(lactic-co-glycolic acid) microspheres. *Journal of Pharmaceutical Sciences* **2009,** 98, (7), 2377-2389.
153. Luan, X.; Bodmeier, R., Modification of the tri-phasic drug release pattern of leuprolide acetate-loaded poly(lactide-co-glycolide) microparticles. *European Journal of Pharmaceutics and Biopharmaceutics* **2006,** 63, (2), 205-214.
154. Batycky, R. P.; Hanes, J.; Langer, R.; Edwards, D. A., A Theoretical Model of Erosion and Macromolecular Drug Release from Biodegrading Microspheres. *Journal of Pharmaceutical Sciences* **1997,** 86, (12), 1464-1477.
155. Miyajima, M.; Koshika, A.; Okada, J. i.; Ikeda, M.; Nishimura, K., Effect of polymer crystallinity on papaverine release from poly (L-lactic acid) matrix. *Journal of Controlled Release* **1997,** 49, (2,3), 207-215.
156. Kuhn, H.; Medlin, D., *ASM Handbook - Mechanical Testing and Evaluation*. ASM International: 2000; Vol. 8, p 143, 146,147.
157. Carneiro, F.; Barcellos, A., Résistance a la traction des bétons. *Bulletin RILEM* **1953,** 1 13, (1953), 97-108.
158. Ginebra, M. P.; Driessens, F. C. M.; Planell, J. A., Effect of the particle size on the micro and nanostructural features of a calcium phosphate cement: a kinetic analysis. *Biomaterials* **2004,** 25, (17), 3453-3462.
159. Driessens, F. C. M.; Boltong, M. G.; Zapatero, M. I.; Verbeeck, R. M. H.; Bonfield, W.; Bermudez, O.; Fernandez, E.; Ginebra, M. P.; Planell, J. A., In vivo behavior of three calcium phosphate cements and a magnesium phosphate cement. *Journal of Materials Science: Materials in Medicine* **1995,** 6, (5), 272-8.
160. Pittet, C.; Lemaitre, J., Mechanical characterization of brushite cements: a Mohr circles' approach. *Journal of Biomedical Materials Research* **2000,** 53, (6), 769-780.
161. Takagi, S.; Chow, L. C., Formation of macropores in calcium phosphate cement implants. *JOURNAL OF MATERIALS SCIENCE: MATERIALS IN MEDICINE* **2001,** 12, (2), 135-139.
162. Galea, L. G.; Bohner, M.; Lemaitre, J.; Kohler, T.; Mueller, R., Bone substitute: Transforming beta - tricalcium phosphate porous scaffolds into monetite. *Biomaterials* **2008,** 29, (24-25), 3400-3407.
163. Schnieders, J.; Gbureck, U.; Thull, R.; Kissel, T., Controlled release of gentamicin from calcium phosphate-poly(lactic acid-co-glycolic acid) composite bone cement. *Biomaterials* **2006,** 27, (23), 4239-4249.
164. Combes, C.; Miao, B.; Bareille, R.; Rey, C., Preparation, physical-chemical characterization and cytocompatibility of calcium carbonate cements. *Biomaterials* **2006,** 27, (9), 1945-1954.
165. Lin, Z.; Wood, L., Concrete Uniaxial Tensile Strength and Cylinder Splitting Test. *Journal of Structural Engineering* **2003,** 129, (5), 692-698.
166. Skalak, R.; Fox, C. F., *Tissue Engineering*. Alan R. Liss, Inc.: New York, 1988.
167. Viola, J.; Lal, B. L.; Grad, O. The Emergence of Tissue Engineering as a Research Field. http://www.nsf.gov/pubs/2004/nsf0450/start.htm (10-02),
168. Wolter, J. R.; Meyer, R. F., Sessile macrophages forming clear endothelium-like membrane on inside of successful keratoprosthesis. *Transactions of the American Ophthalmological Society* **1984,** 82, 187-202.
169. Matsuda, T.; Akutsu, T.; Kira, K.; Matsumoto, H., Development of hybrid compliant graft: rapid preparative method for reconstruction of a vascular wall. *ASAIO transactions / American Society for Artificial Internal Organs* **1989,** 35, (3), 553-5.
170. Langer, R.; Vacanti, J. P., Tissue engineering. *Science (New York, NY)* **1993,** 260, (5110), 920-926.
171. Bruder, S. P.; Fox, B. S., Tissue engineering of bone. Cell based strategies. *Clinical orthopaedics and related research* **1999**, (367 Suppl), S68-83.
172. Bodnar, A. G.; Ouellette, M.; Frolkis, M.; Holt, S. E.; Chiu, C.-P.; Morin, G. B.; Harley, C. B.; Shay, J. W.; Lichsteiner, S.; Wright, W. E., Extension of life-span by introduction of telomerase into normal human cells. *Science (Washington, D C)* **1998,** 279, (5349), 349-352.
173. Tuan Rocky, S.; Boland, G.; Tuli, R., Adult mesenchymal stem cells and cell-based tissue engineering. *Arthritis research & therapy* **2003,** 5, (1), 32-45.
174. Zhao, L.; Weir, M. D.; Xu, H. H. K., An injectable calcium phosphate-alginate hydrogel-umbilical cord mesenchymal stem cell paste for bone tissue engineering. *Biomaterials* **2010,** 31, (25), 6502-6510.
175. Schaefer, D. J.; Klemt, C.; Zhang, X. H.; Stark, G. B., Tissue engineering with mesenchymal stem cells for cartilage and bone regeneration. *Der Chirurg; Zeitschrift für alle Gebiete der operativen Medizin* **2000,** 71, (9), 1001-8.

176. Boo Jae, S.; Yamada, Y.; Okazaki, Y.; Hibino, Y.; Okada, K.; Hata, K.-I.; Yoshikawa, T.; Sugiura, Y.; Ueda, M., Tissue-engineered bone using mesenchymal stem cells and a biodegradable scaffold. *The Journal of craniofacial surgery* **2002,** 13, (2), 231-9; discussion 240-3.
177. Evans, N. D.; Polak, J. M., The potential of stem cells in tissue engineering. *Stem Cell Repair and Regeneration* **2007,** 2, 85-105.
178. Richardson, S. M.; Hoyland, J. A.; Mobasheri, R.; Csaki, C.; Shakibaei, M.; Mobasheri, A., Mesenchymal stem cells in regenerative medicine: Opportunities and challenges for articular cartilage and intervertebral disc tissue engineering. *Journal of Cellular Physiology* **2009,** 222, (1), 23-32.
179. Hutmacher, D. W., Scaffold design and fabrication technologies for engineering tissues. State of the art and future perspectives. *Journal of Biomaterials Science, Polymer Edition* **2001,** 12, (1), 107-124.
180. Ignatius, A. A.; Betz, O.; Augat, P.; Claes, L. E., In vivo investigations on composites made of resorbable ceramics and poly(lactide) used as bone graft substitutes. *Journal of Biomedical Materials Research* **2001,** 58, (6), 701-709.
181. Acuna, V.; Li, J.; Soremark, R., Composites of lactic acid polymer and calcium phosphate or calcium carbonate as degradable bone fillers. *Advances in Biomaterials* **1992,** 10, (Biomaterial-Tissue Interfaces), 391-8.
182. Sun, J. S.; Lin, F. H.; Hung, T. Y.; Tsuang, Y. H.; Chang, W. H.; Liu, H. C., The influence of hydroxyapatite particles on osteoclast cell activities. *Journal of biomedical materials research* **1999,** 45, (4), 311-21.
183. Pioletti, D. P.; Takei, H.; Lin, T.; Van Landuyt, P.; Ma, Q. J.; Kwon, S. Y.; Sung, K. L. P., The effects of calcium phosphate cement particles on osteoblast functions. *Biomaterials* **2000,** 21, (11), 1103-1114.
184. Gelb, H.; Schumacher, H. R.; Cuckler, J.; Ducheyne, P.; Baker, D. G., In vivo inflammatory response to polymethylmethacrylate particulate debris: effect of size, morphology, and surface area. *Journal of orthopaedic research : official publication of the Orthopaedic Research Society* **1994,** 12, (1), 83-92.
185. Van Sliedregt, A.; Knook, M.; Hesseling, S. C.; Koerten, H. K.; De Groot, K.; Van Blitterswijk, C. A., Cellular reaction on the intraperitoneal injection of four types of polylactide particulates. *Biomaterials* **1992,** 13, (12), 819-24.
186. Sachlos, E.; Czernuszka, J. T., Making tissue engineering scaffolds work. Review on the application of solid freeform fabrication technology to the production of tissue engineering scaffolds. *European Cells and Materials* **2003,** 5, 29-40.
187. Kim, T. G.; Park, T. G., Biomimicking Extracellular Matrix: Cell Adhesive RGD Peptide Modified Electrospun Poly(D,L-lactic-co-glycolic acid) Nanofiber Mesh. *Tissue Engineering* **2006,** 12, (2), 221-233.
188. Grzesiak, J. J.; Pierschbacher, M. D.; Amodeo, M. F.; Malaney, T. I.; Glass, J. R., Enhancement of cell interactions with collagen/glycosaminoglycan matrices by RGD derivatization. *Biomaterials* **1997,** 18, (24), 1625-32.
189. Walluscheck, K. P.; Steinhoff, G.; Kelm, S.; Haverich, A., Improved endothelial cell attachment on ePTFE vascular grafts pretreated with synthetic RGD-containing peptides. *European journal of vascular and endovascular surgery* **1996,** 12, (3), 321-30.
190. Smith, I. O.; Liu, X. H.; Smith, L. A.; Ma, P. X., Nanostructured polymer scaffolds for tissue engineering and regenerative medicine. *Wiley Interdisciplinary Reviews: Nanomedicine and Nanobiote* **2009,** 1, (2), 226-236.
191. Seunarine, K.; Gadegaard, N.; Tormen, M.; Meredith, D. O.; Riehle, M. O.; Wilkinson, C. D. W., 3D polymer scaffolds for tissue engineering. *Nanomedicine (London, United Kingdom)* **2006,** 1, (3), 281-296.
192. Place, E. S.; George, J. H.; Williams, C. K.; Stevens, M. M., Synthetic polymer scaffolds for tissue engineering. *Chemical Society Reviews* **2009,** 38, (4), 1139-1151.
193. Lu, L.; Mikos, A. G., The importance of new processing techniques in tissue engineering. *MRS bulletin / Materials Research Society* **1996,** 21, (11), 28-32.
194. Farhat, W. A.; Geutjes, P. J., Artificial biomaterials for urological tissue engineering. *Biomaterials and Tissue Engineering in Urology* **2009**, 243-254.
195. Tabata, Y., Significant role of naturally occurring materials in drug delivery technology for tissue regeneration therapy. *ACS Symposium Series* **2008,** 992, (New Delivery Systems for Controlled Drug Release from Naturally Occurring Materials), 81-105.
196. Swetha, M.; Sahithi, K.; Moorthi, A.; Srinivasan, N.; Ramasamy, K.; Selvamurugan, N., Biocomposites containing natural polymers and hydroxyapatite for bone tissue engineering. *International Journal of Biological Macromolecules* 47, (1), 1-4.
197. Puppi, D.; Chiellini, F.; Piras, A. M.; Chiellini, E., Polymeric materials for bone and cartilage repair. *Progress in Polymer Science* **2010,** 35, (4), 403-440.
198. Göpferich, A., Mechanisms of polymer degradation and erosion. *Biomaterials* **1996,** 17, (2), 103-114.

199. Siepmann, J.; Gopferich, A., Mathematical modeling of bioerodible, polymeric drug delivery systems. *Advanced Drug Delivery Reviews* **2001,** 48, (2-3), 229-247.
200. Lu, L.; Peter, S. J.; Lyman, M. D.; Lai, H. L.; Leite, S. M.; Tamada, J. A.; Uyama, S.; Vacanti, J. P.; Langer, R.; Mikos, A. G., In vitro and in vivo degradation of porous poly(DL-lactic-co-glycolic acid) foams. *Biomaterials* **2000,** 21, (18), 1837-45.
201. Barbanti, S. H.; Santos, A. R., Jr.; Zavaglia, C. A. C.; Duek, E. A. R., Porous and dense poly(L-lactic acid) and poly(D,L-lactic acid-co-glycolic acid) scaffolds: in vitro degradation in culture medium and osteoblasts culture. *Journal of materials science Materials in medicine* **2004,** 15, (12), 1315-21.
202. Vert, M.; Li, S.; Garreau, H., New insights on the degradation of bioresorbable polymeric devices based on lactic and glycolic acids. *Clinical materials* **1992,** 10, (1-2), 3-8.
203. Pitt, C. G.; Chasalow, F. I.; Hibionada, Y. M.; Klimas, D. M.; Schindler, A., Aliphatic polyesters. I. The degradation of poly(e-caprolactone) in vivo. *Journal of Applied Polymer Science* **1981,** 26, (11), 3779-87.
204. Huang, M.-H.; Li, S.; Hutmacher, D. W.; Coudane, J.; Vert, M., Degradation characteristics of poly(e-caprolactone)-based copolymers and blends. *Journal of Applied Polymer Science* **2006,** 102, (2), 1681-1687.
205. Thomson, L. A.; Law, F. C.; James, K. H.; Matthew, C. A.; Rushton, N., Biocompatibility of particulate polymethylmethacrylate bone cements: a comparative study in vitro and in vivo. *Biomaterials* **1992,** 13, (12), 811-8.
206. Lemperle, G.; Ott, H.; Charrier, U.; Hecker, J.; Lemperle, M., PMMA microspheres for intradermal implantation: Part I. Animal research. *Annals of plastic surgery* **1991,** 26, (1), 57-63.
207. Garcia, D. A.; Sullivan, T. M.; O'Neill, D. M., The biocompatibility of dental implant materials measured in an animal model. *Journal of Dental Research* **1981,** 60, (1), 44-9.
208. Santin, M.; Motta, A.; Borzachiello, A.; Nicolais, L.; Ambrosio, L., Effect of PMMA cement radical polymerization on the inflammatory response. *Journal of Materials Science: Materials in Medicine* **2004,** 15, (11), 1175-1180.
209. Boger, A.; Wheeler, K.; Montali, A.; Gruskin, E., NMP-modified PMMA bone cement with adapted mechanical and hardening properties for the use in cancellous bone augmentation. *Journal of Biomedical Materials Research, Part B: Applied Biomaterials* **2009,** 90B, (2), 760-766.
210. Yang, D. H.; Ko, J. T.; Kim, Y. S.; Kim, M. S.; Shin, H. S.; Rhee, J. M.; Khang, G.; Lee, H. B., Surface and chemical properties of surface-modified UHMWPE powder and mechanical and thermal properties of its impregnated PMMA bone cement. IV: Effect of MMA/accelerator on the surface modification of UHMWPE powder. *Journal of Biomaterials Science, Polymer Edition* **2006,** 17, (7), 807-820.
211. Serbetci, K.; Korkusuz, F.; Hasirci, N., Mechanical and thermal properties of hydroxyapatite-impregnated bone cement. *Turkish Journal of Medical Sciences* **2000,** 30, (6), 543-549.
212. Nelson, D. A.; Barker, M. E.; Hamlin, B. H., Thermal effects of acrylic cementation at bone tumor sites. *International Journal of Hyperthermia* **1997,** 13, (3), 287-306.
213. Lewis, G., Properties of acrylic bone cement: state of the art review. *Journal of Biomedical Materials Research* **1997,** 38, (2), 155-182.
214. Berman, A. T.; Reid, J. S.; Yanicko, D. R., Jr.; Sih, G. C.; Zimmerman, M. R., Thermally induced bone necrosis in rabbits. Relation to implant failure in humans. *Clinical orthopaedics and related research* **1984**, (186), 284-92.
215. Olerud, S.; Ponten, B., PGA--a new absorbable suture material. *Nordisk medicin* **1970,** 84, (29), 930-1.
216. Racey, G. L.; Wallace, W. R.; Cavalaris, C. J.; Marguard, J. V., Comparison of a polyglycolic-polylactic acid suture to black silk and plain catgut in human oral tissues. *Journal of oral surgery (American Dental Association : 1965)* **1978,** 36, (10), 766-70.
217. Tauber, R.; Seidel, W.; Mees, P., Studies concerning the usefulness of catgut, PGA and polyester for abdominal fascia closure (author's transl). *Research in experimental medicine* **1975,** 165, (2), 153-61.
218. Hollinger, J. O.; Battistone, G. C., Biodegradable bone repair materials. Synthetic polymers and ceramics. *Clinical orthopaedics and related research* **1986**, (207), 290-305.
219. Miller, R. A.; Brady, J. M.; Cutright, D. E., Degradation rates of oral resorbable implants (polylactates and polyglycolates): rate modification with changes in PLA/PGA copolymer ratios. *Journal of Biomedical Materials Research* **1977,** 11, (5), 711-19.
220. Okada, H., One- and three-month release injectable microspheres of the LH-RH superagonist leuprorelin acetate. *Advanced Drug Delivery Reviews* **1997,** 28, (1), 43-70.
221. Tsuji, H., In vitro hydrolysis of blends from enantiomeric poly(lactide)s. Part 4: well-homo-crystallized blend and nonblended films. *Biomaterials* **2003,** 24, (4), 537-47.
222. Labet, M.; Thielemans, W., Synthesis of polycaprolactone: a review. *Chemical Society Reviews* **2009,** 38, (12), 3484-3504.
223. Porter, J. R.; Henson, A.; Popat, K. C., Biodegradable poly(e-caprolactone) nanowires for bone tissue engineering applications. *Biomaterials* **2009,** 30, (5), 780-788.

224. Sinha, V. R.; Bansal, K.; Kaushik, R.; Kumria, R.; Trehan, A., Poly-epsilon-caprolactone microspheres and nanospheres: an overview. *International journal of pharmaceutics* **2004,** 278, (1), 1-23.
225. Siparsky, G. L.; Voorhees, K. J.; Miao, F., Hydrolysis of polylactic acid (PLA) and polycaprolactone (PCL) in aqueous acetonitrile solutions: autocatalysis. *Journal of Environmental Polymer Degradation* **1998,** 6, (1), 31-41.
226. Woodward, S. C.; Brewer, P. S.; Moatamed, F.; Schindler, A.; Pitt, C. G., The intracellular degradation of poly(epsilon-caprolactone). *Journal of biomedical materials research* **1985,** 19, (4), 437-44.
227. Chen, D. R.; Bei, J. Z.; Wang, S. G., Polycaprolactone microparticles and their biodegradation. *Polymer Degradation and Stability* **2000,** 67, (3), 455-459.
228. Tsuji, H.; Ikada, Y., Blends of aliphatic polyesters. II. Hydrolysis of solution-cast blends from poly(L-lactide) and poly (e-caprolactone) in phosphate-buffered solution. *Journal of Applied Polymer Science* **1998,** 67, (3), 405-415.
229. Pitt, C. G.; Gu, Z. W., Modification of the rates of chain cleavage of poly(e-caprolactone) and related polyesters in the solid state. *Journal of Controlled Release* **1987,** 4, (4), 283-92.
230. Vandamme, T. F.; Legras, R., Physico-mechanical properties of poly (epsilon-caprolactone) for the construction of rumino-reticulum devices for grazing animals. *Biomaterials* **1995,** 16, (18), 1395-400.
231. Woodruff, M. A.; Hutmacher, D. W., The return of a forgotten polymer--Polycaprolactone in the 21st century. *Progress in Polymer Science* **2010,** In Press, Corrected Proof.
232. Le Ray, A. M.; Chiffoleau, S.; Iooss, P.; Grimandi, G.; Gouyette, A.; Daculsi, G.; Merle, C., Vancomycin encapsulation in biodegradable poly(.vepsiln.-caprolactone) microparticles for bone implantation. Influence of the formulation process on size, drug loading, in vitro release and cytocompatibility. *Biomaterials* **2002,** 24, (3), 443-449.
233. Hombreiro Perez, M.; Zinutti, C.; Lamprecht, A.; Ubrich, N.; Astier, A.; Hoffman, M.; Bodmeier, R.; Maincent, P., The preparation and evaluation of poly(e-caprolactone) microparticles containing both a lipophilic and a hydrophilic drug. *Journal of Controlled Release* **2000,** 65, (3), 429-438.
234. Karatas, A.; Sonakin, O.; KiliCarslan, M.; Baykara, T., Poly (e-caprolactone) microparticles containing Levobunolol HCl prepared by a multiple emulsion (W/O/W) solvent evaporation technique: Effects of some formulation parameters on microparticle characteristics. *Journal of Microencapsulation* **2009,** 26, (1), 63-74.
235. Jeong, J.-C.; Lee, J.; Cho, K., Effects of crystalline microstructure on drug release behavior of poly(e-caprolactone) microspheres. *Journal of Controlled Release* **2003,** 92, (3), 249-258.
236. Goodwin, C. J.; Braden, M.; Downes, S.; Marshall, N. J., Release of bioactive human growth hormone from a biodegradable material: poly(epsilon-caprolactone). *Journal of biomedical materials research* **1998,** 40, (2), 204-13.
237. Pitt, C. G.; Gratzl, M. M.; Jeffcoat, A. R.; Zweidinger, R.; Schindler, A., Sustained drug delivery systems II: Factors affecting release rates from poly(epsilon-caprolactone) and related biodegradable polyesters. *Journal of pharmaceutical sciences* **1979,** 68, (12), 1534-8.
238. Lin, W. J.; Huang, L. I., Fabrication of porous poly(e-caprolactone) microparticles for protein release. *Journal of Microencapsulation* **2001,** 18, (5), 577-584.
239. Hafeman, A. E.; Li, B.; Yoshii, T.; Zienkiewicz, K.; Davidson, J. M.; Guelcher, S. A., Injectable Biodegradable Polyurethane Scaffolds with Release of Platelet-derived Growth Factor for Tissue Repair and Regeneration. *Pharmaceutical Research* **2008,** 25, (10), 2387-2399.
240. Gogolewski, S.; Gorna, K., Biodegradable polyurethane cancellous bone graft substitutes in the treatment of iliac crest defects. *Journal of Biomedical Materials Research, Part A* **2006,** 80A, (1), 94-101.
241. Gorna, K.; Gogolewski, S., Preparation, degradation, and calcification of biodegradable polyurethane foams for bone graft substitutes. *Journal of Biomedical Materials Research, Part A* **2003,** 67A, (3), 813-827.
242. Strunz, V.; Bunte, M.; Gross, U. M.; Manner, K.; Bromer, H.; Deutscher, K., Coating of metal implants with the bioactive glass ceramics Ceravital. *Deutsche zahnarztliche Zeitschrift* **1978,** 33, (12), 862-5.
243. Kenny, S. M.; Buggy, M., Bone cements and fillers: a review. *Journal of Materials Science: Materials in Medicine* **2003,** 14, (11), 923-938.
244. Ishaug, S. L.; Crane, G. M.; Miller, M. J.; Yasko, A. W.; Yaszemski, M. J.; Mikos, A. G., Bone formation by three-dimensional stromal osteoblast culture in biodegradable polymer scaffolds. *Journal of biomedical materials research* **1997,** 36, (1), 17-28.
245. Lo, H.; Ponticiello, M. S.; Leong, K. W., Fabrication of controlled release biodegradable foams by phase separation. *Tissue Engineering* **1995,** 1, (1), 15-28.
246. Thomson, R. C.; Yaszemski, M. J.; Powers, J. M.; Mikos, A. G., Fabrication of biodegradable polymer scaffolds to engineer trabecular bone. *Journal of Biomaterials Science, Polymer Edition* **1995,** 7, (1), 23-38.

247. Thomson, R. C.; Yaszemski, M. J.; Powers, J. M.; Harrigan, T. P.; Mikos, A. G., Poly(alpha -hydroxy ester)/short fiber hydroxyapatite composite foams for orthopedic application. *Materials Research Society Symposium Proceedings* **1995,** 394, (Polymers in Medicine and Pharmacy), 25-30.
248. Schmitz, J. P.; Hollinger, J. O., A preliminary study of the osteogenic potential of a biodegradable alloplastic-osteoinductive alloimplant. *Clinical orthopaedics and related research* **1988**, (237), 245-55.
249. Tsuruga, E.; Takita, H.; Itoh, H.; Wakisaka, Y.; Kuboki, Y., Pore size of porous hydroxyapatite as the cell-substratum controls BMP-induced osteogenesis. *Journal of Biochemistry (Tokyo)* **1997,** 121, (2), 317-324.
250. Kuboki, Y.; Jin, Q.; Takita, H., Geometry of carriers controlling phenotypic expression in BMP-induced osteogenesis and chondrogenesis. *The Journal of bone and joint surgery American volume* **2001,** 83-A Suppl 1, (Pt 2), S105-15.
251. Predecki, P.; Auslaender, B. A.; Stephan, J. E.; Mooney, V. L.; Stanitski, C., Attachment of bone to threaded implants by ingrowth and mechanical interlocking. *Journal of biomedical materials research* **1972,** 6, (5), 401-12.
252. Götz, H. E.; Müller, M.; Emmel, A.; Holzwarth, U.; Erben, R. G.; Stangl, R., Effect of surface finish on the osseointegration of laser-treated titanium alloy implants. *Biomaterials* **2004,** 25, (18), 4057-4064.
253. Itala, A. I.; Ylanen, H. O.; Ekholm, C.; Karlsson, K. H.; Aro, H. T., Pore diameter of more than 100 mm is not requisite for bone ingrowth in rabbits. *Journal of Biomedical Materials Research* **2001,** 58, (6), 679-683.
254. Schliephake, H.; Neukam, F. W.; Klosa, D., Influence of pore dimensions on bone ingrowth into porous hydroxylapatite blocks used as bone graft substitutes. A histometric study. *International journal of oral and maxillofacial surgery* **1991,** 20, (1), 53-8.
255. Wang, F. R., Experimental study of osteogenic activity of sintered hydroxyapatite--on the relationship of sintering temperature and pore size. *Nippon Seikeigeka Gakkai zasshi* **1990,** 64, (9), 847-59.
256. Eggli, P. S.; Mueller, W.; Schenk, R. K., Porous hydroxyapatite and tricalcium phosphate cylinders with two different pore size ranges implanted in the cancellous bone of rabbits. A comparative histomorphometric and histologic study of bony ingrowth and implant substitution. *Clinical Orthopaedics and Related Research* **1988,** 232, 127-38.
257. Pamula, E.; Bacakova, L.; Filova, E.; Buczynska, J.; Dobrzynski, P.; Noskova, L.; Grausova, L., The influence of pore size on colonization of poly(L-lactide-glycolide) scaffolds with human osteoblast-like MG 63 cells in vitro. *Journal of Materials Science: Materials in Medicine* **2008,** 19, (1), 425-435.
258. Rose, F. R.; Cyster, L. A.; Grant, D. M.; Scotchford, C. A.; Howdle, S. M.; Shakesheff, K. M., In vitro assessment of cell penetration into porous hydroxyapatite scaffolds with a central aligned channel. *Biomaterials* **2004,** 25, (24), 5507-5514.
259. Goller, G.; Oktar, F. N.; Agathopoulos, S.; Tulyaganov, D. U.; Ferreira, J. M. F.; Kayali, E. S.; Peker, I., Effect of sintering temperature on mechanical and microstructural properties of bovine hydroxyapatite (BHA). *Journal of Sol-Gel Science and Technology* **2006,** 37, (2), 111-115.
260. Peelen, J. G. J.; Rejda, B. V.; Vermeiden, J. P. W., Sintered hydroxylapatite as a bioceramic. *Philips Technical Review* **1978,** 37, (9-10), 234-6.
261. Li Shi, H.; De Wijn Joost, R.; Layrolle, P.; de Groot, K., Synthesis of macroporous hydroxyapatite scaffolds for bone tissue engineering. *Journal of biomedical materials research* **2002,** 61, (1), 109-20.
262. Li, S. H.; de Groot, K.; Layrolle, P., Bioceramic scaffold with controlled porous structure for bone tissue engineering. *Key Engineering Materials* **2002,** 218-220, (Bioceramics-14), 25-30.
263. Habibovic, P.; Gbureck, U.; Doillon Charles, J.; Bassett David, C.; van Blitterswijk Clemens, A.; Barralet Jake, E., Osteoconduction and osteoinduction of low-temperature 3D printed bioceramic implants. *Biomaterials* **2008,** 29, (7), 944-53.
264. Lin, L.; Chow, K. L.; Leng, Y., Study of hydroxyapatite osteoinductivity with an osteogenic differentiation of mesenchymal stem cells. *Journal of Biomedical Materials Research, Part A* **2009,** 89A, (2), 326-335.
265. Sawyer, A. A.; Hennessy, K. M.; Bellis, S. L., The effect of adsorbed serum proteins, RGD and proteoglycan-binding peptides on the adhesion of mesenchymal stem cells to hydroxyapatite. *Biomaterials* **2007,** 28, (3), 383-392.
266. Planell, J. A.; Fernandez, E.; Ginebra, M. P.; Sarda, S.; Nilsson, M., Calcium phosphate based bone cements. *Advances in Science and Technology (Faenza, Italy)* **2003,** 41, (Materials in Clinical Applications VI), 3-10.
267. Roether, J. A.; Deb, S., The effect of surface treatment of hydroxyapatite on the properties of a bioactive bone cement. *Journal of Materials Science: Materials in Medicine* **2004,** 15, (4), 413-418.
268. Dreesman, H., Über Knochenplombierung. *Beitr Klin Chir* **1892,** 9, 804 - 810.
269. Peltier, L. F.; Jones, R. H., Treatment of unicameral bone cysts by curettage and packing with plaster-of-Paris pellets. *The Journal of bone and joint surgery American volume* **1978,** 60, (6), 820-2.

270. Peltier, L. F.; Bickel, E. Y.; Lillo, R.; Thein, M. S., The use of plaster of paris to fill defects in bone. *Annals of surgery* **1957,** 146, (1), 61-9.
271. Gourley, I. M.; Arnold, J. P., The experimental replacement of segmental defects in bone with a plaster of Paris-epoxy resin mixture. *American journal of veterinary research* **1960,** 21, 1119-22.
272. Frame, J. W., Porous calcium sulfate dihydrate as a biodegradable implant in bone. *Journal of Dentistry* **1975,** 3, (4), 177-87.
273. Komath, M.; Varma, H. K.; Sivakumar, R., On the development of an apatitic calcium phosphate bone cement. *Bulletin of Materials Science* **2000,** 23, (2), 135-140.
274. Grover, L. M.; Gbureck, U.; Wright, A. J.; Barralet, J. E., Cement formulations in the calcium phosphate H2O-H3PO4-H4P2O7 system. *Journal of the American Ceramic Society* **2005,** 88, (11), 3096-3103.
275. Barralet, J. E.; Lilley, K. J.; Grover, L. M.; Farrar, D. F.; Ansell, C.; Gbureck, U., Cements from nanocrystalline hydroxyapatite. *Journal of Materials Science: Materials in Medicine* **2004,** 15, (4), 407-411.
276. Xu, H. H. K.; Weir, M. D.; Burguera, E. F.; Fraser, A. M., Injectable and macroporous calcium phosphate cement scaffold. *Biomaterials* **2006,** 27, (24), 4279-4287.
277. Xu, H. H. K.; Quinn, J. B.; Takagi, S.; Chow, L. C., Processing and properties of strong and non-rigid calcium phosphate cement. *Journal of Dental Research* **2002,** 81, (3), 219-224.
278. Flautre, B.; Lemaitre, J.; Maynou, C.; Van Landuyt, P.; Hardouin, P., Influence of polymeric additives on the biological properties of brushite cements: An experimental study in rabbit. *Journal of Biomedical Materials Research, Part A* **2003,** 66A, (2), 214-223.
279. Liu, H.; Zhou, C., Self-hardening calcium phosphate composite scaffold for bone tissue engineering. *Advanced Materials Research (Zuerich, Switzerland)* **2009,** 79-82, (Pt. 1, Multi-Functional Materials and Structures II), 19-22.
280. Habib, M.; Baroud, G.; Gitzhofer, F.; Bohner, M., Mechanisms underlying the limited injectability of hydraulic calcium phosphate paste. *Acta Biomaterialia* **2008,** 4, (5), 1465-1471.
281. Habib, M.; Baroud, G.; Gitzhofer, F.; Bohner, M., Mechanisms underlying the limited injectability of hydraulic calcium phosphate paste. Part II: Particle separation study. *Acta Biomaterialia* In Press, Corrected Proof.
282. Bohner, M.; Baroud, G., Injectability of calcium phosphate pastes. *Biomaterials* **2005,** 26, (13), 1553-1563.
283. Ishikawa, K., Effects of spherical tetracalcium phosphate on injectability and basic properties of apatitic cement. *Key Engineering Materials* **2003,** 240-242, (Bioceramics), 369-372.
284. Khairoun, I.; Boltong, M. G.; Driessens, F. C. M.; Planell, J. A., Some factors controlling the injectability of calcium phosphate bone cements. *Journal of Materials Science: Materials in Medicine* **1998,** 9, (8), 425-428.
285. Ginebra, M. P.; Fernandez, E.; Boltong, M. G.; Bermudez, O.; Planell, J. A.; Driessens, F. C. M., Compliance of an apatitic calcium phosphate cement with the short-term clinical requirements in bone surgery, orthopedics and dentistry. *Clinical Materials* **1994,** 17, (2), 99-104.
286. Cherng, A.; Takagi, S.; Chow, L. C., Effects of hydroxypropyl methyl cellulose and other gelling agents on the handling properties of calcium phosphate cement. *Journal of Biomedical Materials Research* **1997,** 35, (3), 273-277.
287. Ishikawa, K.; Miyamoto, Y.; Kon, M.; Nagayama, M.; Asaoka, K., Non-decay type fast-setting calcium phosphate cement: composite with sodium alginate. *Biomaterials* **1995,** 16, (7), 527-32.
288. Khairoun, I.; Driessens, F. C.; Boltong, M. G.; Planell, J. A.; Wenz, R., Addition of cohesion promotors to calcium phosphate cements. *Biomaterials* **1999,** 20, (4), 393-8.
289. Markovic, M.; Takagi, S.; Chow, L. C., Formation of macropores in calcium phosphate cements through the use of mannitol crystals. *Key Engineering Materials* **2001,** 192-195, (Bioceramics), 773-776.
290. Charriere, E.; Terrazzoni, S.; Pittet, C.; Mordasini, P.; Dutoit, M.; Lemaitre, J.; Zysset, P., Mechanical characterization of brushite and hydroxyapatite cements. *Biomaterials* **2001,** 22, (21), 2937-2945.
291. Suzuki, S.; Ohgaki, M.; Ichiyanagi, M.; Ozawa, M., Preparation of needle-like hydroxyapatite. *Journal of Materials Science Letters* **1998,** 17, (5), 381-383.
292. Li, H.; Zhu, M.; Li, L.; Zhou, C., Preparation of bone-like hydroxyapatite via a reverse microemulsion. *Journal of Wuhan University of Technology, Materials Science Edition* **2005,** 20, (Suppl.), 132-134.
293. Hofmann, M. P.; Mohammed, A. R.; Perrie, Y.; Gbureck, U.; Barralet, J. E., High-strength resorbable brushite bone cement with controlled drug-releasing capabilities. *Acta Biomaterialia* **2009,** 5, (1), 43-49.
294. Grover, L. M.; Gbureck, U.; Hutton, A.; Farrar, D. F.; Ansell, C.; Barralet, J. E., Low porosity CaHPO4.2H2O cement. *Key Engineering Materials* **2004,** 254-256, (Bioceramics), 205-208.
295. Chow, L. C.; Hirayama, S.; Takagi, S.; Parry, E., Diametral tensile strength and compressive strength of a calcium phosphate cement: effect of applied pressure. *Journal of Biomedical Materials Research* **2000,** 53, (5), 511-517.

296. Grover, L. M.; Gbureck, U.; Wright, A. J.; Tremayne, M.; Barralet, J. E., Biologically mediated resorption of brushite cement in vitro. *Biomaterials* **2006,** 27, (10), 2178-2185.
297. Cho, S.-H.; Joo, S.-M.; Cho, J.-S.; Leea, J.-K.; Kimb, H., Mechanical properties and workability of self-hardening calcium phosphate cement as a function of the particle size distribution. *Journal of Ceramic Processing Research* **2004,** 6, (1), 57-62.
298. Takagi, S.; Chow, L. C.; Hirayama, S.; Sugawara, A., Premixed calcium-phosphate cement pastes. *Journal of Biomedical Materials Research, Part B: Applied Biomaterials* **2003,** 67B, (2), 689-696.
299. Carey, L. E.; Xu, H. H. K.; Simon, C. G.; Takagi, S.; Chow, L. C., Premixed rapid-setting calcium phosphate composites for bone repair. *Biomaterials* **2005,** 26, (24), 5002-5014.
300. Hamanishi, C.; Kitamoto, K.; Tanaka, S.; Otsuka, M.; Doi, Y.; Kitahashi, T., A self-setting TTCP-DCPD apatite cement for release of vancomycin. *Journal of Biomedical Materials Research* **1996,** 33, (3), 139-143.
301. Otsuka, M.; Matsuda, Y.; Kokubo, T.; Yoshihara, S.; Nakamura, T.; Yamamuro, T., A novel skeletal drug delivery system using self-setting bioactive glass bone cement IV: Cephalexin release from cement containing polymer-coated bulk powder. *Bio-Medical Materials and Engineering* **1993,** 3, (4), 229-36.
302. Bohner, M.; Lemaitre, J.; Van Landuyt, P.; Zambelli, P.-Y.; Merkle, H. P.; Gander, B., Gentamicin-Loaded Hydraulic Calcium Phosphate Bone Cement as Antibiotic Delivery System. *Journal of Pharmaceutical Sciences* **1997,** 86, (5), 565-572.
303. Tung, I. C., In vitro drug release of antibiotic-loaded porous hydroxyapatite cement. *Artificial Cells, Blood Substitutes,* **1995,** 23, (1), 81-8.
304. Ratier, A.; Gibson, I. R.; Best, S. M.; Freche, M.; Lacout, J. L.; Rodriguez, F., Setting characteristics and mechanical behaviour of a calcium phosphate bone cement containing tetracycline. *Biomaterials* **2001,** 22, (9), 897-901.
305. Otsuka, M.; Matsuda, Y.; Suwa, Y.; Fox, J. L.; Higuchi, W. I., A novel skeletal drug-delivery system using self-setting calcium phosphate cement: Effects of the mixing solution volume on the drug release rate of heterogeneous aspirin-loaded cement. *Journal of Pharmaceutical Sciences* **1994,** 83, (2), 259-63.
306. Otsuka, M.; Nakahigashi, Y.; Matsuda, Y.; Fox, J. L.; Higuchi, W. I.; Sugiyama, Y., Effect of geometrical cement size on in vitro and in vivo indomethacin release from self-setting apatite cement. *Journal of Controlled Release* **1998,** 52, (3), 281-289.
307. Otsuka, M.; Matsuda, Y.; Suwa, Y.; Fox, J. L.; Higuchi, W. I., A Novel Skeletal Drug Delivery System Using a Self-Setting Calcium Phosphate Cement. 5. Drug Release Behavior from a Heterogeneous Drug-Loaded Cement Containing an Anticancer Drug. *Journal of Pharmaceutical Sciences* **1994,** 83, (11), 1565-8.
308. Otsuka, M.; Matsuda, Y.; Suwa, Y.; Fox, J. L.; Higuchi, W. I., A novel skeletal drug-delivery system using self-setting calcium phosphate cement. 3. Physicochemical properties and drug-release rate of bovine insulin and bovine albumin. *Journal of Pharmaceutical Sciences* **1994,** 83, (2), 255-8.
309. Ruhe, P. Q.; Boerman, O. C.; Russel, F. G. M.; Mikos, A. G.; Spauwen, P. H. M.; Jansen, J. A., In vivo release of rhBMP-2 loaded porous calcium phosphate cement pretreated with albumin. *Journal of Materials Science: Materials in Medicine* **2006,** 17, (10), 919-927.
310. Urist, M. R.; Lietze, A.; Dawson, E., beta -Tricalcium phosphate delivery system for bone morphogenetic protein. *Clinical Orthopaedics and Related Research* **1984,** 187, 277-80.
311. Ginebra, M. P.; Traykova, T.; Planell, J. A., Calcium phosphate cements as bone drug delivery systems: A review. *Journal of Controlled Release* **2006,** 113, (2), 102-110.
312. Tiselius, A.; Hjerten, S.; Levin, O., Protein chromatography on calcium phosphate columns. *Arch Biochem and Biophys* **1956,** 65, 156-63.
313. Urist, M. R.; Huo, Y. K.; Brownell, A. G.; Hohl, W. M.; Buyske, J.; Lietze, A.; Tempst, P.; Hunkapiller, M.; DeLange, R. J., Purification of bovine bone morphogenetic protein by hydroxyapatite chromatography. *Proceedings of the National Academy of Sciences of the United States of America* **1984,** 81, (2), 371-5.
314. Brandes, N.; Welzel, P. B.; Werner, C.; Kroh, L. W., Adsorption-induced conformational changes of proteins onto ceramic particles: Differential scanning calorimetry and FTIR analysis. *Journal of Colloid and Interface Science* **2006,** 299, (1), 56-69.
315. Takechi, M.; Miyamoto, Y.; Ishikawa, K.; Nagayama, M.; Kon, M.; Asaoka, K.; Suzuki, K., Effects of added antibiotics on the basic properties of anti-washout-type fast-setting calcium phosphate cement. *Journal of Biomedical Materials Research* **1998,** 39, (2), 308-316.
316. Higuchi, T., Mechanism of sustained-action medication. Theoretical analysis of rate of release of solid drugs dispersed in solid matrices. *Journal of Pharmaceutical Sciences* **1963,** 52, (12), 1145-9.
317. Zuo, Y.; Yang, F.; Wolke, J. G. C.; Li, Y.; Jansen, J. A., Incorporation of biodegradable electrospun fibers into calcium phosphate cement for bone regeneration. *Acta Biomaterialia* **2010,** 6, (4), 1238-1247.

318. Habraken, W. J. E. M.; Wolke, J. G. C.; Mikos, A. G.; Jansen, J. A., Injectable PLGA microsphere/calcium phosphate cements: physical properties and degradation characteristics. *Journal of Biomaterials Science, Polymer Edition* **2006,** 17, (9), 1057-1074.
319. Gorst, N. J. S.; Perrie, Y.; Gbureck, U.; Hutton, A. L.; Hofmann, M. P.; Grover, L. M.; Barralet, J. E., Effects of fibre reinforcement on the mechanical properties of brushite cement. *Acta biomaterialia* **2006,** 2, (1), 95-102.
320. Lian, Q.; Li, D. C.; He, J. K.; Wang, Z., Mechanical properties and in-vivo performance of calcium phosphate cement-chitosan fibre composite. *Proceedings of the Institution of Mechanical Engineers, Part H: Jo* **2008,** 222, (H3), 347-353.
321. Ruhe, P. Q.; Hedberg Elizabeth, L.; Padron Nestor, T.; Spauwen Paul, H. M.; Jansen John, A.; Mikos Antonios, G., rhBMP-2 release from injectable poly(DL-lactic-co-glycolic acid)/calcium-phosphate cement composites. *The Journal of bone and joint surgery American volume* **2003,** 85-A Suppl 3, 75-81.
322. Brown, W. E.; Chow, L. C. Dental resptorative cement pastes. 4518430, 1985.
323. Ishikawa, K., Calcium phosphate cement. *Bioceramics and Their Clinical Applications* **2008**, 438-463.
324. Liu, C., Research and development of calcium phosphate cement. *Key Engineering Materials* **2007,** 353-358, (Pt. 3, Progresses in Fracture and Strength of Materials and Structures), 2267-2270.
325. Miyamoto, Y.; Ishikawa, K.; Fukao, H.; Sawada, M.; Nagayama, M.; Kon, M.; Asaoka, K., In vivo setting behavior of fast-setting calcium phosphate cement. *Biomaterials* **1995,** 16, (11), 855-60.
326. Gbureck, U.; Barralet, J. E.; Hofmann, M. P.; Thull, R., Nanocrystalline tetracalcium phosphate cement. *Journal of Dental Research* **2004,** 83, (5), 425-428.
327. Ginebra, M. P.; Fernandez, E.; Boltong, M. G.; Bermudez, O.; Planell, J. A.; Driessens, F. C., Compliance of an apatitic calcium phosphate cement with the short-term clinical requirements in bone surgery, orthopaedics and dentistry. *Clinical materials* **1994,** 17, (2), 99-104.
328. Driessens, F. C. M.; Boltong, M. G.; De Maeyer, E. A. P.; Verbeeck, R. M. H.; Wenz, R., Effect of temperature and immersion on the setting of some calcium phosphate cements. *Journal of Materials Science: Materials in Medicine* **2000,** 11, (7), 453-457.
329. Ishikawa, K.; Miyamoto, Y.; Suzuki, K., Comparison of the tissue response to calcium phosphate cements with various setting accelerator. *Bioceramics, Proceedings of the International Symposium on Ceramics* **1998,** 11, 447-450.
330. Romeo, H. E.; Bueno, P. R.; Fanovich, M. A., Application of impedance spectroscopy to evaluate the effect of different setting accelerators on the developed microstructures of calcium phosphate cements. *Journal of Materials Science: Materials in Medicine* **2009,** 20, (8), 1619-1627.
331. Breding, K.; Engqvist, H., Strength and chemical stability due to aging of two bone void filler materials. *Key Engineering Materials* **2008,** 361-363, (Pt. 1, Bioceramics), 315-318.
332. Yuasa, T.; Miyamoto, Y.; Ishikawa, K.; Takechi, M.; Nagayama, M.; Suzuki, K., In vitro resorption of three apatite cements with osteoclasts. *Journal of Biomedical Materials Research* **2000,** 54, (3), 344-350.
333. Costantino, P. D.; Friedman, C. D.; Jones, K.; Chow, L. C.; Pelzer, H. J.; Sisson, G. A., Sr., Hydroxyapatite cement. I. Basic chemistry and histologic properties. *Archives of otolaryngology--head & neck surgery* **1991,** 117, (4), 379-84.
334. Wolke, J. G. C.; Ooms, E. M.; Jansen, J. A., In vivo resorption behavior of a high strength injectable calcium phosphate cement. *Key Engineering Materials* **2001,** 192-195, (Bioceramics), 793-796.
335. Mirtchi, A. A.; Lemaitre, J.; Terao, N., Calcium phosphate cements: study of the beta -tricalcium phosphate-monocalcium phosphate system. *Biomaterials* **1989,** 10, (7), 475-80.
336. Ohura, K.; Bohner, M.; Hardouin, P.; Lemaitre, J.; Pasquier, G.; Flautre, B., Resorption of, and bone formation from, new b-tricalcium phosphate-monocalcium phosphate cements: an in vivo study. *Journal of Biomedical Materials Research* **1996,** 30, (2), 193-200.
337. Oh, K.-S.; Choi, H.-W.; Kim, S.-R., Temperature rise and setting of [beta]-TCP-MCPM bone cement containing dense [beta]-TCP granules. *Current Applied Physics* **2005,** 5, (5), 489-492.
338. Mirtchi, A. A.; Lemaître, J.; Hunting, E., Calcium phosphate cements: action of setting regulators on the properties of the [beta]-tricalcium phosphate-monocalcium phosphate cements. *Biomaterials* **1989,** 10, (9), 634-638.
339. Bohner, M.; Van Landuyt, P.; Merkle, H. P.; Lemaitre, J., Composition effects on the pH of a hydraulic calcium phosphate cement. *Journal of Materials Science: Materials in Medicine* **1997,** 8, (11), 675-681.
340. Munting, E.; Mirtchi, A. A.; Lemaitre, J., Bone repair of defects filled with a phosphocalcic hydraulic cement: An in vivo study. *JOURNAL OF MATERIALS SCIENCE: MATERIALS IN MEDICINE* **1993,** 4, (3), 337-44.
341. Grover, L. M.; Gbureck, U.; Young, A. M.; Wright, A. J.; Barralet, J. E., Temperature dependent setting kinetics and mechanical properties of beta -TCP-pyrophosphoric acid bone cement. *Journal of Materials Chemistry* **2005,** 15, (46), 4955-4962.

342. Bohner, M.; Merkle, H. P.; Lemaitre, J., In vitro aging of a calcium phosphate cement. *JOURNAL OF MATERIALS SCIENCE: MATERIALS IN MEDICINE* **2000,** 11, (3), 155-162.
343. Bohner, M.; Brunner, T. J.; Stark, W. J., Controlling the reactivity of calcium phosphate cements. *Key Engineering Materials* **2008,** 361-363, (Pt. 1, Bioceramics), 295-298.
344. Van Landuyt, P.; Lowe, C.; Lemaitre, J., Optimization of setting time and mechanical strength of beta - TCP/MCPM cements. *Bioceramics, Proceedings of the International Symposium on Ceramics* **1997,** 10, 477-480.
345. Bohner, M.; Lemaitre, J.; Ring, T. A., Effects of sulfate, pyrophosphate, and citrate ions on the physicochemical properties of cements made of b-tricalcium phosphate-phosphoric acid-water mixtures. *Journal of the American Ceramic Society* **1996,** 79, (6), 1427-1434.
346. Marino, F. T.; Torres, J.; Hamdan, M.; Rodriguez, C. R.; Cabarcos, E. L., Advantages of using glycolic acid as a retardant in a brushite forming cement. *Journal of Biomedical Materials Research, Part B: Applied Biomaterials* **2007,** 83B, (2), 571-579.
347. Hofmann, M. P.; Gbureck, U.; Grover, L. M.; Barralet, J. E., Stearate salts as brushite bone cement setting retardants. *Key Engineering Materials* **2005,** 284-286, 19-22.
348. Tamimi-Marino, F.; Mastio, J.; Rueda, C.; Blanco, L.; Lopez-Cabarcos, E., Increase of the final setting time of brushite cements by using chondroitin 4-sulfate and silica gel. *Journal of Materials Science: Materials in Medicine* **2007,** 18, (6), 1195-1201.
349. Shugar, D., The measurement of lysozyme activity and the ultra-violet inactivation of lysozyme. *Biochimica et biophysica acta* **1952,** 8, (3), 302-9.
350. Hawthorne, J. R., Note on the products formed on lysis of Micrococcus lysodeikticus by egg white lysozyme. *Biochimica et biophysica acta* **1950,** 6, (1), 94-6.
351. Litwack, G., Photometric determination of lysozyme activity. *Proceedings of the Society for Experimental Biology and Medicine* **1955,** 89, (3), 401-3.
352. Bradford, M. M., A rapid and sensitive method for the quantitation of microgram quantities of protein utilizing the principle of protein-dye binding. *Analytical biochemistry* **1976,** 72, 248-54.
353. Pietrzak, W. S.; Ronk, R., Calcium sulfate bone void filler: a review and a look ahead. *The Journal of craniofacial surgery* **2000,** 11, (4), 327-33; discussion 334.
354. Mahan, K. T.; Carey, M. J., Hydroxyapatite as a bone substitute. *Journal of the American Podiatric Medical Association* **1999,** 89, (8), 392-7.
355. Erbe, E. M.; Clineff, T. D.; Gualtieri, G., Comparison of a new bisphenol-a-glycidyl dimethacrylate-based cortical bone void filler with polymethyl methacrylate. *European spine journal* **2001,** 10 Suppl 2, S147-52.
356. Gunzburg, R.; Szpalski, M., Use of a novel beta-tricalcium phosphate-based bone void filler as a graft extender in spinal fusion surgeries. *Orthopedics* **2002,** 25, (5 Suppl), s591-5.
357. Pomrink, G. J.; DiCicco, M. P.; Clineff, T. D.; Erbe, E. M., Evaluation of the reaction kinetics of CORTOSS, a thermoset cortical bone void filler. *Biomaterials* **2003,** 24, (6), 1023-31.
358. Kühne, J. H.; Bartl, R.; Frisch, B.; Hammer, C.; Jansson, V.; Zimmer, M., Bone formation in coralline hydroxyapatite. Effects of pore size studied in rabbits. *Acta orthopaedica Scandinavica* **1994,** 65, (3), 246-52.
359. Barralet, J. E.; Tremayne, M.; Lilley, K. J.; Gbureck, U., Modification of Calcium Phosphate Cement with alpha -Hydroxy Acids and Their Salts. *Chemistry of Materials* **2005,** 17, (6), 1313-1319.
360. Freytag, T.; Dashevsky, A.; Tillman, L.; Hardee, G. E.; Bodmeier, R., Improvement of the encapsulation efficiency of oligonucleotide-containing biodegradable microspheres. *Journal of Controlled Release* **2000,** 69, (1), 197-207.
361. Herrmann, J.; Bodmeier, R., Biodegradable, somatostatin acetate-containing microspheres prepared by various aqueous and non-aqueous solvent evaporation methods. *European Journal of Pharmaceutics and Biopharmaceutics* **1998,** 45, (1), 75-82.
362. Burguera, E. F.; Xu, H. H. K.; Weir, M. D., Injectable and rapid-setting calcium phosphate bone cement with dicalcium phosphate dihydrate. *Journal of Biomedical Materials Research, Part B: Applied Biomaterials* **2006,** 77B, (1), 126-134.
363. Liu, C.; Shao, H.; Chen, F.; Zheng, H., Rheological properties of concentrated aqueous injectable calcium phosphate cement slurry. *Biomaterials* **2006,** 27, (29), 5003-13.
364. Qi, X.; Ye, J., Mechanical and rheological properties and injectability of calcium phosphate cement containing poly (lactic-co-glycolic acid) microspheres. *Materials Science & Engineering, C: Materials for Biological Applications* **2009,** 29, (6), 1901-1906.
365. Bohner, M.; Gbureck, U., Thermal reactions of brushite cements. *Journal of Biomedical Materials Research, Part B: Applied Biomaterials* **2008,** 84B, (2), 375-385.

366. Hofmann, M. P.; Nazhat, S. N.; Gbureck, U.; Barralet, J. E., Real-time monitoring of the setting reaction of brushite-forming cement using isothermal differential scanning calorimetry. *Journal of Biomedical Materials Research, Part B: Applied Biomaterials* **2006,** 79B, (2), 360-364.
367. Hofmann, M. P.; Young, A. M.; Gbureck, U.; Nazhat, S. N.; Barralet, J. E., FTIR-monitoring of a fast setting brushite bone cement: effect of intermediate phases. *Journal of Materials Chemistry* **2006,** 16, (31), 3199-3206.
368. Rau, J. V.; Generosi, A.; Smirnov, V. V.; Ferro, D.; Albertini, V. R.; Barinov, S. M., Energy dispersive X-ray diffraction study of phase development during hardening of calcium phosphate bone cements with addition of chitosan. *Acta Biomaterialia* **2008,** 4, (4), 1089-1094.
369. Fukase, Y.; Eanes, E. D.; Takagi, S.; Chow, L. C.; Brown, W. E., Setting reactions and compressive strengths of calcium phosphate cements. *Journal of Dental Research* **1990,** 69, (12), 1852-6.
370. Epple, M., On the evaluation of dynamic X-ray diffractometric data for kinetic and structural purposes. *Journal of Thermal Analysis* **1995,** 45, (6), 1265-76.
371. Conolly, J. R., Introduction to X-Ray Powder Diffraction. In *Sample Preparation and Systematic Diffractometer Errors*, 2007.
372. Suryanarayanan, R., X-ray powder diffractometry. In *Physical Characterization of Pharmaceutical Solids*, Brittain, H. G., Ed. Informa Healthcare: 1995; Vol. 70, pp 188-221.
373. Hofmann, M. P.; Young, A. M.; Nazhat, S. N.; Gbureck, U.; Barralet, J. E., Setting kinetics observation of a brushite cement by FTIR and DSC. *Key Engineering Materials* **2006,** 309-311, (Pt. 2, Bioceramics), 837-840.
374. Analysis of Polymers by ATR/FT-IR Spectroscopy - Application Note 0603. In Pike Technologies, Madison, WI, USA.
375. Ikenaga, M.; Hardouin, P.; Lemaitre, J.; Andrianjatovo, H.; Flautre, B., Biomechanical characterization of a biodegradable calcium phosphate hydraulic cement: A comparison with porous biphasic calcium phosphate ceramics. *Journal of Biomedical Materials Research* **1998,** 40, (1), 139-144.
376. Lee, S.-A.; Chung, T.-J.; Oh, K.-S., Effect of storage conditions on the setting properties of brushite bone cement containing granular beta -tricalcium phosphate. *Journal of the Korean Ceramic Society* **2008,** 45, (10), 625-630.
377. Lee, S.-A.; Chung, T.-J.; Lee, K.-A.; Kim, H.-M.; Oh, K.-S., Effect of storage conditions prior to mixing in beta -TCP based bone cement on the reaction products and the setting. *Key Engineering Materials* **2008,** 361-363, (Pt. 1, Bioceramics), 351-354.
378. Yamada, H.; Suryanarayanan, R., Calculation of the Penetration Depth of X-rays in Intact Pharmaceutical Film-Coated Tablets by Microdiffractometory. *Pharmaceutical Research* **2006,** 23, (9), 2149-2157.
379. Maasz, J.; Beyer, C., The measureable penetration depth of x-rays in x-ray diffractometry of pharmaceuticals. *Pharmazeutische Industrie* **1988,** 50, (5), 579-88.
380. Tomov, I., A new diffraction method for the determination of the effective depth of x-ray penetration. *Physica Status Solidi A: Applied Research* **1986,** 95, (2), 397-405.

7 Publications and presentations

7.1 Publications

Dickenhorst, B., Bodmeier, R.; DCPD-forming calcium phosphate cements containing polycaprolactone microparticles for controlled protein drug delivery: Release behavior and mechanical properties (in preparation)

Dickenhorst, B., Bodmeier, R.; Effect of temperature and citrate-addition on the setting time of a DCPD-forming calcium phosphate cement and on the mechanical properties of DCPD (in preparation)

Dickenhorst, B., Bodmeier, R.; Time-resolved powder x-ray diffractometry of the setting reaction of a DCPD-forming calcium phosphate cement (in preparation)

Dickenhorst, B., Bodmeier, R.; Storage stability of a DCPD-forming calcium phosphate cement for bone tissue engineering monitored by iDSC, DVS, FTIR, XRD and mechanical testing (in preparation)

7.2 Presentations

Dickenhorst, B., Bodmeier, R.; Observation of the setting behavior of a DCPD forming calcium phosphate cement via XRD and DSC; Annual meeting of the American Association of Pharmaceutical Scientists (AAPS), San Diego, CA, USA, 2007

Dickenhorst, B., Bodmeier, R.; Effects of humidity during storage on the mechanical strength of a brushite forming premixed calcium phosphate cement; Annual meeting of the American Association of Pharmaceutical Scientists (AAPS), Atlanta, GA, USA, 2008

8 Curriculum vitae

Der Lebenslauf ist in der Online-Version aus Gründen des Datenschutzes nicht enthalten.